A STUDY OF UNSTEADY TRANSONIC INTERFERENCE EFFECTS

Paul Barron Schlein

NAVAL POSTGRADUATE SCHOOL
Monterey, California

THESIS

A STUDY OF UNSTEADY TRANSONIC
INTERFERENCE EFFECTS

by

Paul Barron Schlein

March 1975

Thesis Advisor: M.F. Platzer

UNCLASSIFIED

SECURITY CLASSIFICATION OF THIS PAGE (When Data Entered)

REPORT DOCUMENTATION PAGE		READ INSTRUCTIONS BEFORE COMPLETING FORM
1. REPORT NUMBER	2. GOVT ACCESSION NO.	3. RECIPIENT'S CATALOG NUMBER
4. TITLE (and Subtitle) A Study of Unsteady Transonic Interference Effects		5. TYPE OF REPORT & PERIOD COVERED Doctor of Philosophy March 1975 6. PERFORMING ORG. REPORT NUMBER
7. AUTHOR(s) Paul Barron Schlein		8. CONTRACT OR GRANT NUMBER(s)
9. PERFORMING ORGANIZATION NAME AND ADDRESS Naval Postgraduate School Monterey, California 93940		10. PROGRAM ELEMENT, PROJECT, TASK AREA & WORK UNIT NUMBERS
11. CONTROLLING OFFICE NAME AND ADDRESS Naval Postgraduate School Monterey, California 93940		12. REPORT DATE March 1975 13. NUMBER OF PAGES 176
14. MONITORING AGENCY NAME & ADDRESS(if different from Controlling Office)		15. SECURITY CLASS. (of this report) Unclassified 15a. DECLASSIFICATION/DOWNGRADING SCHEDULE

16. DISTRIBUTION STATEMENT (of this Report)

Approved for public release; distribution unlimited.

17. DISTRIBUTION STATEMENT (of the abstract entered in Block 20, if different from Report)

18. SUPPLEMENTARY NOTES

19. KEY WORDS (Continue on reverse side if necessary and identify by block number)

Unsteady Aerodynamics
Aeroelasticity
Cascade Aerodynamics
Transonic Aerodynamics
Wind Tunnel Interference

20. ABSTRACT (Continue on reverse side if necessary and identify by block number)

The unsteady, sonic, small disturbance potential equation was approximated by reduction to parabolic form and solved by Laplace and Fourier Transform and Collocation techniques, including thickness effects through the Oswatitsch parameter. The Transform techniques produced reliable solutions and the Collocation solution was usable with qualifications, for some parameter values, stemming from the choice of approximating series. Stability boundaries for an unstaggered cascade oscillating in sonic flow were calculated with the Fourier

DD FORM 1 JAN 73 1473 (Page 1)

EDITION OF 1 NOV 65 IS OBSOLETE
S/N 0102-014-6601

UNCLASSIFIED

SECURITY CLASSIFICATION OF THIS PAGE (When Data Entered)

(20. ABSTRACT Continued)

Transform technique revealing that blade interference is strongly destabilizing. The Collocation technique was successfully applied to the two-dimensional, unsteady, porous walled, sonic wind tunnel interference problem, heretofore unapproached with the inclusion of thickness effects.

A Study of Unsteady Transonic Interference Effects

by

Paul Barron Schlein
Lieutenant, United States Navy
B.S., United States Naval Academy, 1966

Submitted in partial fulfillment of the requirements for the degree of

DOCTOR OF PHILOSOPHY

from the

NAVAL POSTGRADUATE SCHOOL
March 1975

ABSTRACT

The unsteady, sonic, small disturbance potential equation was approximated by reduction to parabolic form and solved by Laplace and Fourier Transform and Collocation techniques, including thickness effects through the Oswatitsch parameter. The Transform techniques produced reliable solutions and the Collocation solution was usable with qualifications, for some parameter values, stemming from the choice of approximating series. Stability boundaries for an unstaggered cascade oscillating in sonic flow were calculated with the Fourier Transform technique revealing that blade interference is strongly destabilizing. The Collocation technique was successfully applied to the two-dimensional, unsteady, porous walled, sonic wind tunnel interference problem, heretofore unapproached with the inclusion of thickness effects.

TABLE OF CONTENTS

LIST OF TABLES AND FIGURES

TABLES

FIGURES

LIST OF SYMBOLS

A = $K^2/(\lambda^2 + 4K^2)$

A_1 = nondimensional position of pivot location, a divided by reference length

a = position of pivot in pitch oscillation

B = variable in Fourier Transform solution, functions of interblade phase angle or can be = $\lambda P^2/4$

B_1 = nondimensional pivot location, b divided by reference length

b = airfoil or blade semichord

C = dimensionless speed of sound; speed of sound divided by reference velocity

C_L = lift coefficient, positive upward

C_M = moment coefficient, positive leading edge up

C_P = pressure coefficient

c = airfoil or blade chord

D = variable in Fourier Transform solution, function of interblade phase angle

$Exp[\alpha]$ = e^{α}

E = $KP^2/4$

E_1 = constant in solution of Fourier transformed potential equation

F_1 = constant in solution of Fourier transformed potential equation

F_2 = first integral of Ψ, used in Fourier Transform solution

F_n = nth integrals of Ψ, $n > 1$

f = variable necessary in Fourier Transform solution = 1,2

$H(X,T)$ = nondimensional Y position of airfoil or blade surface

$H(Z)$ = Heaviside step function

h = nondimensional interblade distance, P/C

$\bar{h}$ = nondimensional mean Y position of airfoil or blade surface

$h(X)$ = nondimensional amplitude of oscillatory airfoil or blade surface

h_0 = amplitude of plunge oscillation

h_i = nondimensional amplitude of plunge oscillations, divided by reference length, i = 1 or 2

I_n = integrals appearing in Laplace Transform and Collocation solution

$I(X)$ = integral values for Fourier Transform solution

i = imaginary constant, $\sqrt{-1}$, or variable index

$J(X)$ = integral values for Fourier Transform solution

K = reduced frequency; $\omega b/U_1$

K_1 = $\omega c/U_1$

L = Oswatitsch parameter, λ, or number of collocation points to be used

M = Mach number of reference velocity

n = variable index

P = interblade distance, or variable in I_n

p = Laplace Transform transformation variable

Q = $\lambda + 2iK$

R.P. = real part

s = variable of integration for Laplace Transform and Collocation solutions

S_N = see T_N

T = dimensionless time, t multiplied by reference velocity and divided by reference length

T_N = integral values necessary in Fourier Transform solution

t = time

U = X-S, variable used in evaluation of I_n

U_1 = reference velocity, freestream or critical

u_m = interference source distribution, m = 0 or 1 for reference or adjacent blade, respectively

v = nondimensional downwash velocity at blade chordline, used in Laplace Transform and Collocation solutions

v_m = source distribution on airfoil or blade, m = 0,1, for reference or adjacent blade, respectively

$w(X)$ = nondimensional downwash velocity at blade chordline, used in Fourier Transform solution

X = dimensionless coordinate in freestream direction; x divided by reference length

X_0 = nondimensional pivot location, a divided by b

X_1 = X + 1

XA = upper limit of 'correction integral'

x = coordinate in freestream direction

Y = dimensionless coordinate perpendicular to stream direction

y = coordinate perpendicular to stream direction

α_0 = amplitude of pitch oscillation

γ = ratio of specific heats

η_i = perpendicular coordinate from blades, i=0,1

η_n = variable in summation for J(X)

θ_{mn} = coefficients of isolated blade source distribution series, m defines blade (reference or adjacent), n defines sequence number in series

λ = Oswatitsch parameter, $(\gamma+1)\bar{\phi}_{XX}$

μ^2 = variable in transformed potential equations

ν = Fourier Transform transformation variable

ν_n = variable in summation for I(X)

ν_{mn} = coefficients of interference source distribution series, see θ_{mn}

ξ_i = coordinate along airfoil or blade chord from midchord or leading edge, i = 1 or 2, respectively

ρ = nondimensional interblade distance, P divided by b

σ = interblade phase angle

$\sigma_{w\ell}$ = porosity parameter

τ = airfoil or blade thickness/chord ratio

Φ = dimensionless unsteady two-dimensional velocity potential, potential divided by reference length and reference velocity

ϕ = nondimensional perturbation potential, or dummy variable

ϕ_0^0 = isolated blade potential for the reference blade

ϕ_1^0 = isolated blade potential for the adjacent blade

ϕ_0 = interference potential for the reference blade

ϕ_1 = interference potential for the adjacent blade

$\bar{\phi}$ = steady flow perturbation potential, nondimensional

ψ = nonsteady flow perturbation potential, nondimensional

$\bar{\psi}$ = transformed nonsteady perturbation potential

ω = circular frequency of pitch or plunge oscillation

ACKNOWLEDGEMENT

This work could not have been completed were it not for the indefatigability of Dr. Max F. Platzer, the timely assistance of Dr. Craig Comstock, and the inspiration of Louisa May Alcott:

> Far away in the sunshine
> are my highest aspirations. I may
> not reach them, but I can look up
> and see their beauty, believe in them
> and try to follow where they lead.

I. INTRODUCTION

Nonsteady, interfering, transonic flows are of increasing importance to aeroelasticians. Recent design concepts for transonic transports, high maneuverability fighters, biplanar space shuttle configurations, and so called transonic axial flow compressors, to name a few, involve such flows when aeroelastic problems are considered. Ironically, while sub/supersonic flutter problems have been extensively studied, the transonic problem has been circumvented by either rapid acceleration through the regime or operation avoiding it. It is now apparent that the question of the effect of transonic flow, including possible adjacent flow field interference, on flutter must be confronted in a practical way.

Of course, even without interference, nonsteady transonic flows challenge the aeroelastician concerned with aerodynamic damping of structural vibrations. In that regime, pressure perturbations generated by a body and propagated at the local speed of sound tend to accumulate near the body itself. Thus, the magnitude of aerodynamic forces is increased and, perhaps more importantly, a large phase lag can exist between the forces and the motion producing them. It is this phase lag that can lead to negative aerodynamic damping and, potentially, dangerous flutter.

It is not enough to analytically study the flutter character of particular configurations. Wind tunnel experiments

must be conducted to verify analytical results before a configuration can be committed to flight test. However, flow perturbations from a wind tunnel test model may reflect from the tunnel walls back onto the model requiring a correction to test results due to interference. In steady transonic flow, such wall interference has been thoroughly examined and porous or slotted wall tunnels have been utilized for some time to reduce its effect. In nonsteady flow, the porous wall boundary condition is a difficult one for classical analytical approaches to handle. Only Drake [Ref. 6] has included wall porosity in a theoretical analysis of a thin airfoil oscillating in a transonic wind tunnel and his results are by no means complete. Thus, there is a great need for solutions that can yield the magnitude of unsteady wall interference and the effect of wall porosity upon it.

Blade flutter in transonic axial compressors is a complex problem involving, among other things, interference of highly perturbed transonic flow fields. Historically, sub and supersonic axial compressor flows have been simulated by a series of airfoils (or blades) placed in close proximity (a cascade) so that the two dimensional flow models that in a rotating compressor stage. For the transonic compressor stage the mixed flow character of the real flow makes the two-dimensional approximation questionable, e.g., McCune [Ref. 16]. It must be recognized that accurate modeling of such a complex flow field is well beyond the state of the art. However, the

cascade approximation may yield important information relative to the trends of blade flutter.

Nonsteady transonic flow analysis begins with the derivation of the nonlinear small perturbation potential equation which Lin, Reissner, and Tsien [Ref. 15] and Landahl [Ref. 13] have shown can be linearized for sufficiently high frequency. Since aeroelastic analyses are, generally, concerned with the stability of small amplitude oscillations, the solutions to the nonlinear potential equations shall be written as the sum of a steady component and a much smaller nonsteady component. The result is two equations, the usual nonlinear steady flow equation and a linear nonsteady flow equation containing variable coefficients depending upon the steady flow.

Transonic cascade flow for thin blades and in-phase oscillations was approached by Hamamoto [Ref. 10] using Fourier Transform techniques on the linearized potential equation. Gorelov [Ref. 8] solved the linear nonsteady equation for mildly supersonic flow past thin blades with a superposition of isolated blade and interference potentials represented as trigonometric series. See also Samoylovich [Ref. 22]. Elder [Ref. 7] revised Gorelov's Collocation technique by using a power series and solved for the steady sonic flow cascade potential and the coefficients of the series for the nonsteady flow, out-of-phase oscillation case. Elder made use of the Oswatitsch [Ref. 20] parameter (used by Oswatitsch for

steady flows), as extended by Teipel [Ref. 30] and Hosokawa [Ref. 11] for nonsteady flows, to allow for blades of nonzero thickness (nonuniform steady potential flow).

Sonic wind tunnel interference in steady flow was solved by Sandeman [Ref. 23] using Spreiter's local linearization technique, this after Guderley [Ref. 9] and Spreiter et al [Ref. 27] showed that the choked tunnel results can be corrected so as to simulate unbounded flows. Murasaki [Ref. 18] solved steady transonic tunnel flows for porous or slotted walls. Miles [Ref. 17] and Drake [Ref. 5] solved the supersonic nonsteady solid and porous wall cases, respectively. Drake [Ref. 6], then, utilized Laplace Transform techniques and the linear potential equation for a thin airfoil between porous walls for transonic flows. Recently, Savkar [Ref. 24] has Laplaced transformed the linearized equation and studied airfoil stability in a solid walled wind tunnel.

Wind tunnel interference can be approached, according to Sears [Ref. 25], with suitably located sensors within the test section (not on the model) and variable wall shape or porosity and/or plenum pressure behind the wall. The sensors would modify the tunnel parameters until unbounded flow conditions were present at them. Sears argued that unbounded flow conditions are thus obtainable upon the model.

This work began with the object of applying a Collocation technique to the porous wall wind tunnel problem with the conviction that that method could suitably handle the classically

difficult porous wall boundary condition. While proceeding toward that goal, an efficient approximate solution was developed for studying the aerodynamic stability of the sonic oscillating cascade and stability boundaries were calculated for the cascade as well as for a biplanar configuration.

To accomplish the initial objective of this work, the nonsteady potential equation was reduced with the aforementioned Oswatitsch parameter to approximate the variable coefficient therein. The resulting reduced equation was solved by a Collocation technique for the cascade problem following Elder [Ref. 7]. For numerical checks upon the Collocation technique, the equation was Laplace transformed extending the steady flow work of Sandeman [Ref. 23] and Fourier transformed in a manner analogous to Hamamato [Ref. 10]. These extensions were made flexible enough to handle blade thickness variations (through the Oswatitsch parameter) and variable interblade phase angle.

The Elder power series initially utilized in the Collocation solutions to the cascade problem was found to have numerical difficulties that increased computation time requirements and reduced accuracy. Thus, a 'step-wise-linear' series was introduced and the resulting Collocation method solution to the cascade problem agreed well enough with the other two solutions to allow some confidence in its subsequent adaptation to the porous wall wind tunnel problem.

The Collocation solution was found to be quite flexible. It can be altered to allow streamwise variation of the Oswatitsch parameter, in a manner reminiscent of Spreiter's local linearization, to improve accuracy. Further, it allows a variation in wall porosity for possible simulation of the technique mentioned by Sears.

II. UNSTEADY TRANSONIC FLOW THEORY

A. EQUATIONS FOR GENERAL OSCILLATORY MOTION

The governing equation considered below arises from the assumption that the flows of interest are of frictionless perfect gas. Thence, the equation of state and Eulerian equations of motion are invoked and simplified, assuming the absence of heat conduction and strong shock processes. Further, a velocity potential is introduced which reduces the number of dependent variables at the imposition of the requirement of flow irrotationality. Finally, a small disturbance analysis, including the unique properties of transonic flows (see Refs. 12 and 13), yields, in two dimensions

$$\phi_{TT} + 2\phi_{XT} + \left[1 - \frac{1}{M^2} + (\gamma+1)\phi_X\right]\phi_{XX} - \frac{1}{M^2}\phi_{YY} = 0. \qquad \text{(II-1)}$$

This equation is applicable, approximately, to flows containing weak shocks, incidentally (see Ref. 13).

In the study of unsteady aerodynamics, it is customary and convenient to expand the solution into steady and oscillatory nonsteady components. Thus,

$$\phi(X,Y,T) = \overline{\phi}(X,Y) + \text{R.P.}[\psi(X,Y)e^{iKT}], \qquad \text{(II-2)}$$

where K is the reduced frequency.

Substitution in equation (II-1) yields a coupled partial differential equation,

$$(1-M^2)\psi_{XX} + \psi_{YY} - M^2(\gamma+1)[\psi_X\psi_{XX} + \bar{\phi}_X\psi_{XX} + \bar{\phi}_{XX}\psi_X] + M^2K^2\psi - 2iM^2K\psi_X = 0. \qquad \text{(II-3)}$$

This equation is nonlinear, of mixed elliptic-hyperbolic type, and contains variable coefficients. However, because flutter analysis is, generally, concerned with the stability of small perturbations about a steady flow, it is appropriate to assume that the oscillatory nonsteady component is small compared to the steady flow potential. Thus, the governing equation becomes

$$(1-M^2)\psi_{XX} + \psi_{YY} - M^2(\gamma+1)[\bar{\phi}_X\psi_{XX} + \bar{\phi}_{XX}\psi_X] - 2iM^2K\psi_X + M^2K^2\psi = 0, \qquad \text{(II-4)}$$

with the usual nonlinear steady flow equation also resulting. Equation (II-4), though linear, retains variable coefficients dependent upon the steady flow solution, the nature of which (subsonic or supersonic) determines its type (elliptic or hyperbolic).

B. REDUCTION OF THE GOVERNING EQUATION

First, the reference Mach number shall be unity, reducing equation (II-4) to

$$\psi_{YY} - (\gamma+1)[\bar{\phi}_X\psi_{XX} + \bar{\phi}_{XX}\psi_X] - 2iK\psi_X + K^2\psi = 0. \qquad \text{(II-5)}$$

Second, the approach taken by Teipel [Ref. 30] and Hosokawa [Ref. 11] is utilized. That is, the nonconstant coefficients on ψ_{XX} and ψ_X are approximated as follows. First, the steady flow velocity perturbation is assumed to be small in the X direction, implying that the airfoil or blade is of small thickness,

$$\bar{\phi}_X \tilde{-} 0. \qquad \text{(II-6)}$$

Second, the steady flow fluid acceleration over the airfoil or blade is assumed to be a constant (parabolic arc airfoils exhibit nearly this characteristic), which allows the introduction of the Oswatitsch parameter

$$\lambda = (\gamma+1)\bar{\phi}_{XX} = \text{constant} > 0. \qquad \text{(II-7)}$$

The Oswatitsch parameter was originated by Oswatitsch and Keune [Ref. 20] for steady flow, incidentally. Thus, the governing equation has, finally, become

$$\psi_{YY} - (\lambda+2iK)\psi_X + K^2\psi = 0. \qquad \text{(II-8)}$$

Note that this equation is of the parabolic type.

C. BOUNDARY CONDITIONS

1. Flow Tangency

The usual surface boundary condition is

$$\frac{DF}{DT} = 0, \quad \text{on} \quad F(X,Y,T), \tag{II-9}$$

where F(X,Y,T) describes the surface of a body moving as a function of time. The boundary condition requires flow tangency, that is the total derivative of F is zero. Then, considering a thin airfoil restricted to vanishingly small amplitude out of plane oscillations (recall the small nonsteady potential argument), its upper and lower surfaces can be described by

$$\begin{aligned} F_u(X,Y,T) &= Y - H_u(X,T), \\ F_\ell(X,Y,T) &= Y - H_\ell(X,T), \end{aligned} \tag{II-10}$$

where

$$H_u(X,T) = \tau\bar{h}_u(X) + R.P.[h_u(X)e^{iKT}] \ . \tag{II-11}$$

With the definition of $\phi(X,Y,T)$ from equation (II-2) and H(X,Y,T) from above, the linearized flow tangency condition becomes

$$\psi_Y(X,0\pm) = \frac{\partial h(X)}{\partial X} + iKh(X). \qquad \text{(II-12)}$$

2. Zero Upstream Disturbance

The governing equation has become parabolic as shown by equation (II-8), requiring, upstream of the leading edges,

$$\psi(X,Y) = 0. \qquad \text{(II-13)}$$

III. FORMULATION OF SOLUTIONS

A. SOLUTION THROUGH THE LAPLACE TRANSFORMATION

1. Cascade Geometry and Boundary Conditions

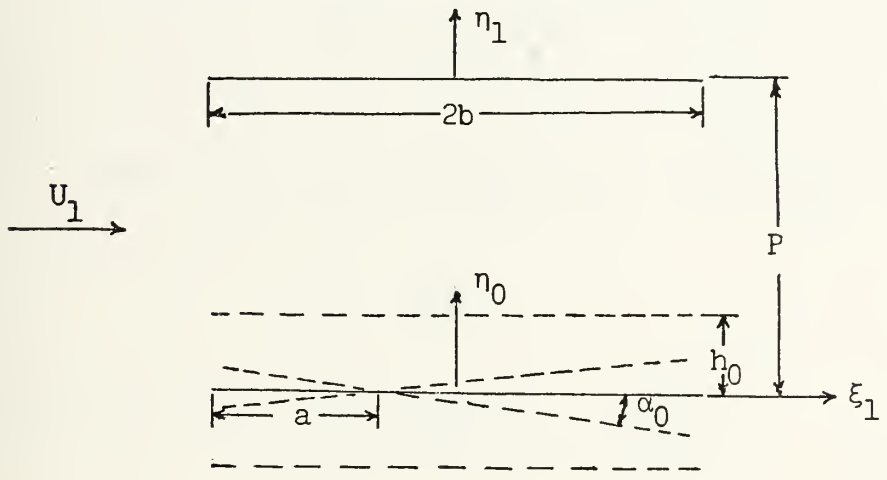

Fig. 1. Unstaggered Cascade.

Consider a pair of the parabolic arc airfoils or blades in an infinite unstaggered cascade (row) immersed within a transonic flow field. The blade chord is 2b, inter-blade spacing is P, the lower blade is the reference blade (variables associated with it are subscripted, zero), and the upper is referred to as the adjacent blade (subscript, one). The coordinate reference is fixed to the reference blade midchord for consistency with Teipel [Ref. 30] with whose work comparisons were made. Pitch and plunge ocsillations can be described, pitch axis at a, magnitude of pitch α_0, of plunge h_o. The adjacent blade performs a harmonic

pitch/plunge oscillation arbitrarily phased with the oscillation of the reference blade.

Two η coordinates are specified, with η_0 and η_1 related such that

$$\eta_1 = \eta_0 + P. \tag{III-1}$$

The following nondimensional variables are defined:

$$\begin{aligned} X &= \frac{\xi_1}{b} , \\ Y_m &= \frac{\eta_m}{b} , \quad m = 0,1, \\ \rho &= \frac{P}{b} , \\ X_0 &= \frac{a}{b} , \\ h_1 &= \frac{h_0}{b} . \end{aligned} \tag{III-2}$$

Note that the linear nondimensionalizing parameter will be the blade semichord for all variables in this analysis. Thus, for example, the reduced frequency

$$K = \frac{\omega b}{U_1} . \tag{III-3}$$

From considerations in Section II, the boundary conditions can be expressed, for the reference and adjacent blades, as

$$\psi_Y(X,Y_0=0) = v_0(X) = \frac{\partial h_u}{\partial X} + iKh_u \ , \qquad \text{(III-4)}$$

and

$$\psi_Y(X,Y_0=\rho) = v_1(X) = e^{i\sigma}v_0(X) \ , \qquad \text{(III-5)}$$

where σ is the interblade phase angle.

Then, for pitch and plunge of small magnitude

$$v_o(X) = - \alpha_0[1+iK(X-X_0] + iKh_1. \qquad \text{(III-6)}$$

For computations for the steady flow case, a parabolic arc airfoil is assumed ($Y = \tau(1-X^2)$, see Ref. 30) and

$$v_0(X) = - 2\tau X. \qquad \text{(III-7)}$$

2. Solution of the Oscillatory Sonic Flow Equation

The governing equation from Section II is

$$\psi_{YY} - Q\psi_X + K^2\psi = 0, \qquad \text{(III-8)}$$

where

$$Q = \lambda + 2iK. \tag{III-9}$$

For utilization of the Laplace Transformation define a new streamwise coordinate

$$X_1 = X + 1. \tag{III-10}$$

Denoting the Laplace transformation of a function with respect to X_1 with an overbar, i.e.,

$$\bar{f}(p) = \mathcal{L}[f(X_1)] = \int_0^\infty e^{-pX_1} f(X_1)\, dX_1 , \tag{III-11}$$

transform equation (II-8) to

$$\bar{\psi}_{YY} - \mu^2 \bar{\psi} = 0 , \tag{III-12}$$

where

$$\mu^2 = Qp - K^2. \tag{III-13}$$

The boundary conditions become

$$\bar{\psi}_Y(p,0) = \bar{v}_o(p), \tag{III-14}$$

$$\bar{\psi}_Y(p,\rho) = e^{i\sigma}\bar{v}_0(p). \qquad \text{(III-15)}$$

The solution to equation (III-12) subject to (III-14 and 15) is

$$\bar{\psi}(p,Y) = \frac{\bar{v}_0(p)}{\mu} \frac{e^{i\sigma}\cosh(\mu Y) - \cosh[\mu(Y-\rho)]}{\sinh(\mu\rho)} . \qquad \text{(III-16)}$$

The hyperbolic functions are expanded, as follows, to allow a term by term inversion

$$\frac{1}{\sinh(\mu\rho)} = \frac{2}{(e^{\mu\rho} - e^{-\mu\rho})} = 2e^{-\mu\rho} \sum_{n=0}^{\infty} e^{-2n\mu\rho} , \qquad \text{(III-17)}$$

then

$$\frac{\cosh(\mu Y)}{\sinh(\mu\rho)} = \sum_{n=0}^{\infty} \{ e^{-\mu[-Y+(2n+1)\rho]} + e^{-\mu[Y+(2n+1)\rho]}\}, \qquad \text{(III-18)}$$

and

$$\frac{\cosh[\mu(Y-\rho)]}{\sinh(\mu\rho)} = \sum_{n=0}^{\infty} \{e^{-\mu[2n\rho+2\rho-Y]} + e^{-\mu[2n\rho+Y]}\}. \qquad \text{(III-19)}$$

Thus,

$$\bar{\psi}(p,Y) = \frac{1}{\mu} \sum_{n=0}^{\infty} \{\bar{v}_0(p)e^{i\sigma}[e^{-\mu[-Y+2n\rho+\rho)} + e^{-\mu(Y+2n\rho+\rho)}] \qquad \text{(III-20)}$$

$$-\bar{v}_0(p)[e^{-\mu(-Y+2n\rho+2\rho)} + e^{-\mu(+Y+2n\rho)}]\}.$$

For inversion, recall the formula

$$\int_0^\infty \frac{e^{-pX_1} e^{-\alpha/4X_1}}{\sqrt{X_1}}\, dX_1 = \sqrt{\pi}\, \frac{e^{-\sqrt{\alpha p}}}{\sqrt{p}}\,, \quad \text{R.P.}[p] > 0. \tag{III-21}$$

Utilizing the above formula and the convolution theorem, recognizing that

$$v_0(X_1) = 0, \quad X_1 < 0\,, \tag{III-22}$$

and reintroducing X after inversion, yields

$$\psi(X,Y) = \frac{1}{\sqrt{\pi Q}} \int_{-1}^{X} \frac{e^{\frac{K^2}{Q}(X-S)}}{\sqrt{X-S}} \sum_{n=0}^{\infty} \{v_0(S)e^{i\sigma}[e^{-\frac{Q(2n\rho+\rho-Y)^2}{4(X-S)}} + e^{-\frac{Q(2n\rho+\rho+Y)^2}{4(X-S)}}] - v_0(S)[e^{-\frac{Q(2n\rho+2\rho+Y)^2}{4(X-S)}} + e^{-\frac{Q(2n\rho-Y)^2}{4(X-S)}}]\}dS. \tag{III-23}$$

Then, for the potential on the reference blade upper surface,

$$\psi(X,0^+) = \frac{1}{\sqrt{\pi Q}} \int_{-1}^{X} \frac{e^{\frac{K^2}{Q}(X-S)}}{\sqrt{X-S}} \sum_{n=0}^{\infty} \{v_0(S)e^{i\sigma}[2e^{-\frac{Q(2n\rho+\rho)^2}{4(X-S)}}] - v_0(S)[e^{-\frac{Q(2n\rho+2\rho)^2}{4(X-S)}} + e^{-\frac{Q(2n\rho)^2}{4(X-S)}}]\}dS. \tag{III-24}$$

This equation was programmed for digital calculation (see Appendix A and Section IV-E).

3. Modification for Sonic Free Jet Problem

The sonic free jet is of interest as an extreme case of wind tunnel wall porosity. That is, the porosity is so great that the wall has vanished and the airfoil is in a sonic jet constrained at its boundaries not by a zero velocity condition but zero pressure differential.

The boundary condition on the reference blade remains the same as before, equation (III-4). The adjacent blade is replaced by the edge of the sonic jet upon which the following pressure perturbation condition is imposed

$$iK\psi(X,Y=\rho) + \psi_X(X,Y=\rho) = 0. \qquad \text{(III-25)}$$

Transforming and substituting as before, the second boundary condition becomes

$$(iK + p)\bar{\psi}(p,\rho) = 0. \qquad \text{(III-26)}$$

Then, using both conditions, the solution to the transformed equation is

$$\bar{\psi}(p,Y) = \frac{v_o(p)}{\mu}\left[\frac{e^{-2\mu\rho}e^{\mu Y} - e^{-\mu Y}}{e^{-2\mu\rho} + 1}\right]$$

$$= \frac{v_o(p)}{\mu}\left[\frac{\sinh[\mu(Y-\rho)]}{\cosh(\mu\rho)}\right]. \qquad \text{(III-27)}$$

With

$$\frac{1}{\cosh(\mu\rho)} = \frac{2e^{-\mu\rho}}{(1+e^{-2\mu\rho})} = 2e^{-\mu\rho} \sum_{n=0}^{\infty} (-1)^n e^{-2n\mu\rho} , \qquad \text{(III-28)}$$

$$\bar{\psi}(p,Y) = \frac{\bar{v}_0(p)}{\mu} \sum_{n=0}^{\infty} (-1)^n \{e^{-\mu(-Y+2n\rho+\rho)} - e^{-\mu[Y+2n\rho]}\}. \qquad \text{(III-29)}$$

The subsequent inversion is similar to that in the previous section.

The result was programmed for digital computation and used as a check case against which the Collocation technique porous wall wind tunnel solution was compared. The Fourier Transformation method (see next section) was also applied to the free jet problem and, by following a derivation similar to that above, it was found that an interblade phase angle of zero in the cascade problem correctly modeled the sonic free jet problem.

B. SOLUTION THROUGH THE FOURIER TRANSFORMATION

1. Cascade Geometry and Boundary Conditions

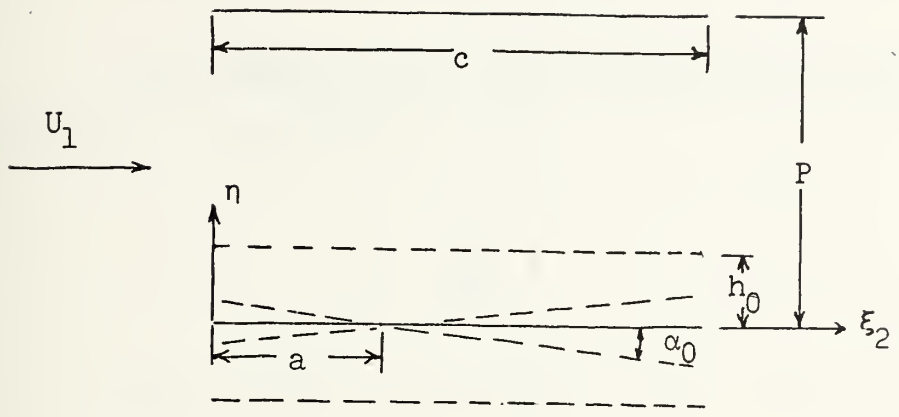

Fig. 2. Unstaggered Cascade.

The arrangement of the cascade is the same as the previous section, however, the coordinate system is changed to simplify the derivation. The origin of the coordinate system is now fixed to the reference blade leading edge. Blade chord is c.

The following nondimensional variables are defined for this phase of the study:

$$X = \frac{\xi_2}{c} ,$$

$$Y = \frac{\eta}{c} ,$$

$$h = \frac{P}{c} , \qquad \text{(III-30)}$$

$$A_1 = \frac{a}{c} ,$$

$$h_2 = \frac{h_0}{c} .$$

All variables will use c (vice b) for nondimensionalization as appropriate, i.e.,

$$K_1 = \frac{\omega c}{U_1} . \qquad \text{(III-31)}$$

The boundary conditions are the same as those expressed in the previous section, though their representation is somewhat different.

$$\psi_Y(X,Y=0) = w(X) ,$$

$$\psi_Y(X,Y=h) = e^{i\sigma} w(X) , \qquad \text{(III-32)}$$

and

$$w(X) = [-1-iK_1(X-A_1)]\alpha_0 + iK_1 h_2 . \qquad \text{(III-33)}$$

2. Transformation of the Sonic Flow Equation

As before, begin with the equation for oscillatory sonic flow from Section II and transform it with the following Fourier Transform,

$$\bar{f}(\nu,Y) = \int_{-\infty}^{+\infty} f(X,Y) e^{i\nu X} \, dX , \qquad \text{(III-34)}$$

Obtain

$$\bar{\psi}_{YY} + \mu^2\bar{\psi} = 0 \ , \qquad \text{(III-35)}$$

and

$$\mu^2 = - i\lambda\nu + 2K_1\nu + K_1{}^2. \qquad \text{(III-36)}$$

This equation is satisfied by

$$\bar{\psi}(\nu,Y) = E_1 e^{i\mu Y} + F_1 e^{-i\mu Y} \ . \qquad \text{(III-37)}$$

Using equation (III-32)

$$\bar{\psi}_Y(\nu,h) = e^{i\sigma}\bar{\psi}_Y(\nu,0) \ ,$$

$$E_1[e^{i\mu h} - e^{i\sigma}] = F_1[e^{-i\mu h} - e^{i\sigma}] \ ,$$

or

$$E_1 = F_1\left[\frac{1 - e^{-i\sigma}e^{i\mu h}}{1 - e^{-i\sigma}e^{-i\mu h}}\right] \ . \qquad \text{(III-38)}$$

Then, with

$$\bar{\psi}_Y(\nu,0) = \bar{w}(\nu),$$

E_1 and F_1 become

$$E_1 = \frac{\bar{w}(\nu)}{i\mu e^{i\sigma}} \left[\frac{1 - e^{-i\sigma} e^{-i\mu h}}{e^{i\mu h} - e^{-i\mu h}}\right] ,$$

and

$$F_1 = \frac{\bar{w}(\nu)}{i\mu e^{i\sigma}} \left[\frac{1 - e^{-i\sigma} e^{i\mu h}}{e^{i\mu h} - e^{-i\mu h}}\right].$$

Finally,

$$\bar{\psi}(\nu,Y) = \frac{\bar{w}(\nu)}{i\mu e^{i\sigma}} \left[\frac{(1-e^{-i\sigma}e^{-i\mu h})e^{i\mu Y} + (1-e^{-i\sigma}e^{i\mu h})e^{-i\mu Y}}{e^{i\mu h} - e^{-i\mu h}}\right] . \qquad \text{(III-39)}$$

Because the pressures on the reference blade are of interest, set Y = 0. With

$$\cos \alpha = \frac{e^{i\alpha} + e^{-i\alpha}}{2} , \qquad \sin \alpha = \frac{e^{i\alpha} - e^{-i\alpha}}{2} ,$$

and

$$\cos 2\alpha = \frac{1 - \tan^2\alpha}{1 + \tan^2\alpha}, \qquad \sin 2\alpha = \frac{2 \tan \alpha}{1 + \tan^2\alpha} ,$$

then

$$\bar{\psi}(\nu,0) = - \frac{\bar{w}(\nu)}{\mu e^{i\sigma}} \left[\frac{2(1-e^{-i\sigma}) + 2(1+e^{-i\sigma})\tan^2 \frac{\mu h}{2}}{4\tan \frac{\mu h}{2}}\right] ,$$

or

$$\bar{\psi}(\nu,0) = -\frac{\bar{w}(\nu)}{\mu}\left[\left(\frac{e^{i\sigma}-1}{2}\right)\cot\frac{\mu h}{2} + \left(\frac{e^{i\sigma}+1}{2}\right)\tan\frac{\mu h}{2}\right]. \qquad \text{(III-40)}$$

It can be shown that equations (III-16) and (III-40) are equivalent and in this sense the two solutions are not independent. However, the inversions are substantially different. The following stems from the work of Hamamoto [Ref. 10] and, apparently, arises from observations of abstract complex variable theory. It differs from standard Fourier Transform inversion techniques and leads to a very computationally convenient result. A further method of inversion, utilizing the Theorem of Residues, was considered and is discussed in Section V-C.

3. Inversion

In order to simplify the inversion of equation (III-40), S_N and T_N will be introduced and evaluated in a subsequent section.

Define S_0 and T_0 as follows,

$$S_0(X) = \frac{1}{2\pi}\int_{-\infty}^{+\infty}\frac{1}{\mu}\tan\frac{\mu h}{2}\, e^{i\nu X}\, dX, \qquad \text{(III-41)}$$

and

$$T_0(X) = \frac{1}{2\pi}\int_{-\infty}^{+\infty}\frac{1}{\mu}\cot\frac{\mu h}{2}\, e^{i\nu X}\, dX. \qquad \text{(III-42)}$$

Also

$$S_{N+1}(\phi) = \int_0^{\phi} S_N(\eta)\, d\eta, \tag{III-43}$$

and

$$T_{N+1}(\phi) = \int_0^{\phi} T_N(\eta)\, d\eta. \tag{III-44}$$

Using the convolution theorem and recognizing that

$$w(X) = 0, \quad \psi(X,Y) = 0, \quad X < 0, \tag{III-45}$$

yields

$$\psi(X,0) = -\int_0^X w(X-\phi)\left[\left(\frac{e^{i\sigma}-1}{2}\right)T_0(\phi) + \left(\frac{e^{i\sigma}+1}{2}\right)S_0(\phi)\right] d\phi. \tag{III-46}$$

Integrate by parts to obtain

$$\psi(X,0) = -\{w(0)[D\cdot T_1(X) + B\cdot S_1(X)] + \int_0^X w(X-\phi)[D\cdot T_1(\phi) + B\cdot S_1(\phi)]\, d\phi\}, \tag{III-47}$$

where

$$B = \frac{e^{i\sigma} - 1}{2}, \qquad D = \frac{e^{i\sigma} + 1}{2}. \tag{III-48}$$

4. Calculation of Lift and Moment Coefficients

This approximate solution of the sonic unsteady cascade problem (III-47) was found to be quite efficient in its usage of computer time. Thus, it was extended, as follows, to calculate pressure, lift, and moment coefficients in addition to velocity potential.

Since

$$C_p(X,0) = -2[\psi_X(X,0) + iK_1\psi(X,0)] , \qquad \text{(III-49)}$$

and

$$C_L = -2 \int_0^1 C_p(X,0)\, dX , \qquad \text{(III-50)}$$

then

$$C_L = 4 \int_0^1 [\psi_X(X,0) + iK_1\psi(X,0)]\, dX$$

$$= 4[\int_0^1 \psi_X(X,0)\, dX + iK_1 \int_0^1 \psi(X,0)\, dX]. \qquad \text{(III-51)}$$

With the previously defined ψ and $w(X)$, and the following definition

$$\int_0^1 \psi(X,0)dX = F_2(1) = -\{(-1+iK_1A_1)[D\cdot T_2(1)+B\cdot S_2(1)]$$

$$-iK_1[D\cdot T_3(1)+B\cdot S_3(1)]\} , \qquad \text{(III-52)}$$

the lift is

$$C_L = 4[\psi(1,0) + iK_1F_2(1)].$$

For the moment coefficient

$$C_M = 2\int_0^1 (X-A_1)\, C_P(X,0)\, dX$$

$$= -4[iK_1 \int_0^1 X\psi(X,0)dX + \int_0^1 X\psi_X(X,0)dX] + A_1 \cdot C_L. \qquad \text{(III-54)}$$

Integrating by parts and continuing the notation started above

$$C_M = -4\{-iK_1[F_2(1)-F_3(1)] + [\psi(1,0)-F_2(1)]\} + A_1 \cdot C_L. \qquad \text{(III-55)}$$

5. Solutions for S_N and T_N

Because $S_0(X)$ and $T_0(X)$ are difficult to evaluate directly, $I(X)$ and $J(X)$ will be defined and calculated. It will be seen that $I(X)$ and $J(X)$ are $S_1(X)$ and $T_1(X)$, respectively, from which all S_N and T_N can be obtained.

Define

$$I(X) = \frac{1}{2\pi i} \int_{-\infty}^{+\infty} \frac{e^{i\nu X}}{\mu\nu} \tan\frac{\mu h}{2}\, d\nu. \qquad \text{(III-56)}$$

Since [Ref. 12]

$$\tan \frac{\pi X}{2} = \sum_{m=0}^{\infty} \frac{4X}{(2m+1)^2 - X^2} ,$$

with

$$\frac{\pi X}{2} = \frac{\mu h}{2} , \quad X = \frac{\mu h}{\pi} , \quad m = n-1,$$

$$\frac{1}{\mu} \tan \frac{\pi h}{2} = - \frac{1}{h} \sum_{n=1}^{\infty} \frac{1}{(\frac{\mu}{2})^2 - (\frac{2n-1}{2})^2 \frac{\pi^2}{h^2}} ,$$

then

$$I(X) = - \frac{1}{2\pi i} \int_{-\infty}^{+\infty} \frac{e^{i\nu X}}{\nu h} [\sum_{n=1}^{\infty} \frac{1}{(\frac{\mu}{2})^2 - (\frac{2n-1}{2})^2 \frac{\pi^2}{h^2}}] \, d\nu .$$

Substitute for μ, using equation (III-35) in the bracket

$$\frac{1}{2} \sum_{n=1}^{\infty} \frac{1}{\frac{-i\lambda\nu + 2K_1\nu + K_1^2}{4} - (\frac{2n-1}{2})^2 \frac{\pi^2}{h^2}} = \frac{1}{K_1} \sum_{n=1}^{\infty} \frac{1}{(1-\frac{i\lambda}{2K_1})(\nu-\nu_n)} ,$$

$$\nu_n = [\frac{(2n-1)^2\pi^2}{h^2} - K_1^2]/[2K_1 - i\lambda] , \qquad \text{(III-57)}$$

so

$$I(X) = - \frac{1}{i\pi h} (\frac{1}{2K_1 - i\lambda}) \sum_{n=1}^{\infty} \int_{-\infty}^{+\infty} \frac{e^{i\nu X}}{\nu(\nu-\nu_n)} \, d\nu . \qquad \text{(III-58)}$$

Now define

$$J(X) = \frac{1}{2\pi i} \int_{-\infty}^{+\infty} \frac{e^{i\nu X}}{\mu\nu} \cot \frac{\mu h}{2} \, d\nu. \qquad \text{(III-59)}$$

With [Ref. 12]

$$\pi X \cot \pi X = 1 + 2X^2 \sum_{m=1}^{\infty} \frac{1}{X^2 - \nu^2} ,$$

obtain

$$J(X) = \frac{1}{2\pi i} \int_{-\infty}^{+\infty} \frac{e^{i\nu X}}{\nu h} \left[\frac{2}{\mu^2} + \sum_{n=2}^{\infty} \frac{1}{(\frac{\mu}{2})^2 - \frac{(n-1)^2\pi^2}{h^2}}\right] d\nu.$$

With

$$\eta_n = \left[\frac{4(n-1)^2\pi^2}{h^2} - K_1^2\right]/[2K_1 - i\lambda] , \qquad \text{(III-60)}$$

then

$$J(X) = \frac{1}{i\pi h} \left(\frac{1}{2K_1 - i\lambda}\right) \sum_{n=1}^{\infty} \frac{1}{f} \int_{-\infty}^{+\infty} \frac{e^{i\nu X}}{\nu(\nu-\eta_n)} \, d\nu. \qquad \text{(III-61)}$$

The integral occurring in equations (III-58 and 61) is, from Campbell and Foster [Ref. 4],

$$\int_{-\infty}^{+\infty} \frac{e^{i\nu X}}{\nu(\nu-\nu_n)} \, d\nu = \frac{2\pi i}{\nu_n} \left[e^{i\nu_n X} - 1\right] . \qquad \text{(III-62)}$$

Thence

$$I(X) = \frac{2}{h(2K_1 - i\lambda)} \sum_{n=1}^{\infty} \frac{(1 - e^{i\nu_n X})}{\nu_n} , \qquad \text{(III-63)}$$

and

$$J(X) = \frac{-2}{h(2K_1 - i\lambda)} \sum_{n=1}^{\infty} \frac{1}{f} \frac{(1 - e^{i\eta_n X})}{\eta_n} . \qquad \text{(III-64)}$$

Now, since

$$S_1(\phi) = \int_0^{\phi} S_0(\eta)\, d\eta , \qquad \text{(III-65)}$$

then

$$S_1(\phi) = \frac{1}{2\pi} \int_0^{\phi} \left[\int_{-\infty}^{+\infty} \frac{1}{\mu} \tan \frac{\mu h}{2} e^{i\nu_n \eta} d\nu \right] d\eta$$

$$= \frac{1}{2\pi} \int_{-\infty}^{+\infty} \frac{1}{\mu} \tan \frac{\mu h}{2} \left[\int_0^{\phi} e^{i\nu_n \eta}\, d\eta \right] d\nu .$$

Therefore,

$$S_1(\phi) = I(\phi) . \qquad \text{(III-66)}$$

Similarly

$$T_1(\phi) = J(\phi) . \qquad \text{(III-67)}$$

Thus,

$$S_1(X) = \frac{2}{h(2K_1-i\lambda)} \sum_{n=1}^{\infty} \frac{1}{\nu_n}[1 - e^{i\nu_n X}] , \qquad \text{(III-68)}$$

and

$$S_2(X) = \int_0^X S_1(\eta)\, d\eta, \qquad \text{(III-69)}$$

so

$$S_2(X) = \frac{2}{h(2K_1-i\lambda)} \sum_{n=1}^{\infty} \frac{1}{\nu_n} \int_0^X [1 - e^{i\nu_n \eta}]\, d\eta$$

$$= \frac{2}{h(2K_1-i\lambda)} \sum_{n=1}^{\infty} \frac{1}{\nu_n} \{X + \frac{i}{\nu_n}[e^{i\nu_n X} - 1]\}, \qquad \text{(III-70)}$$

etc., and likewise for T_N.

C. SOLUTION THROUGH COLLOCATION TECHNIQUE

Utilizing the same geometry, nondimensionalization, and boundary conditions as for the first portion of Section III, the boundary value problem is solved by assuming the potential function is a summation,

$$\psi(X,Y) = \phi_0^0(X,Y) + \phi_0(X,Y) + \phi_1^0(X,Y) + \phi_1(X,Y) , \qquad \text{(III-71)}$$

where ϕ_0^0 and ϕ_1^0 are the isolated blade potential solutions and ϕ_0 and ϕ_1, are the interference potentials for the reference and adjacent blades.

Such an approach was proposed by Gorelov [Ref. 8] for sub/supersonic flows. See also Samoylovich [Ref. 21].

Utilizing the boundary conditions and the known source distributions

$$\phi^0_{mY}(X,0) = v_m(X) \ , \qquad m = 0,1 \ , \tag{III-72}$$

obtain two equations

$$\phi_{0Y}(X,Y_0=0) + \phi^0_{1Y}(X,Y_1=-\rho) + \phi_{1Y}(X,Y_1=-\rho) = 0$$

Reference Blade, (III-73)

$$\phi^0_{0Y}(X,Y_0=\rho) + \phi_{0Y}(X,Y_0=\rho) + \phi_{1Y}(X,Y_1=0) = 0$$

Adjacent Blade. (III-74)

The isolated blade solution is already known from Teipel [Ref. 30] so

$$\phi^0_0(X,Y_0) = -\frac{1}{\sqrt{\pi Q}} \int_{-1}^{X} v_0(S) \frac{\mathrm{Exp}[\frac{K^2}{Q}(X-S) - \frac{QY_0^2}{(X-S)}]}{\sqrt{X-S}} \, dS, \tag{III-75}$$

and

$$\phi_1^0(X,Y_1) = \frac{1}{\sqrt{\pi Q}} \int_{-1}^{X} v_1(S) \frac{\mathrm{Exp}[\frac{K^2}{Q}(X-S) - \frac{QY_1^2}{(X-S)}]}{\sqrt{X-S}}\, dS. \qquad \text{(III-76)}$$

It is expected that interference potentials will have the same form but contain unknown source distributions u_0 and u_1. Thus,

$$\phi_0(X,Y_0) = -\frac{1}{\sqrt{\pi Q}} \int_{-1}^{X} u_0(s) \frac{\mathrm{Exp}[\frac{K^2}{Q}(X-S) - \frac{Q}{4}\frac{Y_0^2}{(X-S)}]\, dS}{\sqrt{X-S}}, \qquad \text{(III-77)}$$

and

$$\phi_1(X,Y_1) = \frac{1}{\sqrt{\pi Q}} \int_{-1}^{X} u_1(s) \frac{\mathrm{Exp}[\frac{K^2}{Q}(X-S) - \frac{Q}{4}\frac{Y_1^2}{(X-S)}\, dS}{\sqrt{X-S}}. \qquad \text{(III-78)}$$

It is the fundamental point of this solution to approximate the unknown and known source distributions by series, the coefficients of which are to be determined by satisfying equations (III-73 and 74) at a sufficient number of points on the blades.

Elder [Ref. 7] utilized a power series,

$$u_m(X) = \sum_{n=0}^{L-1} \nu_{mn} X^n , \qquad \text{(III-79)}$$

and

$$v_m(X) = \sum_{n=0}^{\infty} \theta_{mn} X^n , \qquad m = 0,1. \tag{III-80}$$

Elder obtained the coefficients of these series. Expanding upon his methods, this author obtained potentials. For small numbers of collocation points ($L \leq 10$), $\lambda \neq 0$, $K \leq 1$, agreement with the potential calculated by the other methods was generally good. Numerical difficulties above those parameter ranges and, especially, for $\lambda = 0$ led to the introduction of the 'step-wise-linear' series approximation

$$u_m(X) = \nu_{m0} + \nu_{m1} \cdot X + \sum_{n=2}^{L-1} \nu_{mn}(X-X_n)H(X-X_n) , \tag{III-81}$$

and

$$v_m(X) = \theta_{m0} + \theta_{m1} \cdot X + \sum_{n=2}^{L-1} \theta_{mn}(X-X_n)H(X-X_n) , \tag{III-82}$$

where

$$H(z) = \begin{cases} 0 & z < 0 \\ 1 & z \geq 0 . \end{cases} \tag{III-83}$$

The first two terms were necessary to allow for initial value and slope of the source distributions (subsequent coefficients represent changes in that slope at the selected points, XN). Further, they allow simple representations for

the isolated blade source distribution coefficients. For a pitch oscillation about the midchord,

$$v_0(X) = \theta_{00} + \theta_{01} \cdot X \ ,$$

where

$$\theta_{00} = -1 \ , \qquad \theta_{01} = - iK \ , \tag{III-84}$$

and

$$v_1(X) = \theta_{10} + \theta_{11} \cdot X \ ,$$

where

$$\theta_{10} = - e^{i\sigma} \ , \qquad \theta_{11} = - iKe^{i\sigma} . \tag{III-85}$$

Inserting these step-wise-linear approximations into equations (III-75, 76, 77, and 78) and substituting the resulting expressions into the boundary condition equations for each blade (equations III-73 and 74) obtain

$$\nu_{00} + \frac{\rho}{2}\sqrt{\frac{Q}{\pi}}\,\nu_{10}\int_{-1}^{X}\frac{\mathrm{Exp}[\frac{K^2}{Q}(X-S)-\frac{Q}{4}\frac{\rho^2}{(X-S)}]}{(X-S)^{3/2}}\,dS + \nu_{01}\cdot X$$

$$+ \frac{\rho}{2}\sqrt{\frac{Q}{\pi}}\,\nu_{11}\int_{-1}^{X} S\,\frac{\mathrm{Exp}[\frac{K^2}{Q}(X-S)-\frac{Q}{4}\frac{\rho^2}{(X-S)}]}{(X-S)^{3/2}}\,dS + \sum_{n=2}^{\infty}\{\nu_{0n}(X-X_n)H(X-X_n)$$

$$+ \frac{\rho}{2}\sqrt{\frac{Q}{\pi}}\,\nu_{1n}\int_{-1}^{X}\frac{(S-X_n)H(S-X_n)}{(X-S)^{3/2}}\,\mathrm{Exp}[\frac{K^2}{Q}(X-S)-\frac{Q}{4}\frac{\rho^2}{(X-S)}]\,dS\}$$

$$= -\frac{\rho}{2}\sqrt{\frac{Q}{\pi}}\,[\theta_{10}\int_{-1}^{X}\frac{\mathrm{Exp}[\frac{K^2}{Q}(X-S)-\frac{Q}{4}\frac{\rho^2}{(X-S)}]}{(X-S)^{3/2}}\,dS$$

$$+ \theta_{00}\int_{-1}^{X} S\,\frac{\mathrm{Exp}[\frac{K^2}{Q}(X-S)-\frac{Q}{4}\frac{\rho^2}{(X-S)}]}{(X-S)^{3/2}}\,dS]$$

Reference Blade, (III-86)

$$\nu_{10} + \frac{\rho}{2}\sqrt{\frac{Q}{\pi}}\,\nu_{00}\int_{-1}^{X}\frac{\mathrm{Exp}[\frac{K^2}{Q}(X-S)-\frac{Q}{4}\frac{\rho^2}{(X-S)}]\,dS}{(X-S)^{3/2}} + \nu_{11}\cdot X$$

$$+ \frac{\rho}{2}\sqrt{\frac{Q}{\pi}}\,\nu_{01}\int_{-1}^{X} S\,\frac{\mathrm{Exp}[\frac{K^2}{Q}(X-S)-\frac{Q}{4}\frac{\rho^2}{(X-S)}]\,dS}{(X-S)^{3/2}} + \sum_{n=2}^{\infty}\{\nu_{1n}(X-X_n)H(X-X_n)$$

$$+ \frac{\rho}{2}\sqrt{\frac{Q}{\pi}}\,\nu_{0N}\int_{-1}^{X}\frac{(S-X_n)H(S-X_n)}{(X-S)^{3/2}}\,\mathrm{Exp}[\frac{K^2}{Q}(X-S)-\frac{Q}{4}\frac{\rho^2}{(X-S)}]dS\}$$

$$= -\frac{\rho}{2}\sqrt{\frac{Q}{\pi}}\,[\theta_{00}\int_{-1}^{X}\frac{\mathrm{Exp}[\frac{K^2}{Q}(X-S)-\frac{Q}{4}\frac{\rho^2}{(X-S)}]\,dS}{(X-S)^{3/2}}$$

$$+ \theta_{01}\int_{-1}^{X} S\,\frac{\mathrm{Exp}[\frac{K^2}{Q}(X-S)-\frac{Q}{4}\frac{\rho^2}{(X-S)}]\,dS}{(X-S)^{3/2}}]$$

(III-87)

Adjacent Blade.

These equations are satisfied at each collocation point to obtain the unknown coefficients. The coefficients can then be used in the following equation for the potential,

$$\psi(X,Y_0=0) = -\frac{1}{\sqrt{\pi Q}}\{[\theta_{00}+\nu_{00}]\int_{-1}^{X}\frac{\mathrm{Exp}[\frac{K^2}{Q}(X-S)]}{(X-S)^{1/2}}\,dS$$

$$+[\theta_{01}+\nu_{01}]\int_{-1}^{X}\frac{S\,\mathrm{Exp}[\frac{K^2}{Q}(X-S)]}{(X-S)^{1/2}}\,dS$$

$$+\sum_{n=2}^{\infty}\nu_{0n}\int_{-1}^{X}\frac{(S-X_n)H(S-X_n)}{(X-S)^{1/2}}\mathrm{Exp}[\frac{K^2}{Q}(X-S)]\,dS\}$$

$$+\frac{1}{\sqrt{\pi Q}}\{[\theta_{10}+\nu_{10}]\int_{-1}^{X}\frac{\mathrm{Exp}[\frac{K^2}{Q}(X-S)-\frac{Q}{4}\frac{\rho^2}{(X-S)}]}{(X-S)^{1/2}}\,dS$$

$$+[\theta_{11}+\nu_{11}]\int_{-1}^{X}\frac{S\,\mathrm{Exp}[\frac{K^2}{Q}(X-S)-\frac{Q}{4}\frac{\rho^2}{(X-S)}]}{(X-S)^{1/2}}\,dS$$

$$+\sum_{n=2}^{\infty}\nu_{1n}\int_{-1}^{X}\frac{(S-X_n)H(S-X_n)}{(X-S)^{1/2}}\mathrm{Exp}[\frac{K^2}{Q}(X-S)-\frac{Q}{4}\frac{\rho^2}{(X-S)}]dS\}. \qquad \text{(III-88)}$$

D. EVALUATION OF THE INTEGRALS OCCURRING IN EQUATIONS (III-24,86,87 AND 88)

The integrals encountered are of the form

$$I_N = \int_{-1}^{X}\frac{S^N}{(X-S)^{m/2}}\mathrm{Exp}[\frac{K^2}{Q}(X-S)-\frac{QP^2}{(X-S)}]\,dS, \qquad \text{(III-89)}$$

$$N = 0,1; \quad m = 1,3.$$

Introducing the substitution, U = X-S, separating I_N into its real and imaginary parts, and simplifying as did Elder, obtain

$$I_{NR} = \int_0^{X+1} \frac{(X-U)^N}{U^{m/2}} \text{Exp}[\lambda AU - \frac{B}{U}] \cos[2KAU + \frac{E}{U}]\, dU, \qquad \text{(III-90)}$$

and

$$I_{NI} = \int_0^{X+1} \frac{(X-U)^N}{U^{m/2}} \text{Exp}[\lambda AU - \frac{B}{U}] \sin[2KAU + \frac{E}{U}]\, dU, \qquad \text{(III-91)}$$

where

$$I_N = I_{NR} - iI_{NI} \; ; \quad N = 0,1, \qquad \text{(III-92)}$$

$$A = \frac{K^2}{\lambda^2 + 4K^2} \; , \quad B = \frac{\lambda P^2}{4} \; , \quad E = \frac{KP^2}{4} \qquad \text{(III-93)}$$

Then, it is necessary to evaluate six integrals

$$I^R_{N_I} = \int_0^{X+1} U^{j-5/2} \text{Exp}[\lambda AU - \frac{B}{U}] \begin{matrix}\cos \\ \sin\end{matrix}[2KAU + \frac{E}{U}]\, dU, \qquad \text{(III-94)}$$

where j = 1,2,3.

These are four cases of treatment of these integrals:

1. <u>The Steady Case</u>

Setting K = 0 reduces the integrals to a relatively simple case which may be evaluated through the use of the error function or by numerous numerical techniques, one of

which is utilized in the routines described in the Appendices.

2. The Oscillatory Case with $\lambda = 0$

In this case the integrals are of the form,

$$I_{\substack{c\\s}} = \int_0^{X+1} U^{j-5/2} \begin{matrix}\cos\\ \sin\end{matrix}[2KAU+\frac{E}{U}]\, dU, \qquad \text{(III-95)}$$

requiring a distasteful integration near the lower limit for $j < 5/2$, due to the rapid oscillations and increasing magnitude of the integrand there.

To avoid difficulties at the lower limit, the range of integration is dissected, i.e.,

$$\int_0^{X+1} U^{j-5/2} \begin{matrix}\cos\\ \sin\end{matrix}[2KAU+\frac{E}{U}]\, dU = \int_0^{XA} U^{j-5/2} \begin{matrix}\cos\\ \sin\end{matrix}[2KAU+\frac{E}{U}]\, dU$$

$$+ \int_{XA}^{X+1} U^{j-5/2} \begin{matrix}\cos\\ \sin\end{matrix}[2KAU+\frac{E}{U}]\, dU. \qquad \text{(III-96)}$$

The limit XA will be chosen so as to allow the second integral to be evaluated numerically while not greatly affecting accuracy. The first integral, hereafter the 'correction integral', will be approximated in the manner that follows.

Recall

$$\cos[2KAU+\frac{E}{U}] = \cos[2KAU]\cos[\frac{E}{U}] - \sin[2KAU]\sin[\frac{E}{U}],$$

and

$$\sin[2KAU+\frac{E}{U}] = \sin[2KAU]\cos[\frac{E}{U}] + \cos[2KAU]\sin[\frac{E}{U}] ,$$

and, the truncated series expansion

$$\cos[2KAU] \simeq 1 - \frac{(2KAU)^2}{2} ,$$

and

$$\sin[2KAU] \simeq 2KAU - \frac{(2KAU)^3}{6} .$$

Then, for 2KAU sufficiently small

$$\int_0^{XA} U^{j-5/2} \begin{matrix}\cos\\ \sin\end{matrix}[2KAU+\frac{E}{U}]dU = \int_0^{XA} U^{j-5/2} \begin{matrix}\cos\\ \sin\end{matrix}[\frac{E}{U}]\, dU$$

$$\mp (2KA) \int_0^{XA} U^{j-3/2} \begin{matrix}\sin\\ \cos\end{matrix}[\frac{E}{U}]dU - \frac{(2KA)^3}{2} \int_0^{XA} U^{j-1/2} \begin{matrix}\cos\\ \sin\end{matrix}[\frac{E}{U}]dU$$

$$\pm \frac{(2KA)^3}{6} \int_0^{XA} U^{j+1/2} \begin{matrix}\sin\\ \cos\end{matrix}[\frac{E}{U}]\, dU. \qquad \text{(III-97)}$$

Since integrals of the form

$$\int_0^{XA} U^{m/2} \begin{matrix}\cos\\ \sin\end{matrix}[\frac{E}{U}]\, dU \qquad \text{(III-98)}$$

may be expressed in terms of the Fresnel Integrals, the integrals in (III-97) can be calculated after integrating by parts

$$\int_0^{XA} U^{j-5/2} \begin{matrix}\cos\\ \sin\end{matrix}\left[\frac{E}{U}\right]dU = \frac{2}{2j-3}XA^{j-3/2} \begin{matrix}\cos\\ \sin\end{matrix}\left[\frac{E}{XA}\right]$$

$$\mp 2E \int_0^{XA} \frac{U^{j-3/2}}{(2j-3)U^2} \begin{matrix}\sin\\ \cos\end{matrix}\left[\frac{E}{U}\right] dU, \qquad \text{(III-99)}$$

where, $j > 3/2$. From Elder [Ref. 7] for $j = 1$

$$\int_0^{XA} U^{-3/2} \begin{matrix}\cos\\ \sin\end{matrix}\left[\frac{E}{U}\right]dU = \sqrt{\frac{2\pi}{E}}\left[\frac{1}{2} - \begin{matrix}C\\ S\end{matrix}\left(\frac{E}{XA}\right)\right], \qquad \text{(III-100)}$$

where

$$\begin{matrix}C\\ S\end{matrix}\left(\frac{E}{XA}\right) = \int_0^{\frac{E}{XA}} \frac{\begin{matrix}\cos\\ \sin\end{matrix}(t)\, dt}{\sqrt{2\pi t}}. \qquad \text{(III-101)}$$

Then, for $j = 2$

$$\int_0^{XA} U^{-1/2} \begin{matrix}\cos\\ \sin\end{matrix}\left[\frac{E}{U}\right]dU = 2\cdot XA^{-1/2} \begin{matrix}\cos\\ \sin\end{matrix}\left[\frac{E}{XA}\right] \mp 2\cdot E \int_0^{XA} U^{-3/2} \begin{matrix}\sin\\ \cos\end{matrix}\left[\frac{E}{U}\right]dU. \qquad \text{(III-102)}$$

Thus, the correction integrals can be evaluated sequentially on increasing j.

3. The General Case, $K \neq 0$ and $\lambda \neq 0$

In this case, as the lower limit is approached, the exponential function in the integrand is depended upon to drive the integrand magnitude to zero more rapidly than it is magnified by the negative power of U. Thus, that portion of the integral near zero is neglected by specifying a non-zero lower limit for which a negligibly small error is produced while still allowing numerical integration to be utilized.

4. The Case for $P=0$, $j=2$, $K \neq 0$ and $\lambda \neq 0$

For this case, another approach for that portion of the integral near zero must be taken. Due to the absence of the -B/U in the exponential function, that portion cannot be neglected as in part 3., above.

The range of integration is again dissected, a 'correction integral' is defined, and XA is selected similarly to part 2., above. The 'correction integral' integrand is expanded using the series expansions for the functions within and higher order terms in XA neglected. The resulting series is integrated term by term and programmed for correcting the numerically calculated portion of the integral (see Subroutine ZSUM in the Appendices).

E. APPLICATION AND COMPARISON OF SOLUTIONS TO SEVERAL CASCADE PROBLEMS

In order to gain some confidence in the Collocation method solution before extending it to the porous walled sonic wind

tunnel problem, the solutions obtained for sonic cascade interference in the previous sections were programmed for digital computation (see Appendices A-C). They were applied to cascade problems differing in the parameters of interblade phase angle, reduced frequency, Oswatitsch parameter, and interblade distance with pitch oscillations about the cascade blade midchord position. Many of those results are shown in this section to illustrate the ranges of parameter values for which agreement between solutions can or cannot be expected. Because it is the object of this section to illustrate the basic traits of the solutions, especially those of the Collocation method solution, agreement will be considered to be a 5% or so difference.

The complex velocity potentials calculated by the three methods are presented in three sections. First, reduced frequency, Oswatitsch parameter and interblade distance were fixed, the interblade phase angle varied. Second, interblade distance and phase angle were fixed and the remaining parameters varied to illustrate their interrelationship to the agreement between the Collocation and other methods. Third, the interblade phase angle was fixed, the Oswatitsch parameter set to zero (the governing equation is thereby linearized), and the reduced frequency and interblade distance varied to illustrate the difficulties the Collocation method had satisfying the linearized transonic potential equation.

The results shown indicate that the Collocation method, as applied here, agrees reasonably well for lower frequencies and larger Oswatitsch parameter with the other methods. For larger frequency and/or small Oswatitsch parameter, the step-wise-linear series approximations to the then oscillatory source distributions become oscillations whose amplitude may grow substantially from the blade leading edge aft. For cases in which the amplitude growth is large, agreement between the potential calculations of the Collocation method and the others deteriorates. Furthermore, increasing the number of Collocation points fails to improve agreement. Finally, it should be noted that when agreement was poor, the source distribution series approximation yielded an oscillatory result whose amplitude growth was large.

It has been observed that a step-wise-linear series approximation can exhibit this characteristic when numerical errors of sufficient magnitude are present. Further, the effect of increasing the number of Collocation points (and coefficients) is to increase the growth once it was present, as observed above. Numerical errors of substantial magnitude can be traced to the calculation of the integrals (their values are highly damped oscillations along the chord) in the Collocation method solution above.

The failure to produce accurate potentials when an oscillatory series approximation was obtained can be attributed to the large magnitude of the coefficients near the trailing

edge. The resulting potential calculations will then involve the difference of large numbers.

1. Interblade Phase Angle Variation

Table I shows real and imaginary potentials for $K = .10$, $\lambda = .10$, $\rho = 1.0$ and $\sigma = \pi$, $\pi/2$, and 0 radians (recall, $\sigma = \pi$ corresponds to an out-of-phase oscillation of the blades) for the Collocation, Fourier Transform, and Laplace Transform solutions. Further, the Collocation and Fourier methods are shown for $K = .10$, $\lambda = .50$, $\rho = 1.0$, and $\sigma = 0$.

Agreement is seen to be fairly good for $\sigma > 0$. At $\sigma = 0$, the Collocation method fails to agree with the others aft of about $X = -.70$, unable to fit small amplitude imaginary part's oscillation. An increase in thickness (increased Oswatitsch parameter) improves the agreement slightly.

2. Frequency and Thickness Variation

Figure 3 shows the results of potential calculations versus position along the cascade blades described in Section III-A ($-1 \leq X \leq 1$), for Collocation (step-wise-linear series approximation), Fourier Transform, and two cases each of the Laplace Transform and Collocation (power series) methods. Interblade distance, rho, was fixed at one and interblade phase angle, σ, at pi radians (out-of-phase oscillation produces greatest interference). Reduced frequency, K, was given values .01, .1, .3, .5, 1.0, and 1.5. The Oswatitsch parameter, λ, took values .05, .1, .2, and .5. For all but

TABLE I

COMPARISON OF POTENTIAL (REAL/IMAGINARY) CALCULATIONS OF COLLOCATION, FOURIER, AND LAPLACE SOLUTIONS FOR VARIOUS PHASE ANGLES

X	COLLOCATION	FOURIER	LAPLACE
K = 0.10, τ = 0.10, ρ = 1.00			
For σ = 3.10 rad			
-.9	0.391/ -0.946	0.486/ -0.854	0.489/ -0.854
-.7	1.048/ -2.574	1.146/ -2.525	1.150/ -2.527
-.5	1.741/ -4.286	1.827/ -4.196	1.836/ -4.193
-.3	2.426/ -5.937	2.530/ -5.860	2.540/ -5.861
-.1	3.163/ -7.607	3.254/ -7.522	3.264/ -7.508
0.1	3.900/ -9.266	4.000/ -9.180	4.017/ -9.176
0.3	4.672/-10.920	4.768/-10.834	4.782/-10.810
0.5	5.459/-12.570	5.558/-12.486	5.580/-12.480
0.7	6.271/-14.220	6.370/-14.134	6.392/-14.110
0.9	7.104/-15.870	7.204/-15.780	7.209/-15.740
For σ = 1.60 rad			
-.9	0.007/ -0.448	0.092/- 0.404	0.094/ -0.404
-.7	-0.497/ -1.574	-0.425/ -1.605	-0.423/ -1.604
-.5	-1.005/ -2.783	-0.923/ -2.776	-0.918/ -2.776
-.3	-1.503/ -3.927	-1.410/ -3.956	-1.403/ -3.956
-.1	-1.960/ -5.156	-1.883/ -5.144	-1.872/ -5.142
0.1	-2.446/ -6.299	-2.344/ -6.342	-2.334/ -6.343
0.3	-2.865/ -7.589	-2.794/ -7.548	-2.776/ -7.544
0.5	-3.340/ -8.670	-3.228/ -8.764	-3.214/ -8.743
0.7	-3.715/-10.110	-3.652/ -9.990	-3.631/ -9.987
0.9	-4.187/-11.000	-4.064/-11.226	-4.039/-11.210
For σ = 0.0 rad			
-.9	0.505/ -0.064	0.542/ -0.009	0.545/ -0.009
-.7	0.503/ -0.029	0.498/ -0.034	0.500/ -0.035
-.5	0.498/ -0.037	0.499/ -0.025	0.501/ -0.025
-.3	0.507/ 0.002	0.499/ -0.015	0.501/ -0.016
-.1	0.490/ -0.033	0.499/ -0.005	0.501/ -0.006
0.1	0.521/ 0.047	0.499/ 0.005	0.501/ 0.005
0.3	0.466/ -0.052	0.499/ 0.015	0.501/ 0.014
0.5	0.563/ 0.129	0.499/ 0.024	0.501/ 0.024
0.7	0.393/ -0.128	0.499/ 0.034	0.502/ 0.034
0.9	0.686/ 0.296	0.499/ 0.044	0.503/ 0.045

TABLE I (Continued)

X	COLLOCATION	FOURIER	LAPLACE
K = 0.10, τ = 0.50, ρ = 1.00			
For σ = 0.0 rad			
-.9	0.434/ -0.088	0.437/ -0.088	
-.7	0.509/ -0.042	0.500/ -0.039	
-.5	0.489/ -0.024	0.499/ -0.027	
-.3	0.515/ -0.023	0.499/ -0.017	
-.1	0.485/ 0.001	0.499/ -0.007	
0.1	0.520/ -0.009	0.499/ 0.003	
0.3	0.480/ 0.030	0.499/ 0.013	
0.5	0.525/ 0.000	0.499/ 0.023	
0.7	0.476/ 0.063	0.499/ 0.033	
0.9	0.528/ 0.003	0.499/ 0.043	

Fig. 3-c, in which twenty were used, ten potentials were calculated along the blade and those positions were used as node points for the Collocation routines.

Fourier results were machine plotted as a solid curve connecting individual points, which can result in a jagged curve for some parameter combinations because of plotter limitations. Collocation (step-wise-linear) results are plotted as crosses. Laplace Transform calculations were made for $K = .01$, $\lambda = .05$ (computer time usage = 6 minutes) and $K = 1.0$, $\lambda = .1$ (usage = 40 minutes) and plotted as squares. Power series Collocation results were also plotted as squares for $K = \lambda = .1$ (usage = 14 minutes) and $K = .5$, $\lambda = .1$ (usage = 50 minutes). Typical times for similar calculations by Fourier routine are 2-5 seconds and step-wise-linear Collocation, 10-20 seconds. Interestingly, though not surprising considering the method by which integrals were calculated, the Collocation results for 20 points were obtained in slightly less time than 10 points.

Figure 3 is arranged in order of ascending frequency with λ varying at each to show the characteristics of the Collocation method solution. Generally good agreement in the calculation of the interference potentials for all four methods used is shown. Because Fourier and Laplace agree very well at the points shown and for many others not shown, the Fourier solution was concluded to be a good standard. It was further concluded that increasing frequency adversely affects the

accuracy of Collocation results and increasing thickness, as represented by the Oswatitsch parameter, improves it. Furthermore, increasing Collocation points does not necessarily improve accuracy as illustrated by Fig. 3-c compared to Fig. 3-b.

It was observed that in those cases for which relatively poor potential agreement between the Collocation and the other methods was obtained, the step-wise-linear series source distribution approximation was an oscillation whose amplitude grew toward the trailing edge. The coefficients of those series, because they represent the changes in the slope of the approximation, can illustrate the point. For example, for $K = .3$, $\lambda = .05$, which shows good agreement, the first and last coefficients are (real/imaginary) -.7280/1.760 and 1.488/-.0269, respectively. For $K = .5$, $\lambda = .05$, poorer agreement, with -.1357/1.879 and -1.664/-2.942. For $K = 1.0$, $\lambda = .1$, very poor agreement, with 3.549/1.402 and -164.4/-392.7. For $K = .3$ and $\lambda = .1$ and 20 collocation points, poor agreement, with -.4969/3.505 and 1714.0/-2466.0. The same result is seen in the reduction in accuracy shown for $\sigma = 0.0$ in the previous section.

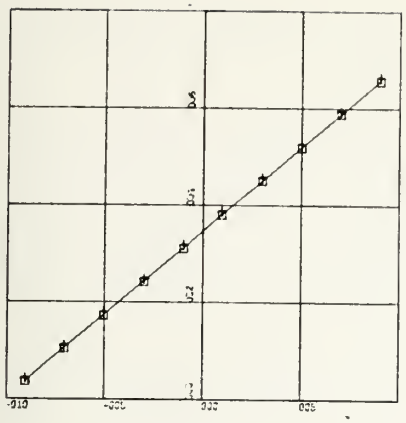

K=.01, λ=.05

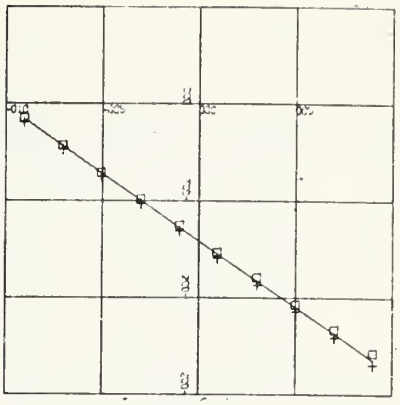

Yscale = 40 units/inch

Yscale = 20 units/inch

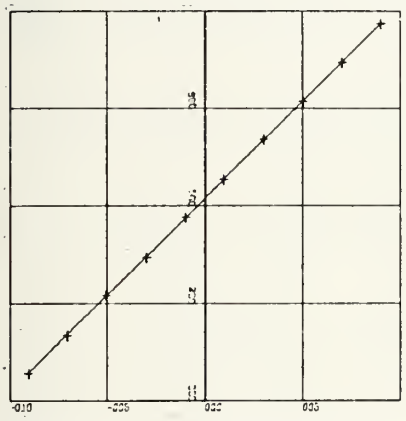

K=.01, λ=.50

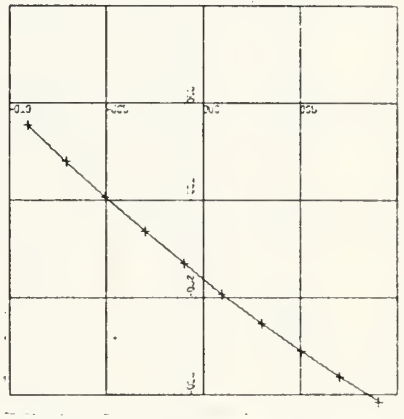

Yscale = 4 units/inch

Yscale = 20 units/inch

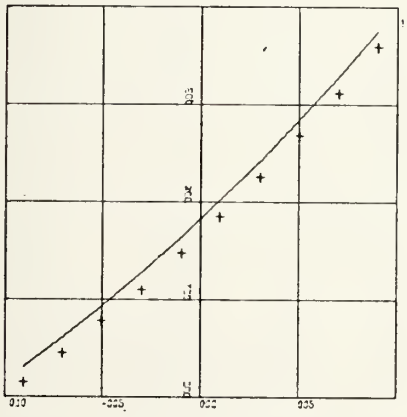

K=.10, λ=.05

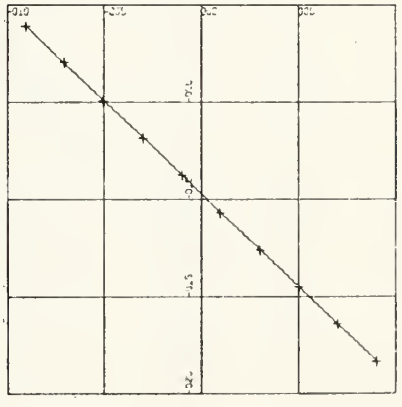

Yscale = 2 units/inch

Real Part

Yscale = 10 units/inch

Imaginary Part

Fig. 3-a. Complex Velocity Potential Comparisons for $\sigma=\pi$ and $\rho=1.0$ with Varying Frequency and Oswatitsch Parameter. Velocity Potential vs. X (1 unit/inch).

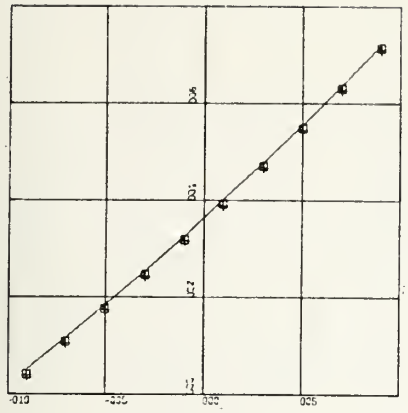

K=.10, λ=.10

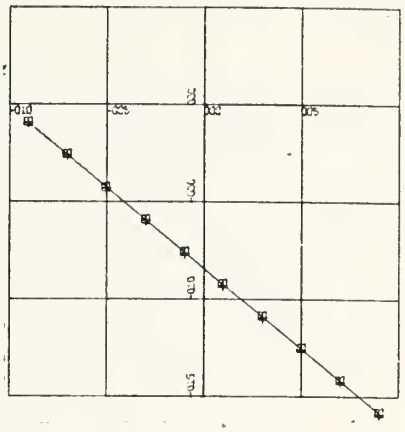

Yscale = 4 units/inch

Yscale = 10 units/inch

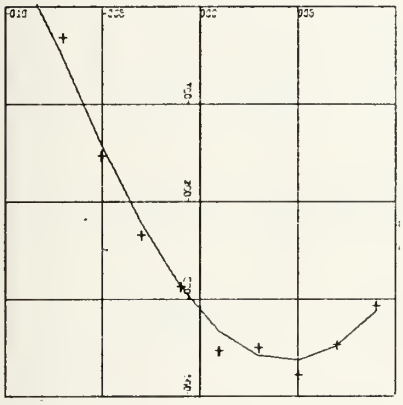

K=.30, λ=.05

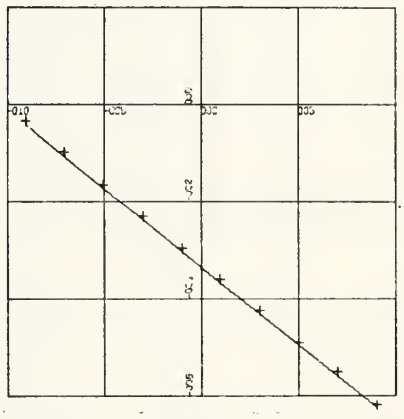

Yscale = .2 units/inch

Yscale = 4 units/inch

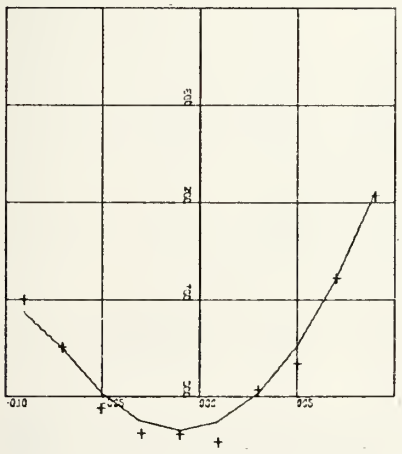

K=.30, λ=.10

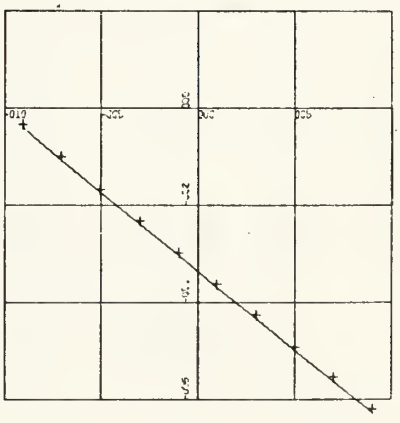

Yscale = .2 units/inch

Yscale = 4 units/inch

Real Part

Imaginary Part

Fig. 3b. Complex Velocity Potential Comparisons for $\sigma=\pi$ and $\rho=1.0$ with Varying Frequency and Oswatitsch Parameter. Velocity Potential vs. X (1 unit/inch).

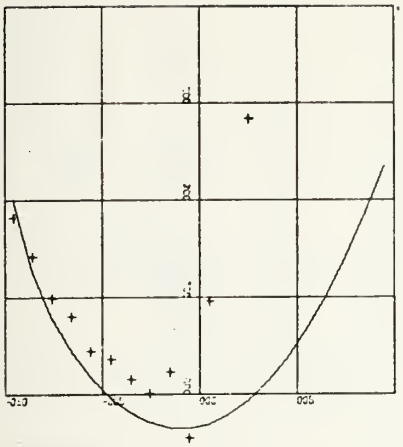

K=.30, λ=.10

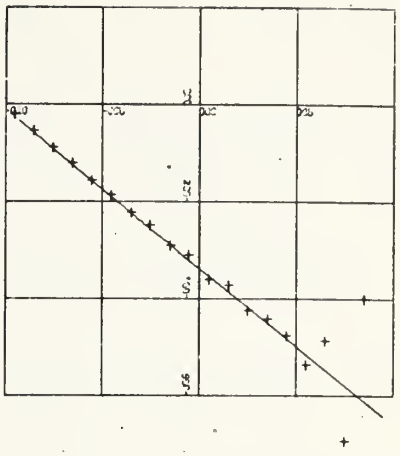

Yscale = .2 units/inch

Yscale = 4 units/inch

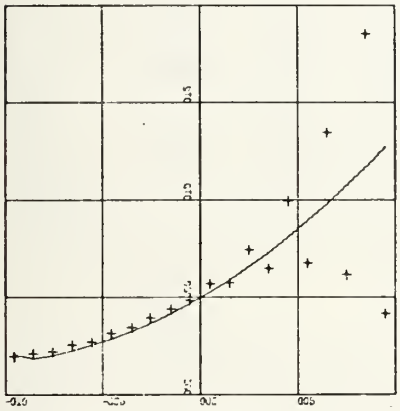

K=.30, λ=.20

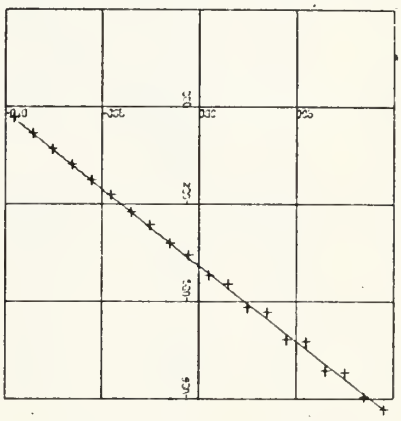

Yscale = 1 unit/inch

Yscale = 4 units/inch

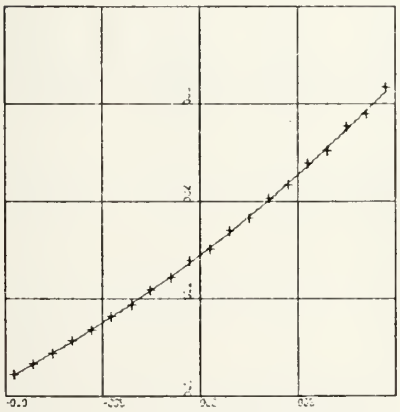

K=.30, λ=.50

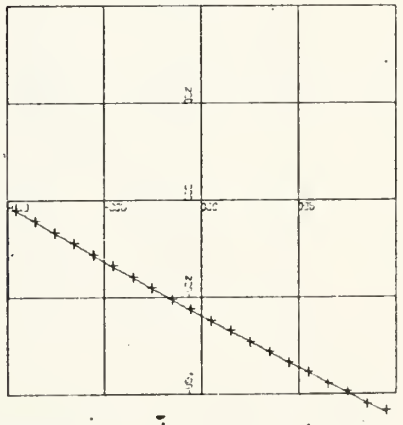

Yscale = 2 units/inch

Yscale = 4 units/inch

Real Part

Imaginary Part

Fig. 3c. Complex Velocity Potential Comparisons for $\sigma=\pi$ and $\rho=1.0$ with Varying Frequency and Oswatitsch Parameter. Velocity Potential vs. X (1 unit/inch).

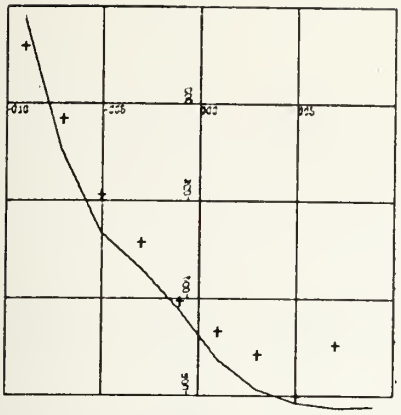

K=.50, λ=.05

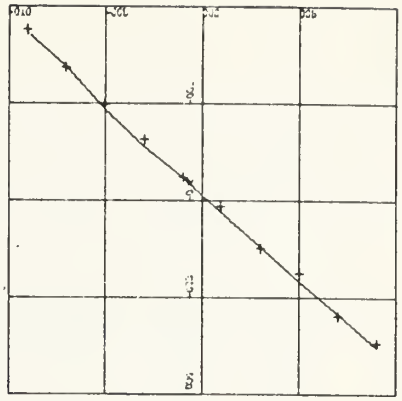

Yscale = .4 units/inch

Yscale = 2 units/inch

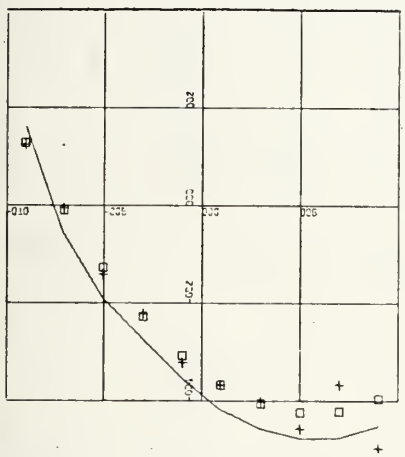

K=.50, λ=.10

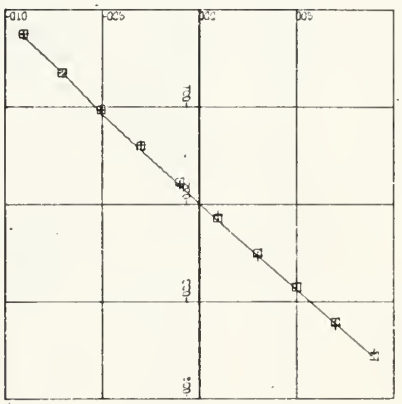

Yscale = .4 units/inch

Yscale = 2 units/inch

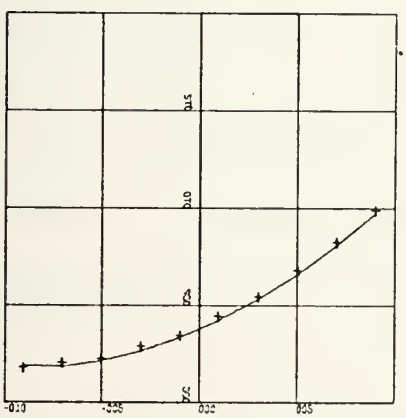

K=.50, λ=.50

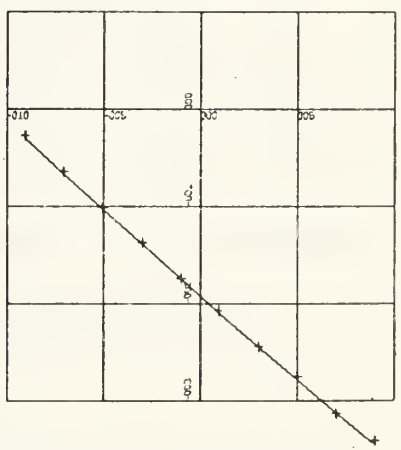

Yscale = 1 unit/inch

Yscale = 2 units/inch

Real Part

Imaginary Part

Fig. 3d. Complex Velocity Potential Comparisons for $\sigma=\pi$ and $\rho=1.0$ with Varying Frequency and Oswatitsch Parameter. Velocity Potential vs. X (1 unit/inch).

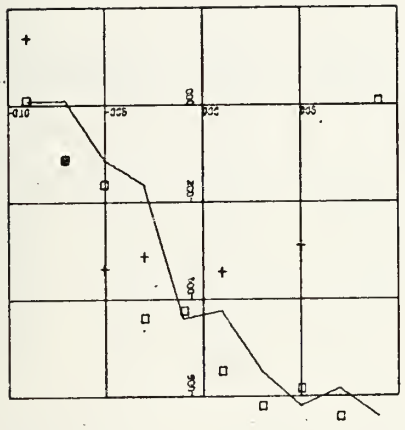

K=1.0, λ=.10

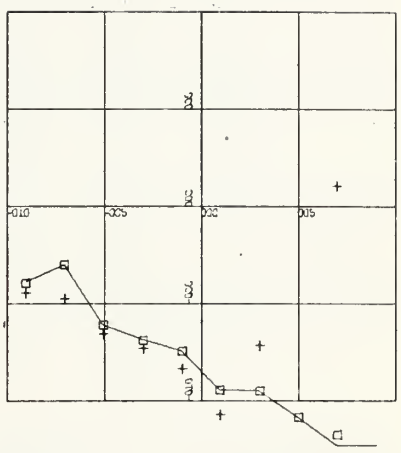

Yscale = .4 units/inch

Yscale = 1 unit/inch

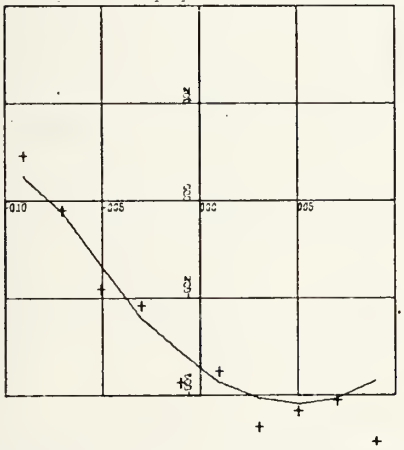

K=1.0, λ=.50

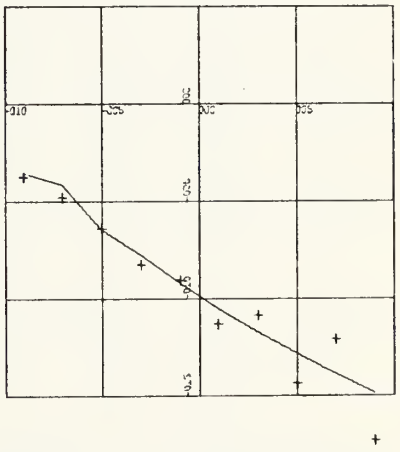

Yscale = .4 units/inch

Yscale = 1 unit/inch

Real Part

Imaginary Part

Fig. 3e. Complex Velocity Potential Comparisons for $\sigma=\pi$ and $\rho=1.0$ with Varying Frequency and Oswatitsch Parameter. Velocity Potential vs. X (1 unit/inch).

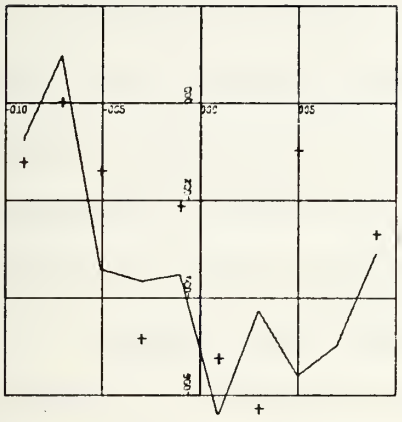

K=1.5, λ=.10

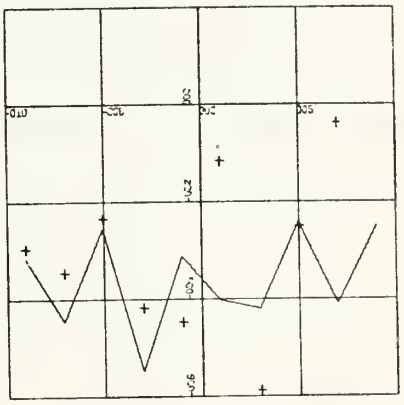

Yscale = .4 units/inch

Yscale = .4 units/inch

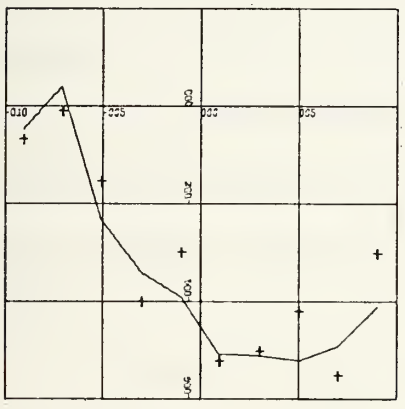

K=1.5, λ=.50

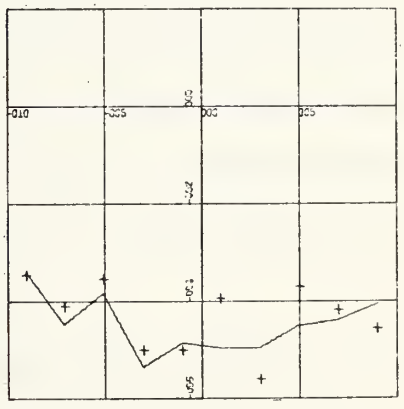

Yscale = .4 units/inch

Yscale = .4 units/inch

Real Part

Imaginary Part

Fig. 3f. Complex Velocity Potential Comparisons for $\sigma=\pi$ and $\rho=1.0$ with Varying Frequency and Oswatitsch Parameter. Velocity Potential vs. X (1 unit/inch).

3. Oswatitsch Parameter = 0.0

Fig. 4 is a compilation of selected interference potential calculations for $\lambda = 0.0$. Because the accuracy of the correction integral technique used in the Collocation method (and Laplace Transform method) (see Appendix A-II), connects accuracy to frequency and interblade spacing, various interblade distances were chosen to illustrate the effect of frequency on the Collocation method solution.

Again, the values of potential are plotted against position, X, along the cascade blade ($-1 \leq X \leq 1$), Fourier Transform results are plotted as a solid line connecting points, Collocation (step-wise-linear series) results are plotted as crosses (except at $\rho = 12$, where Teipel results for an isolated wing are so plotted), and Laplace Transform results are plotted as squares. The number of collocation points varied from ten to twenty, as can be seen from the plots.

Fig. 4-a shows results for interblade distance rho equal to one. For K = .01, the Collocation results were so bad the real parts would not plot on the graph. For K = .1, the real parts of the potentials agreed fairly well. The bottom plots show the effect of increasing the number of points. It is seen again that the Laplace and Fourier Transform solutions agree rather well, as indicated in the few results shown and others not shown.

Fig. 4-b and c show results for $\rho = 4$ (ρ is increased so that frequency can be increased while still attempting to maintain accuracy in the Collocation routine, see Section III-D and Appendix A-II). Agreement is only fair and the conclusion must be drawn that the derivatives of potentials needed for calculations of pressure coefficients, lifts and moments are likely to be very questionable. As in the previous part of this section, large growth of the source distribution approximation amplitude would signal poorer agreement for the Collocation method.

The bottom graphs of Fig. 4-d are for $\rho = 12.0$. The crosses depict potentials calculated by a routine following the work of Teipel for an isolated wing. The convergence of Fourier Transform solution results into isolated wing values for increasing interblade distance will be discussed later. Here, these data further serve to illustrate the applicability of the Fourier Transformation solution.

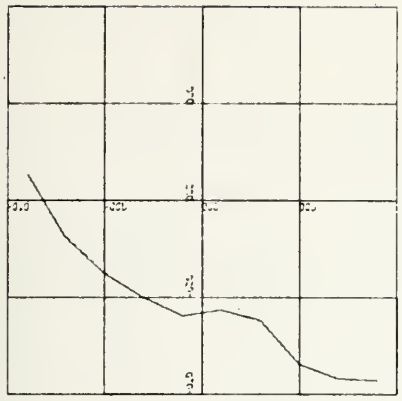

ρ=1.0, K=.01

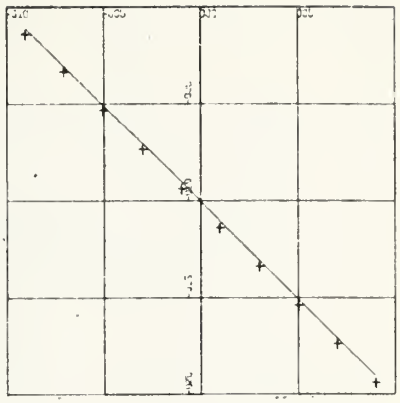

Yscale = 1 unit/inch

Yscale = 100 units/inch

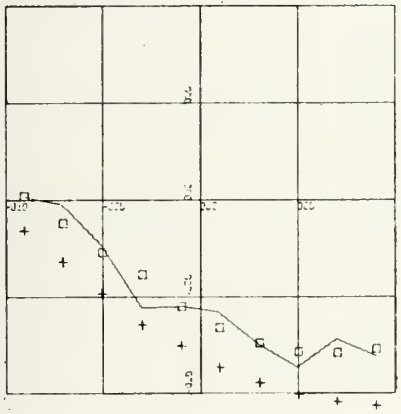

ρ=1.0, K=.10

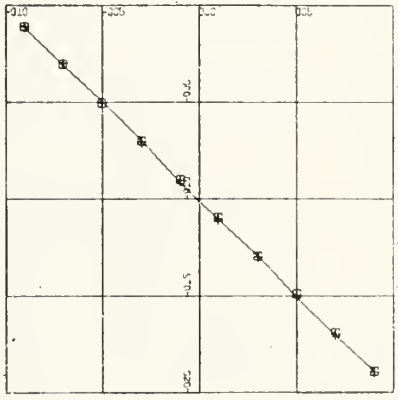

Yscale = 1 unit/inch

Yscale = 10 units/inch

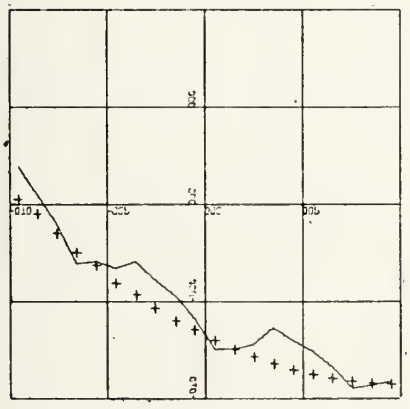

ρ=1.0, K=.10

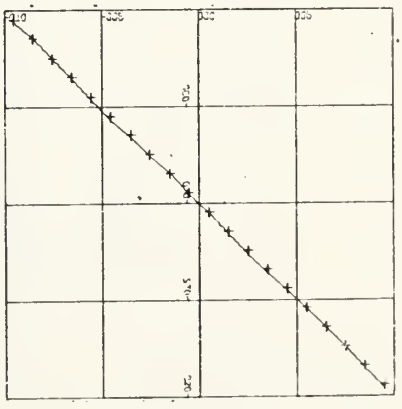

Yscale = 1 unit/inch

Yscale = 10 units/inch

Real Part

Imaginary Part

Fig. 4a. Complex Velocity Potential Comparisons for $\sigma=\pi$ and $\lambda = 0$. Varying Frequency and Interblade Distance. Velocity Potential vs. X (1 unit/inch).

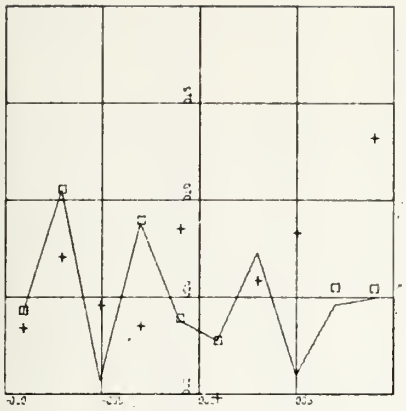

ρ=4.0, K=.10

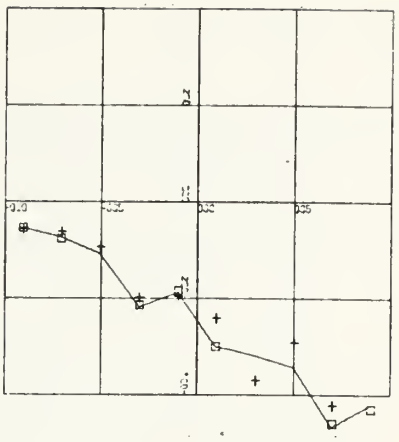

Yscale = 1 unit/inch

Yscale = 4 units/inch

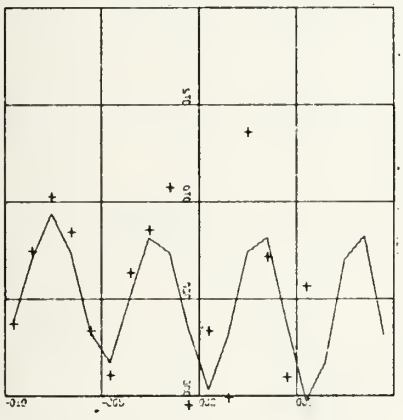

ρ=4.0, K=.10

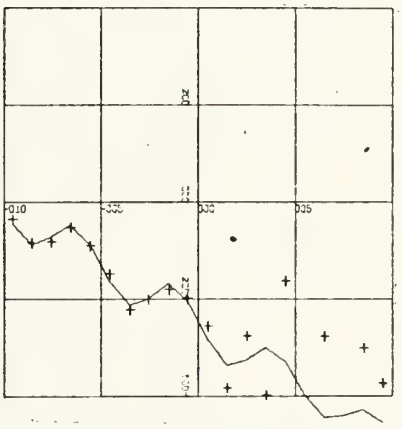

Yscale = 1 unit/inch

Yscale = 4 units/inch

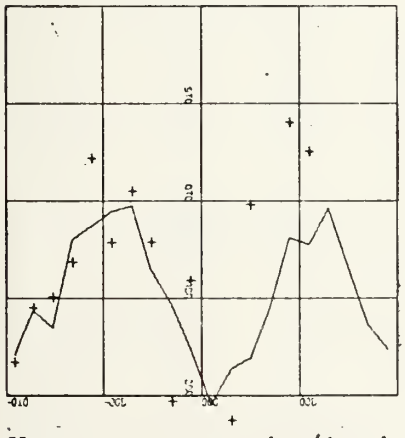

ρ=4.0, K=.20

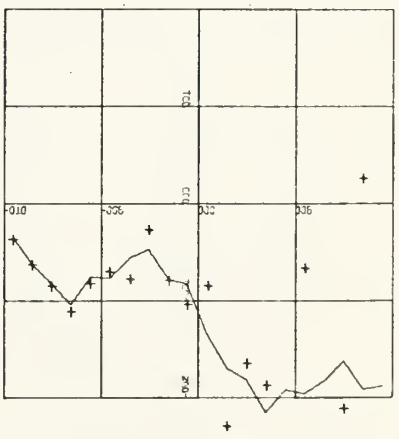

Yscale = 1 unit/inch

Yscale = 2 units/inch

Real Part

Imaginary Part

Fig. 4b. Complex Velocity Potential Comparisons for $\sigma=\pi$ and $\lambda=0$, Varying Frequency and Interblade Distance. Velocity Potential vs. X (1 unit/inch).

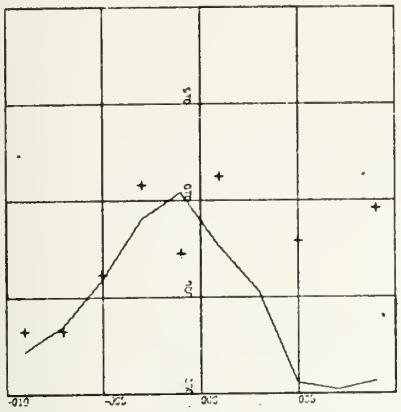

ρ=4.0, K=.30

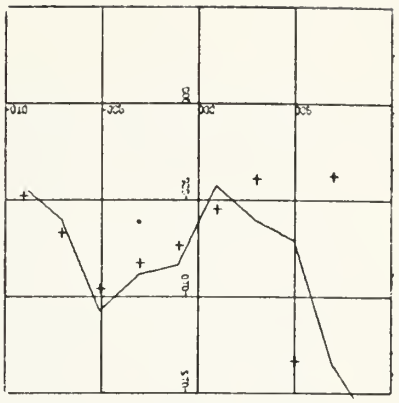

Yscale = 1 unit/inch

Yscale = 1 unit/inch

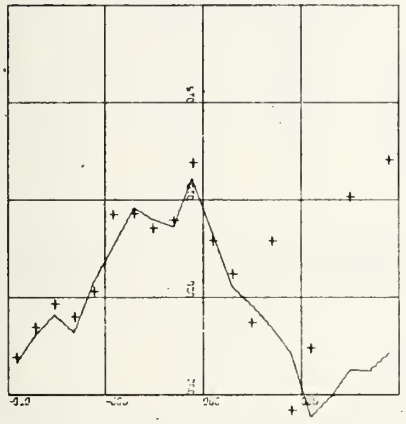

ρ=4.0, K=.30

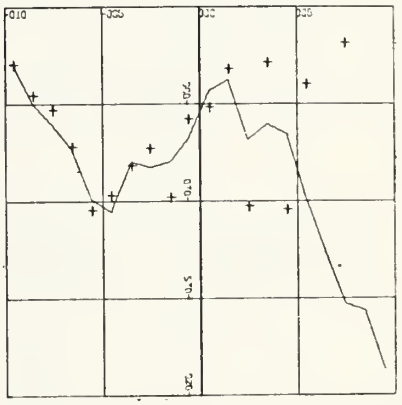

Yscale = 1 unit/inch

Yscale = 1 unit/inch

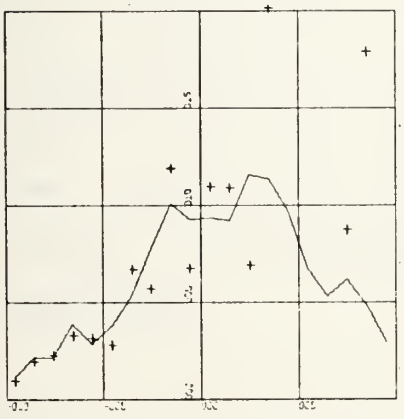

ρ=4.0, K=.40

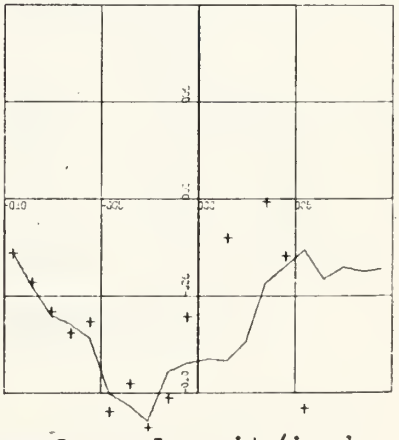

Yscale = 1 unit/inch

Yscale = 1 unit/inch

Real Part

Imaginary Part

Fig. 4c. Complex Velocity Potential Comparisons for $\sigma=\pi$ and $\lambda=0$, Varying Frequency and Interblade Distance. Velocity Potential vs X (1 unit/inch).

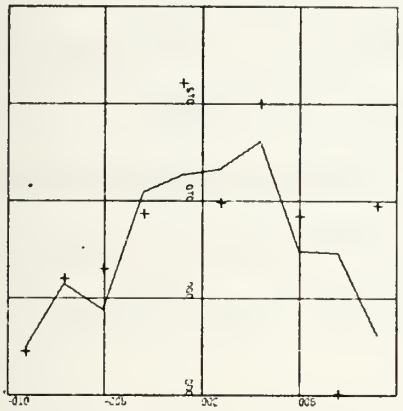

ρ=5.0, K=.25

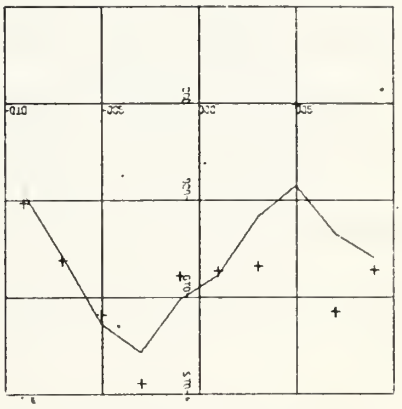

Yscale = 1 unit/inch

Yscale = 1 unit/inch

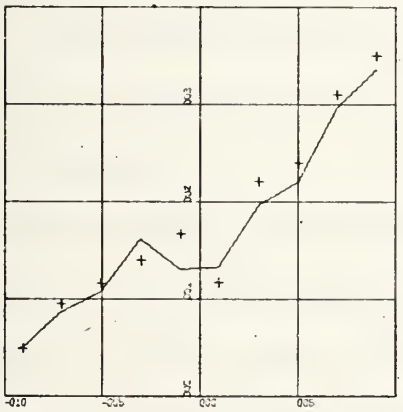

ρ=12, K=.10

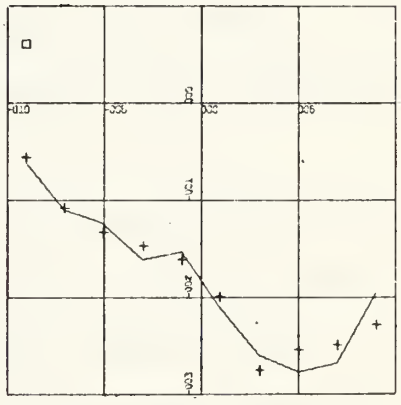

Yscale = 2 units/inch

Real Part

Yscale = 2 units/inch

Imaginary Part

Fig. 4d. Complex Velocity Potential Comparisons for $\sigma=\pi$ and $\lambda=0$, Varying Frequency and Interblade Distance. Velocity Potential vs X (1 unit/inch).

IV. TRANSONIC CASCADE AND BIPLANE STABILITY

A. GENERAL

In the previous sections, the Fourier Transform solution has emerged as a standard. The method has been made flexible by the inclusion of the Oswatitsch parameter and variable interblade phase angle. It has been compared to Laplace Transform, Collocation method, and Teipel [Ref. 30] solutions for many different sets of parameters and has produced good results.

The Fourier Transform solution has been applied to the problem of transonic, unstaggered cascade aerodynamic stability. Selected results are included to show the effects of frequency, blade thickness, interblade distance, and interblade phase angle.

The biplane problem was solved by utilizing the Fourier solution for the interference caused moment upon the upper surface of the lower blade and adding the Teipel [Ref. 30] solution for the isolated wing moment on the lower surface of that blade.

Isolated wing lift and moment results published by Nelson and Berman [Ref. 17], Teipel [Ref. 30], and Hamamoto [Ref. 10] were utilized for comparisons. Barton [Ref. 2] and Rott [Ref. 21] were also checked. The Fourier Transform solution reproduced all of the aforementioned results with reasonable accuracy, even when the interblade distance was about 20 (necessary for comparisons when $\lambda = 0.0$).

B. TRANSONIC, UNSTAGGERED CASCADE STABILITY

Calculations of stability boundaries were made for certain interblade phase angle, σ, blade thickness/chord ratio, τ, and interblade distance, ρ. The moment coefficients were then calculated for varying frequency to find the frequency at which the moment's phase angle was $\simeq$ 180 or 0, for each pivot location. Blade thickness was converted to Oswatitsch parameter as per Teipel [Ref. 30],

$$\lambda = 1.559\ [(\gamma+1)\tau]^{2/3} \qquad \text{(IV-1)}$$

The boundaries are plotted so that stable ranges lie above the curves which represent the boundaries of stability for that ρ.

It is seen that for $\rho = 1$, the boundary frequency lies off the curves for forward pivot locations. Further, frequency, interblade distance, and blade thickness increases were stabilizing as were interblade phase angle reductions and rearward pivot shifts. It should be noted that the effect of interference was destabilizing as indicated by the strong effect of decreasing interblade distance, ρ.

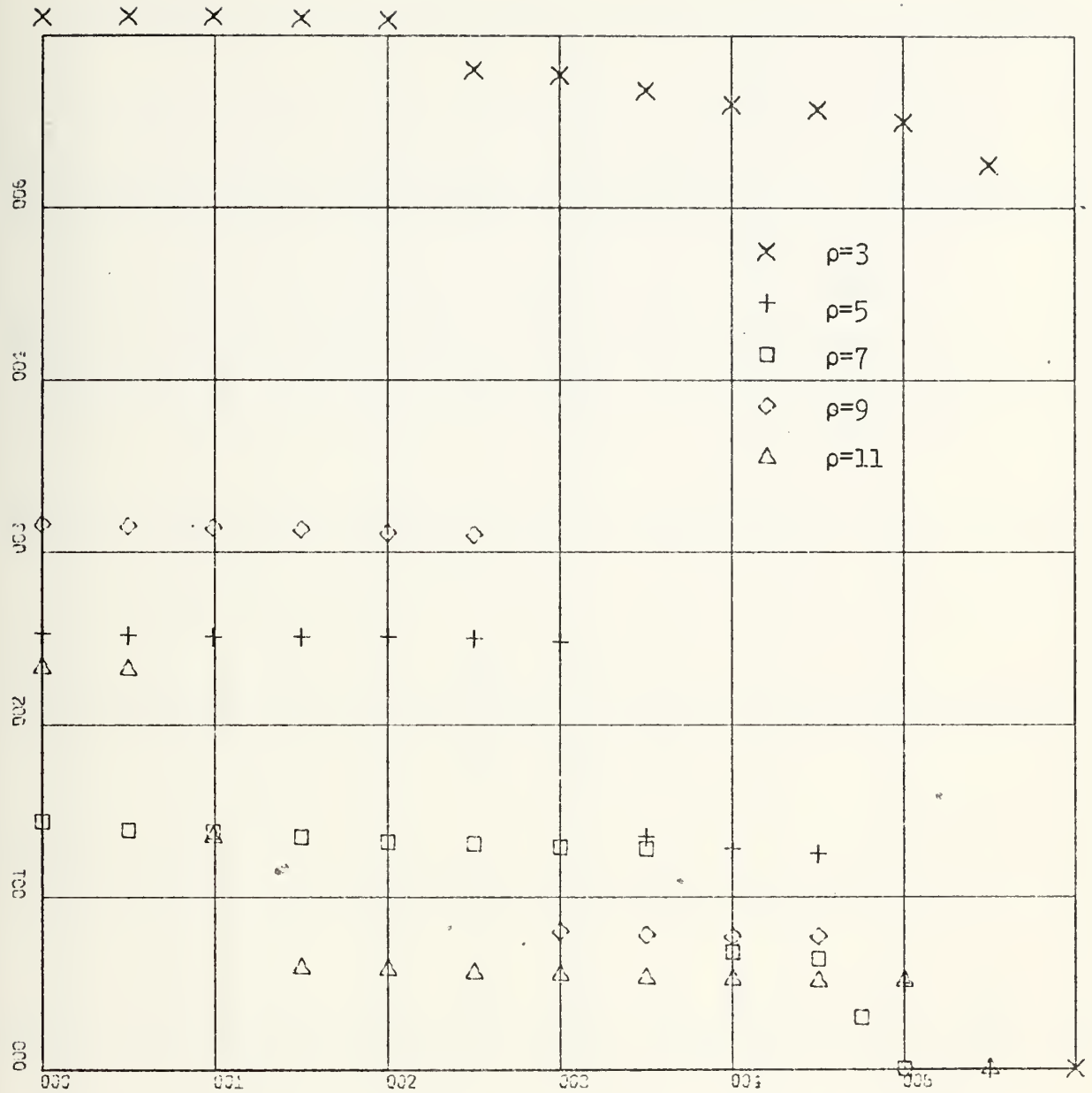

X-SCALE=1.00E-01 UNITS INCH.
Y-SCALE=1.00E-01 UNITS INCH.

Fig. 5a. Cascade Stability Boundary Frequency vs. Pivot Location, A_1 for Tau=0.0, Sigma=π.

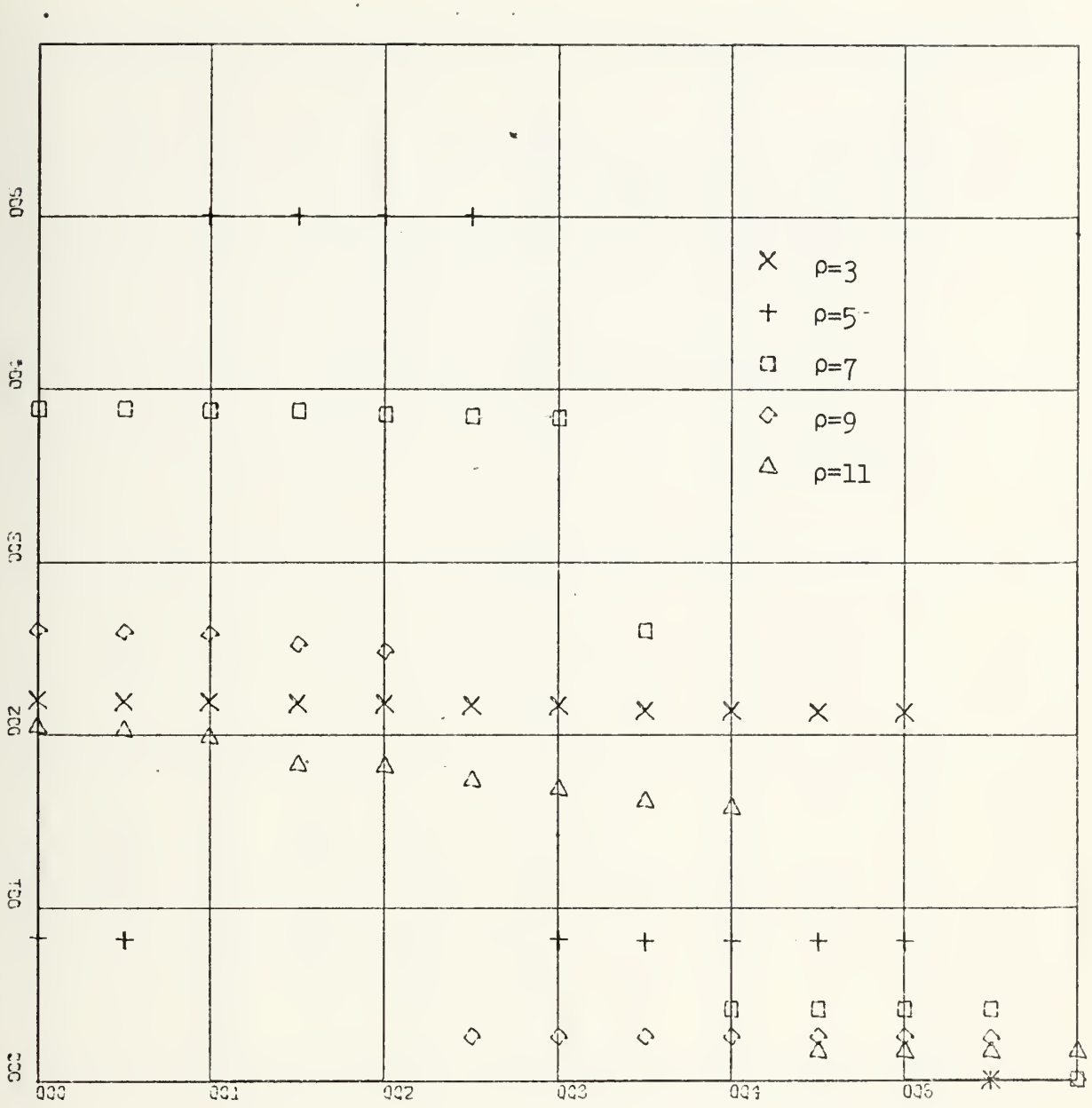

Fig. 5b. Cascade Stability Boundary Frequency vs. Pivot Location, A_1 for Tau = 0.0, Sigma = $\pi/2$.

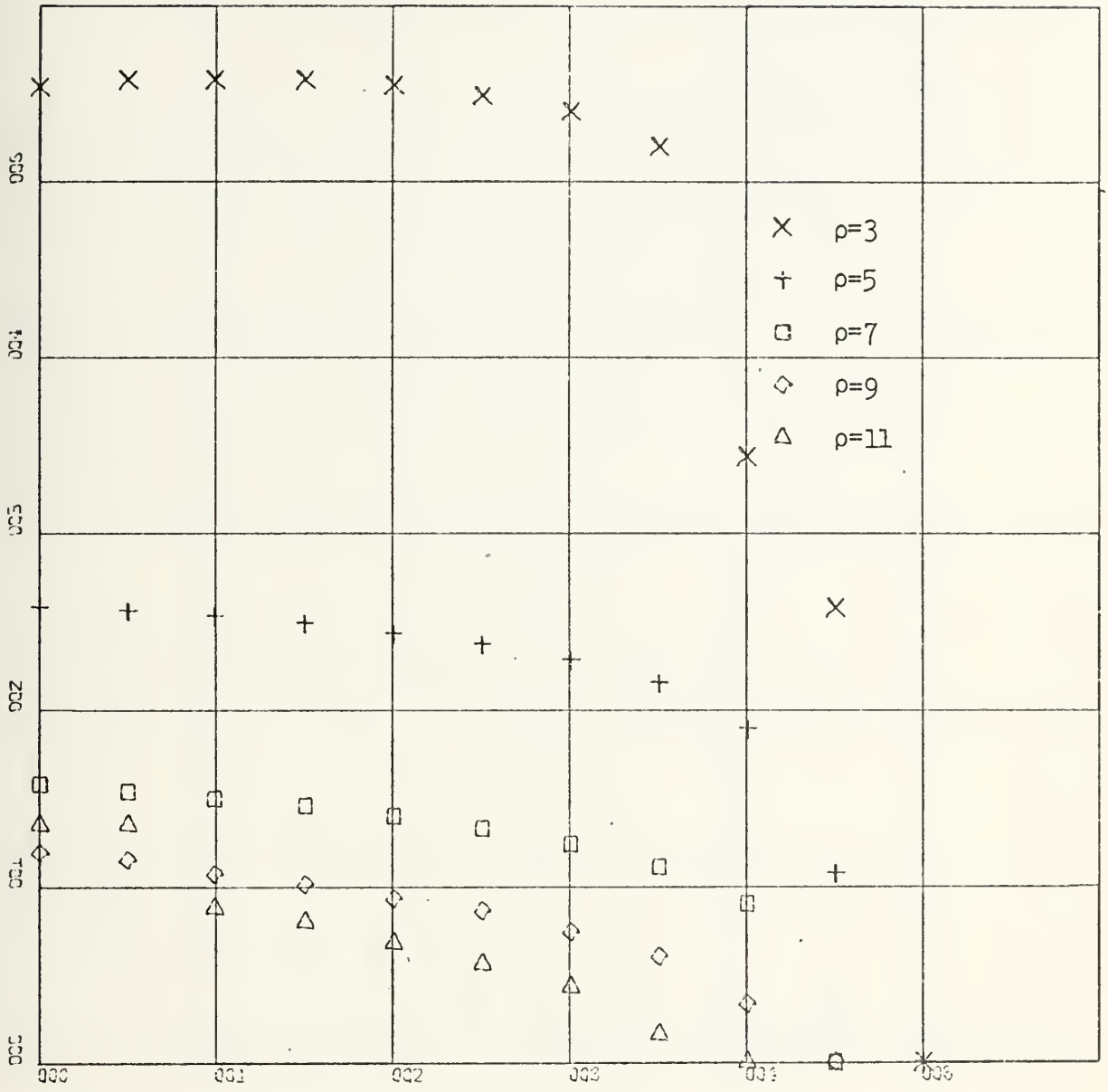

X-SCALE=1.00E-01 UNITS INCH.
Y-SCALE=1.00E-01 UNITS INCH.

Fig. 5c. Cascade Stability Boundary Frequency vs. Pivot Location, A_1 for Tau = .01, Sigma = π.

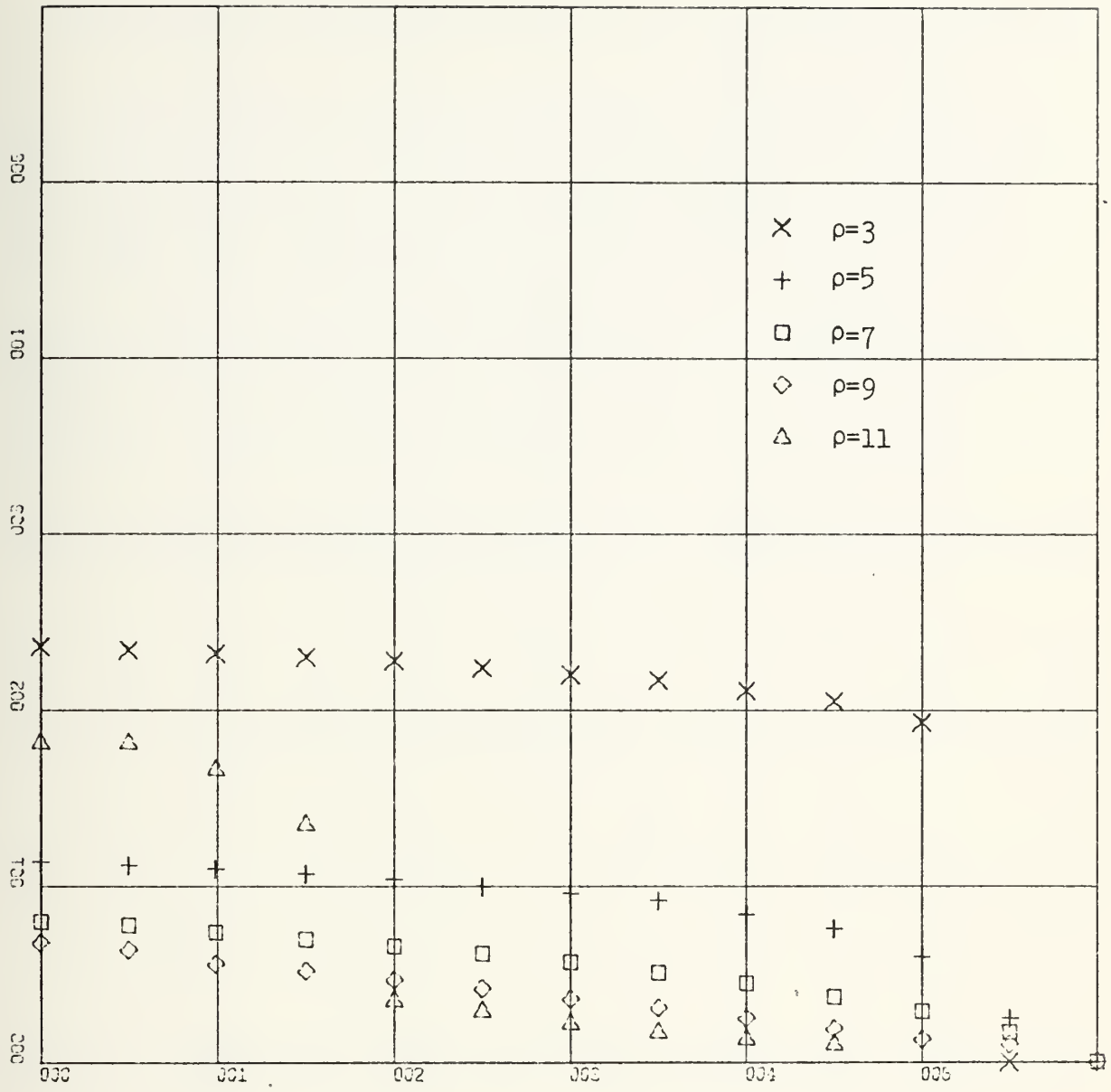

Fig. 5d. Cascade Stability Boundary Frequency vs. Pivot Location, A_1 for Tau = .01, Sigma = $\pi/2$.

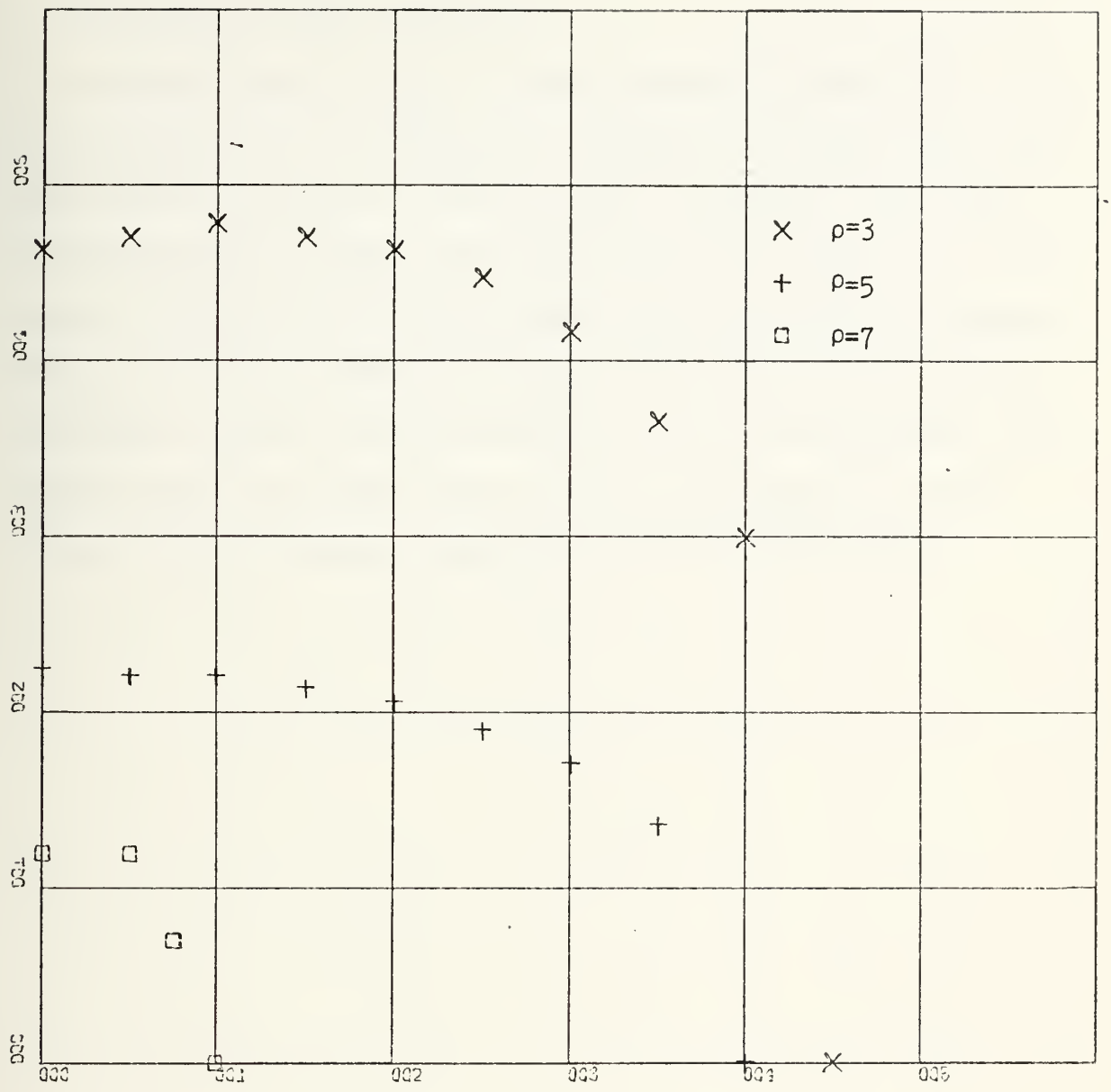

X-SCALE=1.00E-01 UNITS INCH.
Y-SCALE=1.00E-01 UNITS INCH.

Fig. 5e. Cascade Stability Boundary Frequency vs. Pivot Location, A_1 for Tau = .03, Sigma = π.

C. TRANSONIC BIPLANE STABILITY

A single result (Fig. 5-f) was included to show the effect of interference on the Biplane. Because the blades have isolated blade pressures on their 'outer' surfaces, the effect of interference is much less evident than observed in cascade flows. This can be seen by comparing the cascade and biplane curves for $\tau = .01$, and $\sigma = \pi$(Figs. 5-c and 5-f). For close interblade spacing, where interference is most prevalent, the biplane stability curves drop to lower frequencies at more forward pivot locations, indicating greater stability.

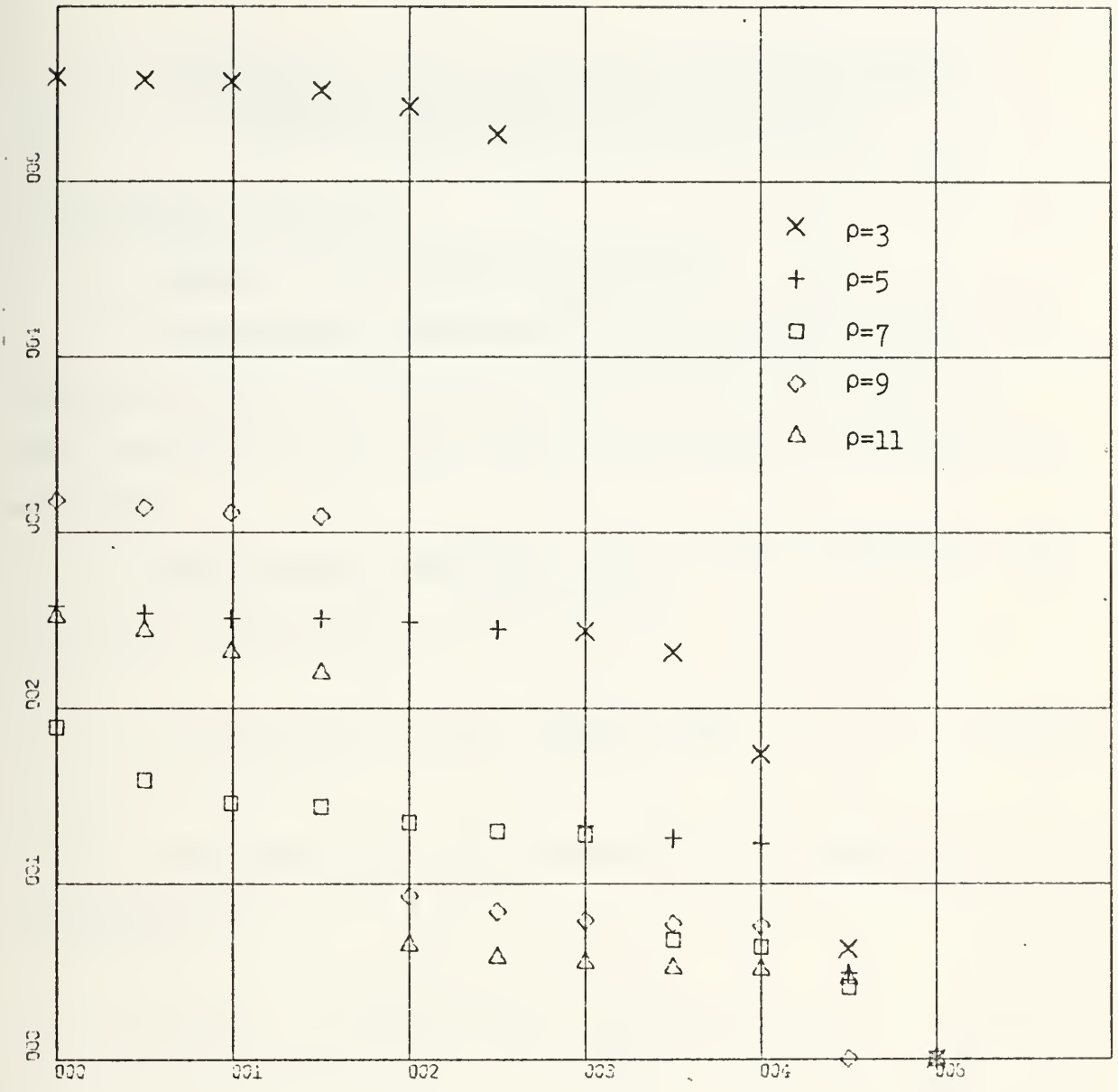

Fig. 5f. Biplane Stability Boundary Frequencies vs. Pivot Location, A_1 for Tau = .01, Sigma = π.

V. EXTENSION OF THE COLLOCATION SOLUTION TO THE POROUS WALLED TRANSONIC WIND TUNNEL

A. PROBLEM FORMULATION

1. Geometry and Boundary Conditions

The geometry considered here will differ in that the adjacent blade of the Collocation method solution for the sonic cascade is now a flat wall, the porosity of which may be varied.

The boundary condition acting at the reference blade (or, now, the airfoil) is as before

$$\psi_Y(X,Y_0=0) = v_0(X) = \frac{\partial h_u}{\partial X} + iKh_u. \qquad \text{(III-4)}$$

From Drake [Ref. 6], the condition at the wall can be stated as

$$\psi_Y(X,Y=\rho) + \sigma_{w\ell}[iK\psi(X,Y=\rho) + \psi_X(X,Y=\rho)] = 0. \qquad \text{(V-1)}$$

The condition of zero upstream disturbance holds as previously. Furthermore, non-dimensionalizations are the same.

2. Solution of the Oscillating Sonic Flow Equation

As in Section III, the source distributions shall be assumed to be series. However, because the 'adjacent blade'

is now a flat wall, its 'isolated blade' potential and derivatives vanish. Thus,

$$\psi(X,Y_0) = \phi_0^0(X,Y_0) + \phi_0(X,Y_0) + \phi_1(X,Y_1). \qquad \text{(V-2)}$$

Now, from the boundary conditions and

$$\phi_{0Y}^0(X,Y_0=0) = v_m, \quad m = 0,1; \qquad \text{(V-3)}$$

the airfoil and wall equations become

$$\phi_{0Y}(X,Y_0=0) + \phi_{1Y}(X,Y_1=-\rho) = 0, \qquad \text{(V-4)}$$

and

$$\phi_{0Y}^0(X,Y_0=\rho) + \phi_{0Y}(X,Y_0=\rho) + \phi_{1Y}(X,Y_1=0) +$$

$$\sigma_{w\ell}\{[\phi_{0X}^0(X,Y_0=\rho) + \phi_{0X}(X,Y_0=\rho) + \phi_{1X}(X,Y_1=0)] +$$

$$iK[\phi_0^0(X,Y_0=\rho) + \phi_0(X,Y_0=\rho) + \phi_1(X,Y_1=0)]\} = 0. \qquad \text{(V-5)}$$

3. Derivation of Expressions for Derivatives of the Potential

In Section III-C the isolated and interference potentials are expressed by integrals of the appropriate source

distributions (see equations III-71, 75, 76, 77, and 78). The wall boundary condition requires derivatives on the X variable of those potentials. Thus, the following derivatives must be evaluated,

$$DIN = \frac{\partial}{\partial X} \int_{XN}^{X} S^N \frac{\mathrm{Exp}[\frac{K^2}{Q}(X-S) - \frac{Q}{4}\frac{P^2}{(X-S)}]}{\sqrt{X-S}}\, dS, \qquad \text{(V-6)}$$

$$n = 0,1; \quad P \geq 0.$$

For n = 0,

$$DI0 = \frac{\partial}{\partial X} \int_{XN}^{X} \frac{\mathrm{Exp}[\frac{K^2}{Q}(X-S) - \frac{Q}{4}\frac{P^2}{(X-S)}]}{\sqrt{X-S}}\, dS. \qquad \text{(V-7)}$$

For n = 1,

$$DI1 = \frac{\partial}{\partial X}\{X \int_{XN}^{X} \frac{\mathrm{Exp}[\frac{K^2}{Q}(X-S) - \frac{Q}{4}\frac{P^2}{(X-S)}]}{\sqrt{X-S}} dS$$

$$- \int_{XN}^{X} \frac{\mathrm{Exp}[\frac{K^2}{Q}(X-S) - \frac{Q}{4}\frac{P^2}{(X-S)}]}{(X-S)^{-1/2}}\, dS\} . \qquad \text{(V-8)}$$

Thus, derivatives are required of two integrals

$$DIM = \frac{\partial}{\partial X} \int_{XN}^{X} (X-S)^m \mathrm{Exp}[\frac{K^2}{Q}(X-S) - \frac{Q}{4}\frac{P^2}{(X-S)}] dS, \quad m = \pm \frac{1}{2}$$

Applying Leibniz' rule

$$\frac{d}{da}\int_p^q f(s,a)dS = \int_p^q \frac{\partial}{\partial a}f(s,a)ds + f(q,a)\frac{dq}{da} - f(p,a)\frac{dp}{da},$$

DIM becomes

$$DIM = \int_{XN}^{X} \frac{\partial}{\partial X}\{(X-S)^m Exp[\frac{K^2}{Q}(X-S) - \frac{Q}{4}\frac{P^2}{(X-S)}]\}dS$$

$$+ (X-S)^m Exp[\frac{K^2}{Q}(X-S) - \frac{Q}{4}\frac{P^2}{(X-S)}]\Big|^X .$$

To differentiate the integrand, let U = X-S,

$$\frac{\partial}{\partial U}\{U^m Exp[AU + B/U]\} =$$

$$\{mU^{m-1} + \frac{K^2}{Q}U^m + \frac{QP^2}{4}U^{m-2}\} Exp[\frac{K^2}{Q}U - \frac{Q}{4}\frac{P^2}{4U}].$$

There are two cases to consider, m = ±1/2 that is

$$DI- = \frac{K^2}{Q}\int_0^{X-X_n} U^{-1/2}Exp[C]dU + \frac{Qp^2}{4}\int_0^{X-X_n} U^{-5/2}\exp[C]\,dU$$

$$- \frac{1}{2}\int_0^{X-X_n} U^{-3/2}Exp[C]\,dU + \frac{Exp[-\frac{Q}{4}\frac{P^2}{U}]}{U^{1/2}}\Big|^0 , \qquad (V\text{-}10)$$

and

$$DI+ = \frac{K^2}{Q} \int_0^{X-X_n} U^{-1/2}\mathrm{Exp}[C]dU + \frac{QP^2}{4} \int_0^{X-X_n} U^{-3/2}\mathrm{Exp}[C]dU$$

$$+ \frac{1}{2} \int_0^{X-X_n} U^{-1/2}\mathrm{Exp}[C]dU + U^{1/2}\mathrm{Exp}[-\frac{Q}{4} \frac{P^2}{U}]\Big|^0 , \quad \text{(V-11)}$$

where

$$C = \frac{K^2}{Q} U - \frac{Q}{4} \frac{P^2}{U} .$$

The last term in equation (V-11) vanishes nicely for all P. As long as P > 0, the last term in (V-10) does as well. For P = 0, however, care must be exercised.

For P = 0,

$$DI-(P=0) = \frac{K^2}{Q} \int_0^{X-X_n} U^{-1/2}\mathrm{Exp}[\frac{K^2}{Q}U]dU$$

$$- \frac{1}{2} \int_0^{X-X_n} U^{-3/2}\mathrm{Exp}[\frac{K^2}{Q}U]dU + \frac{1}{U^{1/2}}\Big|^0 .$$

Since

$$\int \frac{e^{ax}}{x^m} dx = - \frac{1}{m-1} \frac{e^{ax}}{x^{m-1}} + \frac{a}{m-1} \int \frac{e^{ax}}{x^{m-1}} dx,$$

then

$$\int_0^{X-X_n} U^{-3/2}\mathrm{Exp}[\frac{K^2}{Q}U]dU = -2\frac{\mathrm{Exp}[\frac{K^2}{Q}U]}{U^{1/2}}\Big|_0^{X-X_n}$$

$$+ 2 \frac{K^2}{Q} \int_0^{X-X_n} \frac{\mathrm{Exp}[\frac{K^2}{Q}U]}{U^{1/2}} dU.$$

Thus,

$$DI-(P=0) = \frac{\mathrm{Exp}[\frac{K^2}{Q}(X-X_n)]}{\sqrt{X-X_n}} \quad . \qquad (V\text{-}12)$$

B. RESULTS OF POROUS WALL TUNNEL CALCULATION

The results of the preceding analytical work were programmed (see Appendix-D) and pressure coefficients calculated. Comparisons were made with solid wall tunnel and sonic free jet results obtained from the other methods. Experimental comparisons were made in the steady flow case using results of Spreiter, Smith and Hyett [Ref. 27].

Figures 6,7, and 8 plot solid wall tunnel program results as crosses, sonic free jet as squares, and porous wall program results as solid lines connecting data points. Further, the porosity is printed to the right of each curve of collocation method results. Results from [Ref. 27] and for a run of the Collocation method for variable porosity are plotted as diamonds and triangles on Figs. 6 and 7, respectively.

The results from [Ref. 27] plotted on Fig. 6 are for a circular arc airfoil in a choked wind tunnel with no wall porosity. The agreement is relatively good but it must be considered that the use of a constant fluid acceleration (λ) is an approximation. Further, the experimental results indicate a magnitude reduction in the pressure coefficients with introduction of porosity in the manner shown by the results

of the computer routine. Porosities used were 0.0, .05, .5, 10.0, and 100.0.

Figs. 7 and 8 are the results of nonsteady analyses for which there is no experimental or theoretical comparison available. It can be mentioned, however, that for both the increases of porosity produces the expected trend in the porous wall tunnel collocation routine results. Note that the pressure coefficients shown are normalized to the magnitude of the pitch oscillation, α_0.

It should be noted that for K = .5 (Fig. 8), the Collocation method solution was near the limit of its applicability, as expected from the results of Section III-E. In particular, for $\sigma_{w\ell} = 0$, the source distribution series approximation was a mildly divergent oscillation and the result shown in Fig. 8-a is oscillatory as well. Interestingly, as porosity was increased the character of the results improved.

The Collocation routine was modified for the utilization of the following variable porosity,

$$\sigma_{w\ell} = 5.0\ (X + 1.0)$$

Thus, the porosity varies linearly from zero, at the leading edge, to ten at the trailing edge. Of course, there is presently no way to verify the results but they are promising. However, the source distribution series approximation was

more oscillatory for the variable porosity case than that for constant porosity, suggesting further analysis is necessary to confirm the Collocation method's applicability to this technique.

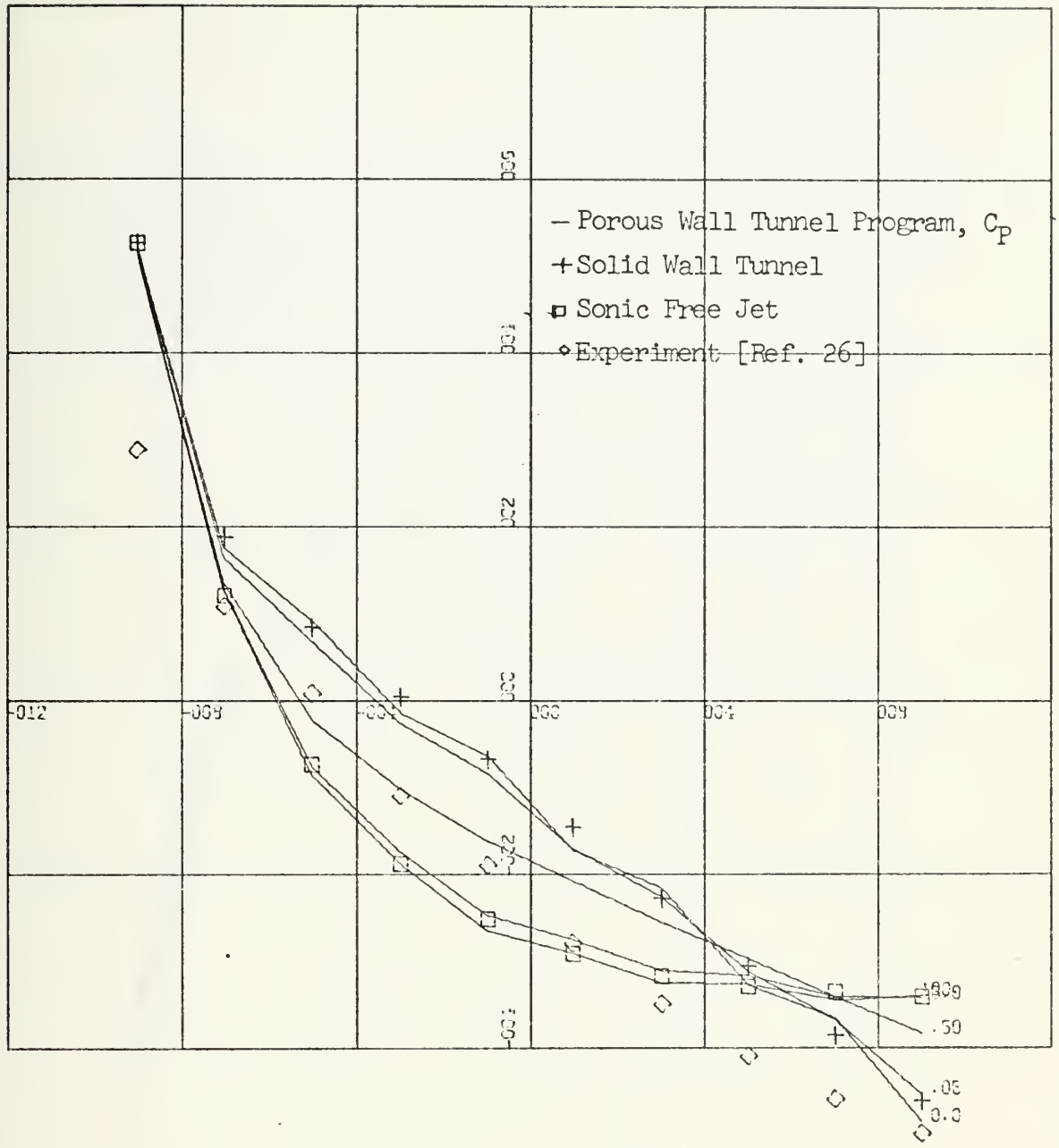

Fig. 6. Steady Flow Pressure Coefficient vs. X, τ = .06, for Various Porosity (0.,.05,.50,10.,100.) and Solid Wall Tunnel, Sonic Free Jet, and Experimental Results.

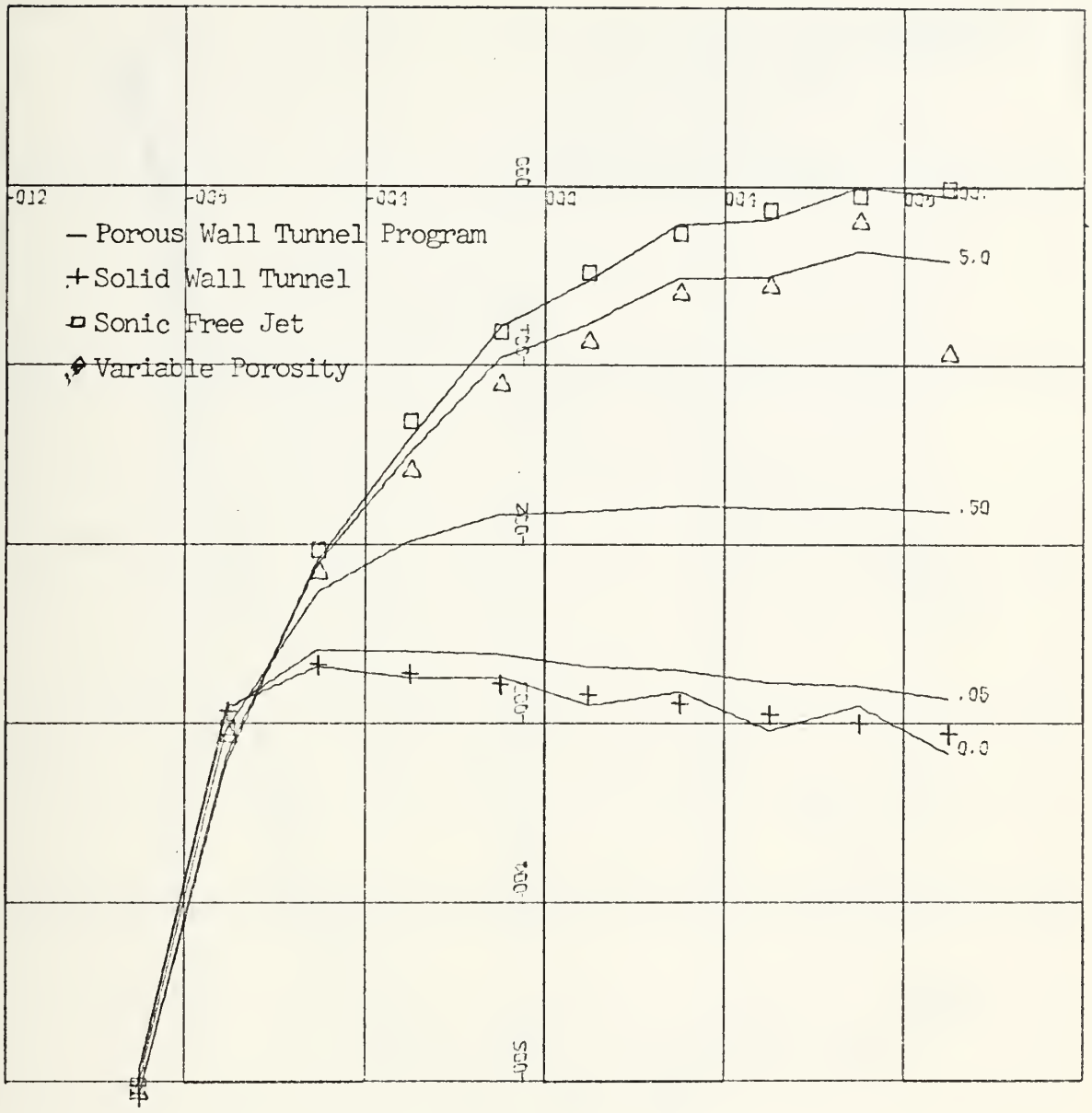

Fig. 7a. Nonsteady Flow Normalized Pressure Coefficient vs. X, K = .1, τ = .06, for Various Porosity (0.,.05,.50,5.0, 100.), Solid Wall Tunnel, Sonic Free Jet, and Variable Porosity Collocation Routine Results. Real Part.

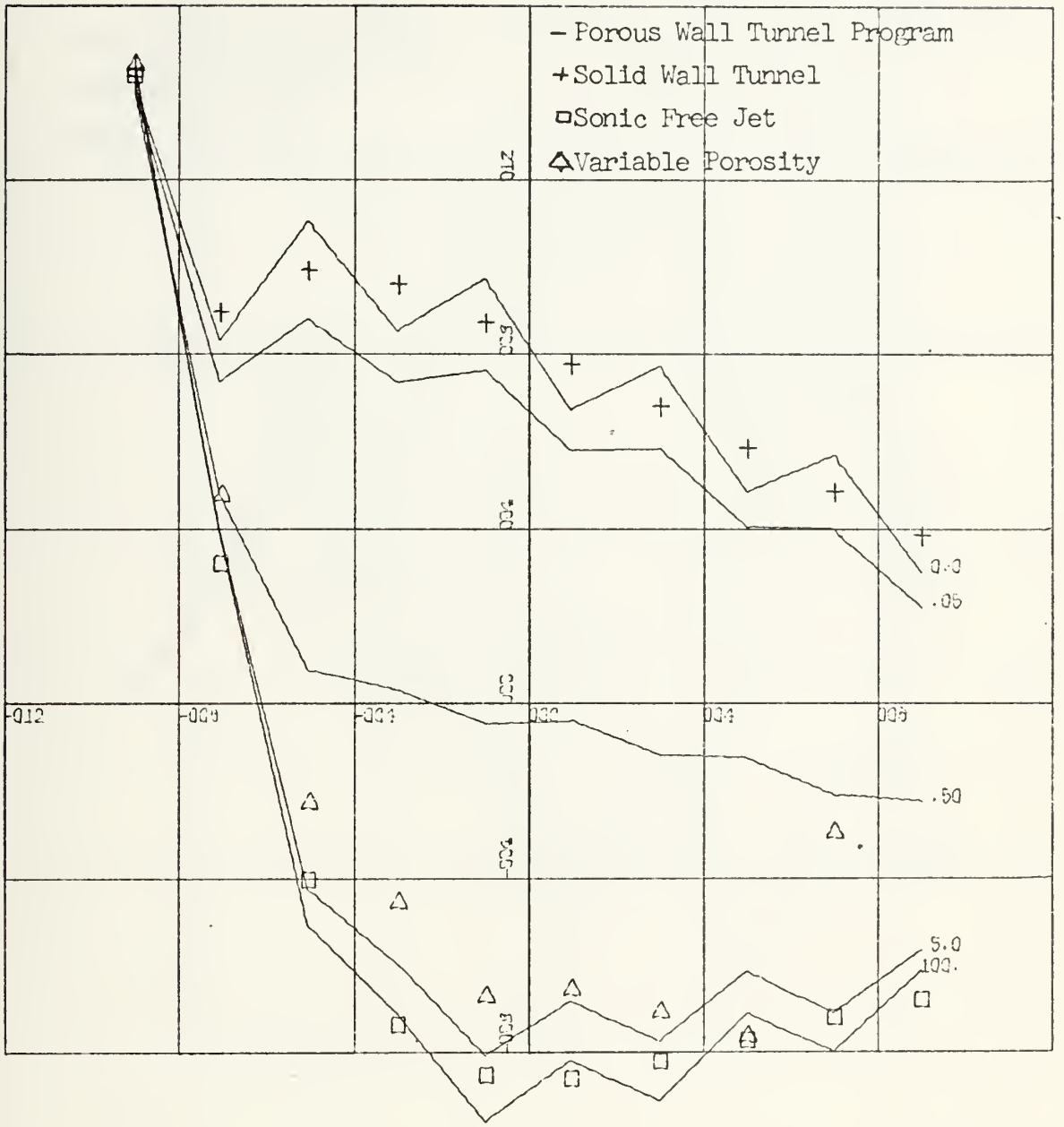

Fig. 7b. Nonsteady Flow Normalized Pressure Coefficient vs. X, K = .1, τ = .06, for Various Porosity (0.,.05,.50, 5.0,100.), Solid Wall Tunnel, Sonic Free Jet, and Variable Porosity Collocation Routine Results. Imaginary Part.

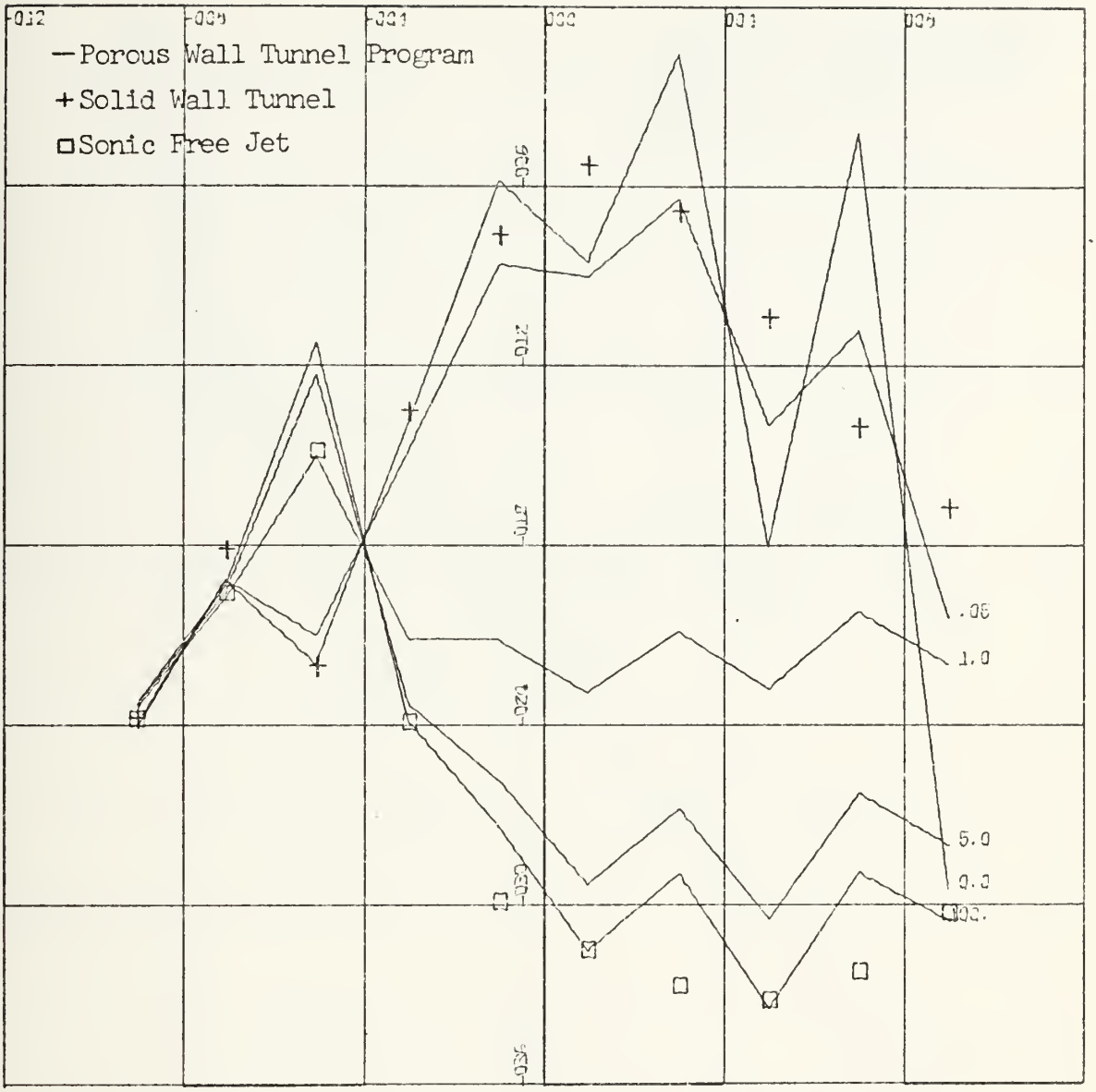

X-SCALE=4.00E-01 UNITS INCH.
Y-SCALE=6.00E-01 UNITS INCH.

Fig. 8a. Nonsteady Flow Normalized Pressure Coefficient vs. X, K = .5, τ = .06, for Various Porosity (0.,.05,1.0, 5.0,100.), Solid Wall Tunnel and Sonic Free Jet Results. Real Part.

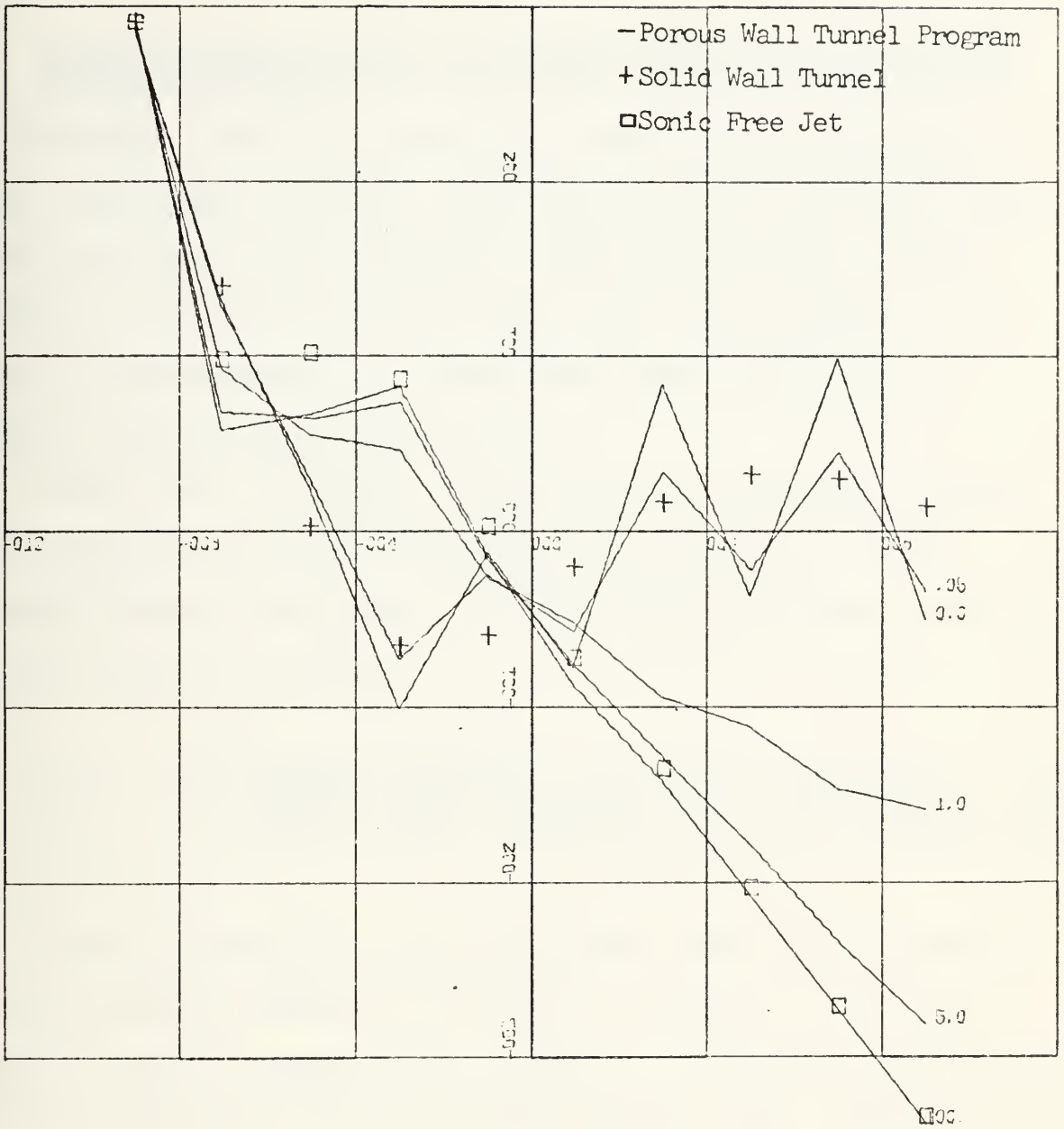

Fig. 8b. Nonsteady Flow Normalized Pressure Coefficient vs. X, K = .5, τ = .06), for Various Porosity (0.,.05,1.0, 5.0,100.), Solid Wall Tunnel and Sonic Free Jet Results. Imaginary Part.

C. DISCUSSION OF MURASAKI AND DRAKE POROUS WALL SONIC WIND TUNNEL SOLUTIONS

Murasaki [Ref. 18] solved the steady sonic flow porous wall wind tunnel problem. His results could not provide more than one check case against the Collocation method, though. However, they show his solution to have good agreement with those of experiment for a solid wall tunnel in [Ref. 27] (those results are shown in Fig. 6).

Drake [Ref. 6] Laplace transformed the nonsteady linearized potential equation and applied the porous wall wind tunnel boundary conditions, leading to the following inversion for the Green's function,

$$g(X,0+) = \mathcal{L}^{-1}\left\{\frac{\sqrt{2iKp}\,\cosh[\sqrt{2ikp}\,\rho] + \sigma(p+iK)\,\sinh[\sqrt{2iKp}\,\rho]}{\sqrt{2iKp}\,[\sqrt{2iKp}\,\sinh[\sqrt{2iKp}\,\rho] + \sigma(p+iK)\cosh[\sqrt{2iKp}\,\rho]]}\right\}.$$

Drake's results of lift coefficient could not be used as a verification because of the known inability of the Collocation method to produce derivatives of the velocity potential for the linearized (zero thickness effect) case. Thus, Drake's solution was modified to include the Oswatitsch parameter and computer programmed. The results of that program did not agree with reasonable estimates so the Drake solution method was followed to produce a solution for $\sigma_{w\ell} = 0$, in order to test the method at as simple a level as possible.

For $\sigma_{w\ell} = 0$, the potential is, using notation of Section III-B

$$\psi(X,0^+) = \int_0^X \alpha(t)\, g(X-t,0^+)\, dt,$$

where

$$\alpha(t) = 1 + iK(t - A) ,$$

$$g(X,0^+) = \frac{e^{\frac{K^2}{Q}}}{2\pi i} \int_{\gamma-i\infty}^{\gamma+i\infty} e^{pX} \frac{\cosh[\sqrt{Qp}\ \rho]}{\sqrt{Qp}\ \sinh[\sqrt{Qp}\ \rho]}\, dp$$

$$= e^{\frac{K^2}{Q}} \sum_{n=0}^{\infty} \frac{2}{\rho Q}\, e^{S_n X} ,$$

and

$$S_n = -\frac{n^2\pi^2}{Q\rho^2} , \quad n = 0,1,2,...$$

Though this result is derived in a parallel manner to Drake's $\sigma_{w\ell} \neq 0$, $\lambda = 0$ result (inversion by the Theorem of Residues), it leads to a series whose convergence is questionable, i.e.,

$$\sum_{n=0}^{\infty} e^{-\frac{n^2\pi^2}{Q\rho^2} X} .$$

In fact, computer generated results using the above formulation showed good agreement with previous results of Fourier and Laplace Transform and Collocation method routines for $K < .3$ and $\lambda \neq 0$. In those cases for which agreement was not obtained, it is believed that the computer routine signaled series convergence at a local minimum of term value.

It was concluded that a Laplace Transform solution of this type needs further analysis before it could be used in a verification of Collocation results.

VI. DISCUSSION AND SUMMARY

A. ANALYSIS OF SOLUTIONS

Reference should be made to Section III-E.

1. Laplace Transform

This solution provided a reliable, if time consuming, check on the others. Despite the principal shortcoming of an unsophisticated integration technique, it always gave reasonable agreement with the Fourier Transform solution. Even for $\lambda = 0$, the case that required the 'correction integral' described in Section III-D, agreement with the Fourier solution was good for the parameters tested. Thus, the calculation of the integrals utilized in the Collocation method solution was verified.

As programmed, this solution was too extravagant in its computation time usage, principally due to the time required for integrating. Presently, integrals are calculated from the leading edge to the X value for which a potential is desired. Perhaps, a better approach would be to calculate the integrals in increments between each X value, as does the Collocation routine (see Appendix-C). Further, an improved integration routine itself may speed the results and improve their accuracy.

2. Fourier Transform

The Hamamoto Fourier Transform method, as extended here for variable blade thickness (via the Oswatitsch

parameter), frequency (to include K = 0), and interblade phase angle, was a reliable and reasonably rapid method for velocity potential, pressure coefficient, lift, and moment calculations (which includes the solid wall tunnel and free jet problems). It must be noted that for large interblade distances, beyond those required to initially obtain isolated wing results, the series involved may not converge. This must be considered principally for the $\lambda = 0$ case.

3. Collocation Method

The Collocation method, as programmed here, was a qualified success due to its agreement limitations for higher frequencies and lower Oswatitsch parameter, as discussed in Section III-E. Whenever the other methods showed that the potential results were not reasonably smooth or large magnitude differences were present between the real and imaginary parts of the potential, the coefficients of the series became large and the computed velocity potentials deviated from those of the Fourier and Laplace Transform solutions. Increasing the number of collocation points did not, in general, improve the agreement. It is believed that the character of the stepwise-linear series approximation in the presence of the numerical inaccuracies of the integral calculations (though not terribly significant in themselves) can lead to large errors in the calculated potential, especially near the trailing edge.

Because of the inability of the method to reliably produce potentials for $\lambda = 0$, it cannot calculate pressure

coefficients for that case, which are needed if lift and moment results are desired.

Perhaps an improvement to the step-wise-linear series is the Fourier series. It might overcome the numerical pitfalls encountered by the power series approach of Elder and the aforementioned qualification of present series by providing a better approximation to the source distribution when more complex behavior is expected.

B. CASCADE STABILITY

Two qualifications must be mentioned as to the applicability of these results, produced by the Fourier Transform solution. First, the $\tau = 0$ results were a solution to the linearized potential equation, the applicability of which is a function of reduced frequency, K, e.g. Landahl [Ref. 13] stated the following requirement for applicability,

$$K >> |1 - M_L|$$

where, M_L = local mach number.

Secondly, for $\tau \neq 0$, the approximation of the Oswatitsch parameter, λ, was utilized. This can only be a rough estimate to the real behavior but, at least, it is an initial step. A more accurate analysis could perhaps be made through the application of Spreiter's local linearization. (See part D of this Section).

C. POROUS WALL WIND TUNNEL INTERFERENCE

The Collocation method applied to the porous walled wind tunnel is subject to the same qualifications discussed earlier in this section for the Collocation method.

The results are difficult to verify experimentally due to the paucity of such data. Further, theoretical verification is difficult to obtain as only Murasaki's approach is available for steady flow and Drake's analysis for nonsteady porous wall tunnel flows. Unfortunately, Murasaki's data could be used to verify only a single steady flow case and the Drake Laplace Transform solution was restricted to the linearized case for which the Collocation method solution would not produce reliable results. However, the trends of the Collocation method solution are correct and the results for very large and very small porosities compared well with the free jet and solid wall results.

The modification of the routine for variation of porosity along the wall appears promising and may allow a numerical test of the Sears [Ref. 25] technique. Further, a kind of local linearization may be applied to collocation methods (see the next part of this section).

D. FUTURE WORK

Various areas of improvement have been recognized.

1. Improve series approximation methods for Collocation methods.

2. Improved numerical integration schemes for those methods.

3. Application of Spreiter's 'local linearization' to Fourier Transform and Collocation methods.

The first two have been discussed. The third requires the following elaboration and description for steady sonic flow.

Recall that the Oswatitsch parameter was used to approximate the nonconstant coefficient of the governing equation, i.e.,

$$\bar{\phi}_{YY} - (\gamma+1)\,\bar{\phi}_{XX}\bar{\phi}_{X} = 0,$$

became,

$$\bar{\phi}_{YY} - \lambda\cdot\bar{\phi}_{X} = 0,$$

where, λ = constant > 0, assuming that the fluid acceleration was slowly varying.

The solution for the steady flow potential on a single foil is,

$$\bar{\phi}(X,0) = \frac{1}{\sqrt{\pi\lambda}} \int_{-1}^{X} \frac{v(S)}{\sqrt{X-S}}\, dS.$$

Now, Spreiter argued [Ref. 25] λ can be replaced by its definition, yielding an ordinary differential equation which admits an analytical solution.

Spreiter recently extended this approach to the oscillating airfoil in transonic flow [Ref. 28]. Start with the oscillating flow potential equation for sonic flow,

$$\psi(X,0) = -\frac{1}{\sqrt{\pi Q}} \int_{-1}^{X} v(S) \frac{e^{\frac{K^2}{Q}(X-S)}}{\sqrt{X-S}} dS,$$

where,

$$Q = \lambda + 2iK,$$

λ = constant, replacing the variable coefficient $(\gamma+1)\phi_{XX}$.

With $\psi(X,0)$, calculate $\psi_{XX}(X,0)$, replace λ by the function it originally represented, and solve the resulting second order differential equation for $\psi(X,0)$ and $\psi_X(X,0)$.

It remains to be investigated whether this approach could be further extended to study nonsteady interference in transonic flows. It appears from the outset, however, that the Collocation method is suited to a form of 'local linearization'.

VII. CONCLUSIONS

The unsteady, sonic, small disturbance potential equation was approximated, following the approach of Teipel [Ref. 30] and Hosokawa [Ref. 11], by replacing the nonconstant coefficients with a constant, the Oswatitsch parameter. The resulting parabolic equation was solved by Laplace and Fourier Transform and Collocation techniques.

Comparison of solutions to numerous sonic cascade problems revealed that the Transform solutions were reliable and convenient in the Fourier Transform case. The Collocation technique was usable with qualifications, growing out of the series approximation and numerical integration methods utilized, which degraded its accuracy for certain parameters.

Sonic cascade stability boundaries were computed utilizing the Fourier Transform solution and interference was found to be strongly destabilizing. Such results must be qualified by the realization that they were obtained by the solution of an approximated equation, though the trends are not expected to be materially affected.

The Collocation method, once some confidence was obtained from its comparison with the other solution as mentioned above, was applied to the sonic porous wall wind tunnel interference problem. Though few experimental results were available for comparison and the Drake [Ref. 6] approach was

questioned, the trends of the results for different values of porosity were as expected and solid wall wind tunnel and sonic free jet results were easily obtainable with reasonable porosity values.

The success of the Collocation solution in handling a range of sonic interference problems leads to the consideration of improvements beyond better series approximations and numerical techniques. It is reasonable to expect application of the Spreiter [Ref. 28] 'local linearization' to improve accuracy. Further, the method appears to be capable of utilizing a streamwise variable porosity in a manner like that proposed by Sears [Ref. 25].

APPENDIX A

FORMULATION OF THE LAPLACE SOLUTION ROUTINE

A-I Main Program

The Main routine serves as the controller for calculation of potential utilizing the Laplace Transform solution derived in Section III-A.

$$\psi(X,0^+) = \frac{1}{\sqrt{\pi Q}} \int_{-1}^{X} \frac{e^{\frac{K^2}{Q}(X-S)}}{\sqrt{X-S}} \sum_{n=0}^{\infty} \{v_0(S)e^{i\sigma}[2e^{-\frac{Q}{4}\frac{(2n\rho+\rho)^2}{(X-S)}}]$$

$$- v_0(S)[e^{-\frac{Q}{4}\frac{(2n\rho+2\rho)^2}{(X-S)}} + e^{-\frac{Q}{4}\frac{(2n\rho)^2}{(X-S)}}]\}dS. \qquad \text{(III-24)}$$

Calculations are made for controlling variables DK, DL, RHO, and SIGMA (corresponding to K, λ, ρ, and σ in equation (III-24)) at each of L selected points along the chord.

To reduce computational redundancy, the Main routine calculates the parameters A, C, and D as described in Section III-D. Also, the boundary condition expressions

$$v_0(S)e^{i\sigma} ,$$

and

$$v_0(S)$$

are treated as they are in the Collocation routine (Appendix C)

$$v_0(S) = \theta_{00} + \theta_{01} \cdot X$$

$$= -1 - iKX \ , \qquad \text{(A-I-1)}$$

$$e^{i\sigma} v_0(S) = \theta_{10} + \theta_{11} \cdot X \qquad \text{(A-I-2)}$$

The Main routine reduces equation (III-22) to

$$POT(J) = R * I, \qquad \text{(A-I-3)}$$

where

$$\eta = \frac{1}{\sqrt{\pi Q}} \ , \qquad Q = \lambda + 2iK \ , \qquad \text{(A-I-4)}$$

and

$$I = \sum_{n=0}^{\infty} \{2\cdot\theta_{10} \int_{-1}^{X} \frac{\mathrm{Exp}[\frac{K^2}{Q}(X-S) - \frac{Q}{4}\frac{(2n\rho+\rho)^2}{(X-S)}]}{\sqrt{X-S}}\,dS$$

$$+ 2\cdot\theta_{11} \int_{-1}^{X} \frac{S\,\mathrm{Exp}[\frac{K^2}{Q}(X-S) - \frac{Q}{4}\frac{(2n\rho+\rho)^2}{(X-S)}]}{\sqrt{X-S}}\,dS$$

$$- \theta_{00}[\int_{-1}^{X} \frac{\mathrm{Exp}[\frac{K^2}{Q}(X-S) - \frac{Q}{4}\frac{(2n\rho+2\rho)^2}{(X-S)}]}{\sqrt{X-S}}\,dS$$

$$+ \int_{-1}^{X} \frac{\mathrm{Exp}[\frac{K^2}{Q}(X-S) - \frac{Q}{4}\frac{(2n\rho)^2}{(X-S)}]}{\sqrt{X-S}}\,dS\ ]$$

$$- \theta_{01}[\int_{-1}^{X} \frac{S\,\mathrm{Exp}[\frac{K^2}{Q}(X-S) - \frac{Q}{4}\frac{(2n\rho+2\rho)}{(X-S)}]}{\sqrt{X-S}}\,dS$$

$$+ \int_{-1}^{X} \frac{S\,\mathrm{Exp}[\frac{K^2}{Q}(X-S) - \frac{Q}{4}\frac{(2n\rho)^2}{(X-S)}]}{\sqrt{X-S}}\,dS]\}, \qquad \text{(A-I-5)}$$

which is calculated by subroutine ISUM.

The Main routine uses the common named SUM to relay boundary condition and integral sum results between itself and subroutine ISUM. Common HOLD relays parameter information between Main and subroutines ISUM, ZSUM, and INTCOR.

```
C
C           THE LAPLACE TRANSFORM SOLUTION FOR A TRANSSONIC,
C                UNSTAGGERRED, OSCILLATING CASCADE.
C
C.....................................................................
C
C                              MAIN ROUTINE
C
C.....................................................................
C
      IMPLICIT REAL*8 (A-H,U-Z)
      IMPLICIT COMPLEX*16 (I,Q,P,R,T)
      REAL*8 SIGMA,RHO,TAU
      COMPLEX*16 EISIG
C
      DIMENSION POT(50),XX(50)
C
      COMMON/SUM/I,TH00,TH01,TH10,TH11,NMAX
      COMMON/HOLD/DK,DL,RHO,B,C,D,E,EPS,LIM
C
C
 9001 FORMAT('1'////////' ',36X,'SOLUTIONS FOR THE FOLLOWING PARAMETERS'/
     1'0',20X,'DL=',F6.3,10X,'DK=',F6.3,10X,'RHO=',F6.3,10X,'SIGMA=',F6.
     23,'RAD',/'0',36X,'X',17X,'POTR',14X,'POTI')
 9002 FORMAT('1'////)
 9003 FORMAT(//,(20X,3(D12.4,6X),/))
C
      PI=3.14159265358979D0
      EPS=1.0D-8
      NMAX=0
      LIM=50
C
C     .................................................................
C
C     SET THE CONTROLLING VARIABLES DK,DL,RHO,AND SIGMA.
C
      SIGMA=PI
C
      RHO=1.0D0
      DK=1.0D0
      TAU=.06D0
C
C     .................................................................
C
C     FOR CONVENIENCE ESTABLISH VARIOUS OTHER FIXED VARIABLES THAT ARE
C     FUNCTIONS OF THE CONTROLLING VARIABLES.
C
```

```
      DL=1.559D0*(2.4D0*TAU)**(2.0D0/3.0D0)
      IF(DK.GT.0) GO TO 11
      A=0.0D0
      GO TO 22
   11 A=DK**2/(DL**2+4.0D0*DK**2)
   22 C=DL*A
      D=2.0D0*DK*A
      Q= DCMPLX(DL,2.0D0*DK)
      P=1.0D0/CDSQRT(PI*Q)
C
C     SET THE NUMBER OF STATIONS ON THE FOIL, STATION ONE, AND INTERVAL
      L=10
      XINT= 2.0D0/DFLOAT(L)
      X=-1.0D0 + XINT/2.0D0
C
C     CALCULATE THE BOUNDARY CONDITIONS.
      TH00= -1.0D0
      TH01= -DCMPLX(0.0D0,DK)
      EISIG= CDEXP(DCMPLX(0.0D0,SIGMA))
      TH10= EISIG*TH00
      TH11= EISIG*TH01
C
CCC   ..................................................................
CCC   ..................................................................
C
      DO 1 J=1,L
C
      CALL ISUM(X)
      POT(J)= P*I
      XX(J)=X
C
      X=X + XINT
    1 CONTINUE
C
C     PRINTOUT RESULTS
      WRITE(6,9002)
      WRITE(6,9001) DL,DK,RHO,SIGMA
      WRITE(6,9003)(XX(J),POT(J),J=1,L)
  800 CONTINUE
C
      STOP
      END
```

A-II Subroutine ISUM

ISUM is called by Main for each X position on the blade at which the potential is to be evaluated. It sequentially calculates each term in the summation comprising I in equation (A-I-5), in the 'n loop'.

ISUM denotes the integrals in equation (A-I-5) as the variables Iji where j = 1,2 and i = 0,1,2. Since ZSUM is used for the evaluation of the integrals, j and a constant denote the power of U required in the integrand (note that this routine's ZSUM calculates the integrals with $U^{j-1.5}$ vice $U^{j-2.5}$ as illustrated in Section III-D).

Because each integral differs not only in j, but in the value of the natural exponent values, the exponent is considered to be of the form

$$\mathrm{Exp}\left[\frac{K^2}{Q}(X-S) - \frac{Q}{4}\frac{(R_i)^2}{(X-S)}\right] ,$$

where R0 = 2nρ, R1 = 2nρ+ρ, R2 = 2nρ+2ρ. Thus, once in the 'n loop', ISUM calculates R0, R1, and R2 and the associated Bi and Ei required for the subsequent integrations.

The integrations are conducted sequentially on i. Since Ij2 for n-1 and Ij0 for n do not differ, integration for Ij0 can be avoided for n > 0.

In the event that λ = 0, correction integrals must be calculated as outlined in Section III-D. Subroutine INTCOR is called for the calculations which are stored matrix

COR(i,j,k). The corrections are to be calculated but once for each n; thus, NMAX is set on the first call of ISUM and subsequent calls use it to determine whether further correction calculations are required (resetting NMAX higher).

Accuracy of the correction integrals is dependent upon the magnitude of the ratio (E/U)/DU, where U takes on the maximum value used in the correction integral, i.e., U = XA (see Section III-D). If we desire (E/U)/DU $\geq$ 10,000, since

$$E = \frac{K}{2} (2n\rho + k\rho)^2, \quad k = 0,1,2,$$

then, the maximum value XA can be

$$XA = (2n + k)\rho/100.$$

Thus, XA is calculated for each n and i. If the calculated XA is less than the required XO, it is used. If it is greater, an XA is chosen smaller than XO.

Of course, for $\lambda \neq 0$ and RO = 0.0, XA is chosen as 1.0D-03 and ZSUM calculates a correction (see Section III-D). Subsequent integrations utilize the arbitrarily small XA = 1.0D-08 as a compromise between computation time and accuracy.

Convergence of the series for I is signaled when successive terms alter it by less than DEL x 100 percent and control is returned to Main with the value for I.

```
      SUBROUTINE ISUM(X)
C
      IMPLICIT REAL*8 (B,D-H,X)
      IMPLICIT COMPLEX*16 (C,I,T,Z)
      REAL*8 CHK,C,RHO
C
      DIMENSION ZERO(200)
C
      COMMON/HOLD/DK,DL,RHO,B,C,D,E,EPS,LIM
      COMMON/SUM/I,TH00,TH01,TH10,TH11,NMAX
      COMMON/CORINT/COR(2,50,2)
      EQUIVALENCE (COR(1,1,1),ZERO(1))
C
C     ZEROIZE COR
      DO 1 J=1,200
    1 ZERO(J)=0.0D0
C
      I=0.0D0
      X0=X + 1.0D0
      XA1=.99D0*X0
      XA2=XA1
C
C     THE N LOOP.
C
      DO 100 N1=1,LIM
      N=N1-1
      R0=DFLOAT(N)*RHO*2.0D0
      R1=R0 + RHO
      R2=R1 + RHO
      B0=.25D0*DL*R0*R0
      B1=.25D0*DL*R1*R1
      B2=.25D0*DL*R2*R2
      E0=.5D0*DK*R0*R0
      E1=.5D0*DK*R1*R1
      E2=.5D0*DK*R2*R2
C
C     CALCULATE IJ0.
      IF(N.GT.0) GO TO 2
C
      XA=1.0D-3
      B=B0
      E=E0
C
      CALL ZSUM(XA,X0,1,I10)
      CALL ZSUM(XA,X0,2,I20)
      I20= X*I10 - I20
      GO TO 3
    2 I10=I12
```

```
      I20=I22
C
C     CALCULATE IJ1.
    3 B=B1
      E=E1
      IF(DL.GT.EPS) GO TO 4
C
      K=1
      XA=DFLOAT(2*N + K)*RHO/100.0D0
      IF(XA.LE.XO) XA1=XA
      XA=XA1
      IF(N1.LE.NMAX) GO TO 5
      CALL INTCOR(N1,K,XA)
      GO TO 5
C
    4 XA=1.0D-08
    5 CALL ZSUM(XA,XO,1,I11)
      CALL ZSUM(XA,XO,2,I21)
      I11=COR(1,N1,1) + I11
      I21=COR(2,N1,1) + I21
      I21= X*I11 - I21
C
C     CALCULATE IJ2.
      B=B2
      E=E2
      IF(DL.GT.EPS) GO TO 6
C
      K=2
      XA=DFLOAT(2*N + K)*RHO/100.0D0
      IF(XA.LE.XO) XA2=XA
      XA=XA2
      IF(N1.LE.NMAX) GO TO 6
      CALL INTCOR(N1,K,XA)
C
    6 CALL ZSUM(XA,XO,1,I12)
      CALL ZSUM(XA,XO,2,I22)
      I12=COR(1,N1,2) + I12
      I22=COR(2,N1,2) + I22
      I22= X*I12 - I22
C
C
      TEMP=I
C
C
      I= 2.0D0*(TH10*I11+TH11*I21) - (TH00*(I12+I10) + TH01*(I22+I20))
     1 +I
C
C
```

```
C       USE THE 1. PERCENT CRITERION.
C
        DEL=1.0D-02
        CHK=CDABS((I - TEMP)/I)
C
        IF(CHK.GT.DEL) GO TO 100
        RETURN
  100 CONTINUE
C
        RETURN
        END
```

A-III. Subroutine INTCOR

Called by ISUM in the case $\lambda = 0$ INTCOR follows the organization of Elder [Ref. 7] in calling the corrections required for the integrals from the subroutine COR.

A-IV. Subroutines COR and ZSUM

COR is a simplification of the more general correction routine developed for the Porous Tunnel Wall Solution. ZSUM is an adaptation of Elder's [Ref. 7] pyramided Simpson's Rule integration routine with $P = 0$ corrections added (see Section III-D).

A-V. Subroutine CS

This is a library routine utilized to provide Fresnel Integral values required in $\lambda = 0$ correction integral calculations.

```
      SUBROUTINE INTCOR(N1,K,XA)
C
C
      IMPLICIT REAL*8 (A-H,O-Z)
      COMPLEX*16 COR,CORR
      COMMON/CORINT/COR(2,50,2)
      COMMON/HOLD/DK,DL,RHO,B,C,D,E,EPS,LIM
C
      PI=3.141592653589793
C
 2500 FORMAT('0','COR1',2D12.4,2X,'COR2',2D12.4,2X,'XA=',D12.4)
C
CC    CASE FOR K.NE.0   DL=0
CC
CC    COMPUTE CORRECTIONS.
C
      AR=E/XA
      SS=DSIN(AR)
      CC=DCOS(AR)
      CALL CS(CCC,SSS,AR)
      ARG=DSQRT(2.0D0*PI/E)
      SSS=ARG*(0.5D0 - SSS)
      CCC=ARG*(0.5D0 - CCC)
C
      CALL COR(XA,D,E,1,CC,SS,SSS,CCC,CORR)
      COR(1,N1,K)= CORR
      CALL COR(XA,D,E,2,CC,SS,SSS,CCC,CORR)
      COR(2,N1,K)= CORR
C
      WRITE(6,2500) COR(1,N1,K),COR(2,N1,K),XA
C
      RETURN
      END
```

```
      SUBROUTINE COR(XA,D,E,J,C,S,SS,CC,CORR)
C
CCCCCCCC
CCCCCCCC
C
      IMPLICIT REAL*8(A-H,O-Z)
      COMPLEX*16 CORR
      COMMON/HELO/SI(4),CI(4)
      SI(4)=0.0D0
      CI(4)=0.0D0
CC
CC CCCC
CCCC
C
      IF(J.GE.2) GO TO 12

      CASE J EQUAL ONE
      UTILIZE THE REDUCTION FORMULA TO OBTAIN THE BASIC CORRECTION TERMS.

      DEN=1.0D0
      Z=DSQRT(XA)
      DO 10 I=1,3
      SI(I)= 2.0D0*(Z*S + E*CC)/DEN
      CI(I)= 2.0D0*(Z*C - E*SS)/DEN
      Z=XA*Z
      DEN=DEN + 2.0D0
      CC=CI(I)
   10 SS=SI(I)
      GO TO 14
   12 DO 13 I=1,3
      SI(I)=SI(I+1)
   13 CI(I)=CI(I+1)
CC
C
   14 CONTINUE
C
CCCC
CCCC
C
      UTILIZE THE SIN AND COS TRUNCATED SERIES TO OBTAIN THE FINAL
      INTEGRAL CORRECTION.

      SCOR=SI(1)+D*(CI(2)-D*(SI(3)/2.0D0+D*CI(4)/6.0D0))
      CCOR=CI(1)-D*(SI(2)+D*(CI(3)/2.0D0-D*SI(4)/6.0D0))
C
      CORR= DCMPLX(CCOR,-SCOR)
      RETURN
      END
```

```
      SUBROUTINE ZSUM(XA,XO,J,SUM)
C     ..................................................................
C
C                        SUBROUTINE ZSUM
C
C     PROGRAM FOR THE COMPUTATION OF THE INTEGRAL
C     U**(J-1.5)EXP(DL*A*U-B/U)SIN OR COS (2KAU+E/U).
C
C     METHOD UTILIZED IS A PYRAMIDED SIMPSON'S RULE WITH END CORRECTION.
C     LIMITS ARE FROM XA TO XO.  PYRAMID LIMIT IS LIM.  CONVERGENCE IS
C     MEASURED BY EPS.  B,C,D,AND E ARE FIXED FUNCTIONS OF DK,DL,AND RHO.
C     TWO INTEGRALS ARE COMPUTED, THE REAL AND IMAGINARY PORTION OF THE
C     INTEGRAL IN THE BOUNDARY EQUATIONS.  THE VALUES ARE RETURNED ON SUMR
C     AND SUMI.
C
C     A WARNING IS GENERATED IN THE CASE OF NON CONVERGENCE.
C
C     ..................................................................
C
      IMPLICIT REAL*8(A-H,O-Z)
      COMPLEX*16 SUM
      COMMON/HOLD/DK,DL,RHO,B,C,D,E,EPS,LIM
      YR(U,J,AA,BB)=U**(J-1)*DEXP(AA)*DCOS(BB)/DSQRT(U)
      YI(U,J,AA,BB)=U**(J-1)*DEXP(AA)*(-DSIN(BB))/DSQRT(U)
    2 FORMAT('1','WARNING-SSUM NON CONVERGENT')
C
C     ESTABLISH LEFT END POINT
C
      U=XA
      AA=C*U-B/U
      IF(AA.LE.(-172.0D0)) GO TO 6
      BB=D*U+E/U
      CC=D*U-E/U
      YAR=YR(U,J,AA,BB)
      YAI=YI(U,J,AA,BB)
      EE=DEXP(AA)*U**(J-2)/DSQRT(U)
      FF=DFLOAT(J)-1.5D0+C*U+B/U
      YARP=EE*(DCOS(BB)*FF-CC*DSIN(BB))
      YAIP=(-EE)*(DSIN(BB)*FF+CC*DCOS(BB))
      GO TO 3
    6 YAR=0.0D0
      YAI=0.0D0
      YARP=0.0D0
      YAIP=0.0D0
    3 CONTINUE
C
```

```
C
CC      ESTABLISH THE RIGHT END POINT
C
        U=XC
        AA=C*U-B/U
        BB=D*U+E/U
        CC=D*U-E/U
        YOR=YR(U,J,AA,BB)
        YOI=YI(U,J,AA,BB)
        EE=DEXP(AA)*U**(J-2)/DSQRT(U)
        FF=DFLOAT(J)-1.5D0+C*U+B/U
        YORP=EE*(DCOS(BB)*FF-CC*DSIN(BB))
        YOIP=(-EE)*(DSIN(BB)*FF+CC*DCOS(BB))
C
CC      ESTABLISH INTERVAL
C
        DINT=XC-XA
        SOR=0.0D0
        SOI=0.0D0
        SER=0.0D0
        SEI=0.0D0
        SUMR=0.0D0
        SUMI=0.0D0
C       INITIAL SPACING AND NUMBER OF TERMS IN EVEN SUM
        SP=2.0D0
        K=1
C
CC      LOOP  SPECIFYING INTERVAL
C
        DO 100 M=1,LIM
        H=DINT/SP
C       SET OLD EVEN SUM INTO ODD SUM
        SOR=SOR+SER
        SOI=SOI+SEI
        XE=XA+H
C       ZEROIZE EVEN SUM
        SER=0.0D0
        SEI=0.0D0
C
CC      LOOP TO ESTABLISH EVEN SUM
C
        DO 10 I=1,K
        AA=C*XE-B/XE
        IF(AA.LE.(-172.0D0)) GO TO 4
        BB=D*XE+E/XE
        YER=YR(XE,J,AA,BB)
        YEI=YI(XE,J,AA,BB)
        GO TO 5
```

```
    4 YEP=0.0D0
      YEI=0.0D0
    5 CONTINUE
      SER=SER+YER
      SEI=SEI+YEI
   10 XE=XE+2.0D0*H
C
CCC     FORM THE INTEGRAL
C
        TEMPR=SUMR
        TEMPI=SUMI
        SUMR=H*(7.0D0*(YAR+YOR)+16.0D0*SER+14.0D0*SOR)/15.0D0
        SUMR=SUMR+H**2*(YARP-YORP)/15.0D0
        SUMI=H*(7.0D0*(YAI+YOI)+16.0D0*SEI+14.0D0*SOI)/15.0D0
        SUMI=SUMI+H**2*(YAIP-YOIP)/15.0D0
        L=M
C
CCC     TEST FOR CONVERGENCE
C
        TTTR=DABS(TEMPR-SUMR)
        TTTI=DABS(TEMPI-SUMI)
        IF(TTTR.LE.EPS.AND.TTTI.LE.EPS) GO TO 101
C
CCC     PROVIDE FOR ERROR STATEMENT IF NO CONVERGENCE
C
        IF(M.EQ.LIM) GO TO 1
        GO TO 9
    1 WRITE(6,2)
    9 K=K*2
      SP=SP*2.0D0
  100 CONTINUE
  101 CONTINUE
C
CCC     IF E=B=0, COMPUTE THE LEFT END POINT TERMS.
C
        IF(B.NE.0.AND.E.NE.0) GO TO 102
        IF(J.NE.1) GO TO 102
        SUMR=2.0D0*(1.0D0 + C*XA/3.0D0 - (D*XA-C*XA)**2/10.0D0)*DSQRT(XA)
       1 + SUMR
        SUMI=-2.0D0*(XA/3.0D0 + C*XA*XA/5.0D0)*D*DSQRT(XA) + SUMI
  102 CONTINUE
      SUM= DCMPLX(SUMR,SUMI)
      RETURN
      END
```

```
      SUBROUTINE CS(C,S,X)                                                  CS    380
C                                                                           CS     10
C     .....................................................................CS     20
C                                                                           CS     30
C        SUBROUTINE CS                                                      CS     40
C                                                                           CS     50
C        PURPOSE                                                            CS     60
C           COMPUTES THE FRESNEL INTEGRALS.                                 CS     70
C                                                                           CS     80
C     INPUT IS STATION=X, OUTPUTS ARE THE COS INTEGRAL ON C AND SIN
C     INTEGRAL ON S.
C                                                                           CS     90
C     .....................................................................CS    100
C                                                                           CS    110
      Z=ABS(X)                                                              CS    120
      IF(Z-4.)1,1,2                                                         CS    130
    1 C=SQRT(Z)                                                             CS    140
      S=Z*C                                                                 CS    150
      Z=(4.-Z)*(4.+Z)                                                       CS    160
      C=C*((((((5.100785E-11*Z+5.244297E-9)*Z+5.451182E-7)*Z                CS    170
     1+3.273308E-5)*Z+1.020418E-3)*Z+1.102544E-2)*Z+1.840965E-1)            CS    180
      S=S*((((((6.677681E-10*Z+5.883158E-8)*Z+5.051141E-6)*Z                CS    190
     1+2.441816E-4)*Z+6.121320E-3)*Z+8.026490E-2)                           CS    200
      RETURN                                                                CS    210
    2 D=COS(Z)                                                              CS    220
      S=SIN(Z)                                                              CS    230
      Z=4./Z                                                                CS    240
      A=((((((((8.768258E-4*Z-4.169289E-3)*Z+7.970943E-3)*Z-6.792801E-3)    CS    250
     1*Z-3.095341E-4)*Z+5.972151E-3)*Z-1.606428E-5)*Z-2.493322E-2)*Z        CS    260
     2-4.444091E-9                                                          CS    270
      B=((((((-6.633926E-4*Z+3.401409E-3)*Z-7.271690E-3)*Z+7.428246E-3)     CS    280
     1*Z-4.027145E-4)*Z-9.314910E-3)*Z-1.207998E-6)*Z+1.994711E-1           CS    290
      Z=SQRT(Z)                                                             CS    300
      C=0.5+Z*(D*A+S*B)                                                     CS    310
      S=0.5+Z*(S*A-D*B)                                                     CS    320
      RETURN                                                                CS    330
      END                                                                   CS    340
```

APPENDIX B

FORMULATION OF THE FOURIER SOLUTION ROUTINE

B-I Main Program

The Main routine satisfies equation (III-47) derived in Section III-B for potential at selected locations, X, along the unit blade chord and equations (III-49, 51, and 55) for pressure coefficient, total lift and moment coefficients.

$$\psi(X,0) = -\{(-1-iK_1A_1)[D\cdot T_1(X)+B\cdot S_1(X)]-iK_1[D\cdot T_2(X)+B\cdot S_2(X)]\} , \tag{III-47}$$

$$C_P(X) = -2[\psi_X(X,0) + iK_1\psi(X,0)] , \tag{III-49}$$

$$C_L = 2[\psi(1,0) + iK_1F_2(1.0)] , \tag{III-51}$$

$$C_M = -2\{iK_1[F_2(1,0)-F_3(1,0)]+[\psi(1,0)-F_2(1,0)]\}-A_1\cdot C_L, \tag{III-55}$$

where T_N and S_N are provided by Subroutine SUM as described in the next section and F_N are successive integrations of ψ.

Main controls the calculation of T_N and S_N with Subroutine SUM in peculiar manner. Since S_N and T_N are actually infinite series, Main calls SUM to produce successive terms in those series, the sums of which are S_N and T_N.

Convergence is signaled for the loop of index n in Main when successive calculations of the potential, for a particular

chordwise position, differ by less than criterion EPS.

When the lift and moment are calculated, the n loop is continued, if necessary, to provide the successive calculations of the magnitude and phase angle of the moment coefficient until convergence is detected in them.

Due to the difference in nondimensionalizations between the Fourier and other solutions, RHO, DK, and DL must be scaled, as shown in the output, to conform to the solution. Further, the results for the potential obtained will be one half those of the other solutions.

```
C      A GENERAL ROUTINE USING FOURIER TRANSFORM APPROACH TO CASCADE
CC     FLOW.
C
       IMPLICIT REAL*8(A-E,G-H,O-R,U-Y)
       IMPLICIT COMPLEX*16(F,S,T)
       REAL*8 TAU,SIGMA
       COMPLEX*16 C,CL,CM,POT,EISIG,D,B,DPOT,CP,I
       DIMENSION POT(25),XX(25),DPOT(25),CP(25)
       COMMON/HOLD/HK,HHO,X,C,N
C
CC     SET PARAMETERS.
       LIM=50
       EPS=1.0D-04
       PI=3.14159265358979300
       I=(0.0D0,1.0D0)
C
CC     THE VARIABLES.
       L=10
C
       A=.5D0
C
       DL=0.1D0
C
       SIGMA=PI
C
       DK=0.1D0
C
       RHO=1.0D0
C
       WRITE(6,7) SIGMA,DL,RHO,A,DK
     7 FORMAT(//,5X,' SIGMA=',D12.4,' DL=',D12.4,' RHO=',D12.4,' A=',D12.
      24,' DK=',D12.4./)
C
CC     CHANGE TO HAMAMOTO VARIABLES.
       HHO=RHO/2.0D0
       HK=2.0D0*DK
       HL=2.0D0*DL
CC
C
       TEST=0.0D0
       CMMAGT=0.0D0
       CMPAT=0.0D0
C
       XINT=1.0D0/DFLOAT(L)
       X=XINT/2.0D0
       L1=L + 1
       C=1.0D0/(2.0D0*HK - I*HL)
       Z= (4.0D0/HHO)*C
```

```
      EISIG=CDEXP(I*SIGMA)
      EISIG=CDEXP( DCMPLX(0.0D0,1.0D0)*SIGMA)
      D=(EISIG - 1.0D0)/2.0D0
      B=D + 1.0D0
      TH00=-1.0D0 + I*HK*A
      TH01=-I*HK
C
C     THE LOOP ON X.
C
      DO 3 J=1,L1
      IF(J.EQ.L1) X=1.0D0
      XX(J)=X
C
C     THE LOOP ON N.
C
      DO 1 N=1,LIM
C
C
C     CALCULATE TN
      CALL SUM(2,T0,T1,T2,T3,T4)
C     CALCULATE SN
      CALL SUM(1,S0,S1,S2,S3,S4)
C
C     CALCULATE THE POTENTIALS.
      POT(J)= -(TH00*(D*T1 + B*S1) + TH01*(D*T2 + B*S2))*Z
      DPOT(J)=-(TH00*(D*T0 + B*S0) + TH01*(D*T1 + B*S1))*Z
      CP(J)= -2.0D0*(DPOT(J) + I*HK*POT(J))
C
      CON=CDABS((POT(J) - TEST)/POT(J))
      IF(CON.LT.EPS.AND.I.LT.L1) GO TO 2
      TEST=POT(J)
      IF(J.LT.L1) GO TO 1
C
      F2=      -(TH00*(D*T2 + B*S2) + TH01*(D*T3 + B*S3))*Z
C
      F3=      -(TH00*(D*T3 + B*S3) + TH01*(D*T4 + B*S4))*Z
C
      CL=4.0D0*(I*HK*F2 + POT(L1))
C
      CM=-4.0D0*(I*HK*(F2 - F3) + (POT(L1) - F2)) + A*CL
      IF(HK.EQ.0.0D0) GO TO 1
C
      CLMAG=CDABS(CL)
      CLR=DREAL(CL)
      CLI=DIMAG(CL)
      CLPA=DATAN2(CLI,CLR)
C
      CMMAG=CDABS(CM)
```

```
      CMR=DREAL(CM)
      CMI=DIMAG(CM)
      CMPA=DATAN2(CMI,CMR)*180.0D0/PI
C
      CON1= DABS((CMMAG - CMMAGT)/CMMAG)
      CON2= DABS((CMPA - CMPAT)/CMPA)
      IF(CON1.LT.EPS.AND.CON2.LT.EPS) GO TO 799
      CMMAGT=CMMAG
      CMPAT=CMPA
C
    1 CONTINUE
C
    2 X=X + XINT
    3 CONTINUE
  799 WRITE(6,6) DK,CLMAG,CLPA,CMMAG,CMPA
    6 FORMAT(10X,' DK=',D12.4,' CLMAG=',D12.4,' CLPA=',D12.4,
     1' CMMAG=',D12.4,' CMPA=',D12.4,/)
      WRITE(6,4) (XX(J),POT(J),DPOT(J),CP(J),J=1,L1)
    4 FORMAT(/,1X,' X=',D12.4,2X,' POT=',2D12.4,2X,' DPOT=',2D12.4,2X,
     1' CP=',2D12.4)
   20 CONTINUE
      STOP
      END
```

B-II. Subroutine SUM

SUM is called by Main, as explained, to calculate the series for S_N and T_N. Recall that $S_1(X)$ and $T_1(X)$ are from equations (III-66 and 67). Main provides the coefficients to the series as Z.

Since

$$S_{N+1} = \int_0^X S_N(\phi)\, d\phi$$

and likewise for T_N, then the dummy variables U_N in SUM provide the appropriate series terms for S_N or T_N for the value of J (J = 2 for T_N) sent to it in the calling statement.

Logic is provided to properly calculate the first term of the series for T_N for the case K = 0.

```
      SUBROUTINE SUM(J,U0,U1,U2,U3,U4)
      IMPLICIT COMPLEX*16 (A-I,O-Z)
      REAL*8 HK,RHO,K,PI,X,F
      COMMON/HOLD/HK,RHO,X,C,N
C
      I=(0.0D0,1.0D0)
      PI=3.14159265358979D0
      IF(N.GT.1) GO TO 1
      U0=0.0D0
      U1=0.0D0
      U2=0.0D0
      U3=0.0D0
      U4=0.0D0
C
    1 F=2.0D0
      IF(J.EQ.2) F=1.0D0
C
      K= -2.0D0
      IF (N.GT.1) K= -1.0D0
      IF(J.EQ.1) K= 1.0D0
C
      VN= ((PI*(F*DFLOAT(N) - 1.0D0))**2/(.25D0*F*F*RHO*RHO) - HK*HK)*C
C
C
      E=CDEXP(I*VN*X)
C
      U0=-I*E/K + U0
C
      IF(DK.NE.0.OR.N.NE.1.OR.J.NE.2) GO TO 4
C
      U1= U0*X
      U2= U1*X/2.0D0
      IF(X.LT.(1.0D0 - EPS)) GO TO 2
      U3= U2*X/3.0D0
      U4= U3*X/4.0D0
      GO TO 2
C
    4 U1=(1.0D0 - E)/(VN*K) + U1
      U2=(X + I*(E - 1.0D0)/VN)/(VN*K) + U2
      IF(X.LT.(1.D0 - EPS)) GO TO 2
C
      U3=  (X*X/2.D0 + (E - 1.0D0)/(VN*VN) - I*X/VN)/(VN*K) + U3
      U4= (X*X*X/6.0D0 - X/(VN*VN) - I*((E - 1.0D0)/(VN**3)
     1+ X*X/(2.0D0*VN)))/(VN*K) + U4
C
    2 RETURN
      END
```

APPENDIX C

FORMULATION OF THE COLLOCATION SOLUTION ROUTINE

C-I. Main Program

Because the derivations have certain parallels in the integrals to be evaluated, much of this routine and the Laplace Transform routine are similar.

Main calculates the necessary variables required by the integrating routine, the boundary condition for coefficient and potential generation, and the step size between collocation points (XINT). With that done, Subroutine INTEGR is called to calculate all integrals required in subsequent steps. Main obtains the coefficients from Subroutine COEFF, then, implements equation (III-88) and calculates the potential.

Main's organization of the solution for the potential is also applied in COEFF and is due to the series chosen. The J loop carries the calculations down the chordwise collocation points and the I loop conducts only those calculations as allowed by the chord position dependent step function in equation (III-88). For any X position, at least two terms must be calculated, the n = 0, 1 terms of the series, and are done when I = 1. For I = 2, no calculations need be made and it is sidestepped and I is cycled to 3.

```
C      MASTER ROUTINE FOR CALCULATION OF CASCADE POTENTIAL. UTILIZES
C      STEP WISE LINEAR SERIES WITH INITIAL VALUE AND SLOPE FOR SOURCE
C      DISTRIBUTION.
C
       IMPLICIT REAL*8 (A-H,S,U-Z)
       IMPLICIT COMPLEX*16 (P,N,Q,R,T)
       REAL*8 RHO,PI,TAU
       COMPLEX*16 EISIG,INT
       INTEGER*4 P,J
C
C
       COMMON/HOLD/B,C,D,E,EPS,RHO,P,LIM
       COMMON/COF/NU(2,24),TH00,TH01,TH10,TH11,R
       COMMON/INTG/INT(5,24)
C
C
       PI=3.141592653589793
       LIM=50
       EPS=1.0D-8
C
CCC    INITIALIZATION SECTION
CCCC
CCCCC  ..................................................................
CCC    SET THE CONTROLLING VARIABLES   DK,DL,RHO, AND SIGMA.
C
       SIGMA=PI
       DL=0.0D0
       DK=0.25D0
       RHO=5.0D0
C
C      ..................................................................
       WRITE(6,6) SIGMA,DK,DL,RHO
C
CCC    FOR CONVENIENCE ESTABLISH VARIOUS OTHER FIXED VARIABLES THAT ARE
CCC    FUNCTIONS OF THE CONTROLLING VARIABLES.  IN ADDITION VARIOUS
C      MATRICES ARE ZEROIZED.
C
       IF(DK.GT.0) GO TO 1
       A=0.0D0
       GO TO 2
     1 A=DK**2/(DL**2+4.0D0*DK**2)
     2 B= DL*RHO**2/4.0D0
       C=DL*A
       D=2.0D0*DK*A
       E= DK*RHO**2/2.0D0
C
       Q=DCMPLX(DL,2.0D0*DK)
```

```
      R=(RHO/2.0D0)*CDSQRT(Q/PI)
C
C     CALCULATE THE BOUNDARY CONDITIONS.
      TH00= -1.0D0
      TH01= -DCMPLX(0.0D0,DK)
C
      EISIG=CDEXP(DCMPLX(0.0D0,1.0D0)*SIGMA)
      TH10= EISIG*TH00
      TH11= EISIG*TH01
C
C     SET THE NUMBER OF STATIONS ON THE FOIL, STATION ONE, AND INTERVAL
      L=10
      XINT= 2.0D0/DFLOAT(L)
C
CCC
CCC   ..................................................................
CCC
C     CALL INTEGRALS FOR CALCULATION.
      CALL INTEGR(XINT,L)
C
CCC
CCC   ..................................................................
CCC
CC    CALCULATION OF THE COEFFICIENTS.
C
      CALL COEFF(XINT,L)
      WRITE(6,9004) (NU(1,I),NU(2,I),I=1,L)
 9004 FORMAT(//,' THE COEFFICIENTS   ',5X,'NU(1,I)',22X,'NU(2,I)',/,
     1(25X,2D12.4,5X,2D12.4,/))
C
CC    SOLVE FOR THE POTENTIALS.
C
      X=-1.0D0 + XINT/2.0D0
      R=-1.0D0/CDSQRT(PI*Q)
      DO 7 J=1,L
C
      XN=-1.0D0
      DO 4 I=1,J
      IF(I.EQ.2) GO TO 4
C
      M=J-I+1
C
C     REFERENCE BLADE
      PI00= INT(4,M)
      PI01= X*PI00 - INT(5,M)
C     ADJACENT BLADE
      PI10= INT(2,M)
      PI11= X*PI10 - INT(3,M)
```

```
      IF(I.GT.1) GO TO 8
C
CC    FIRST, THE CONSTANT TERMS.
C
      POT=R*((TH00 + NU(1,1))*PI00 + (TH01 + NU(1,2))*PI01
     1-(TH10 + NU(2,1))*PI10 - (TH11 + NU(2,2))*PI11)
      XN=XN + 2.0D0*XINT
      GO TO 4
C
CC    NOW THE REMAINING TERMS.
C
    8 POT= POT + R*(NU(1,I)*(PI01 - XN*PI00) - NU(2,I)*(PI11 - XN*PI10))
C
      XN=XN + XINT
    4 CONTINUE
C
   68 WRITE(6,9012) X,POT
 9012 FORMAT(///,5X,'X=',D12.4,'POT=',2D12.4)
      X= X + XINT
    7 CONTINUE
      STOP
      END
```

C-II. Subroutine COEFF

This subroutine is called by Main after all integrals have been calculated for the purpose of solving equations (III-86 and 87) for the coefficients of the series representing the interference source distribution.

For n = 0 and 1, the abovementioned equations can be reduced to matrix form,

$$\begin{matrix} n=0 \\ \\ n=1 \\ \\ \end{matrix} \begin{bmatrix} 1 & X & RI0 & RI1 \\ RI0 & RI1 & 1 & X \\ 1 & X & RI0 & RI1 \\ RI0 & RI1 & 1 & X \end{bmatrix} \begin{bmatrix} \nu_{00} \\ \nu_{01} \\ \nu_{10} \\ \nu_{11} \end{bmatrix} = \begin{bmatrix} -BB0 \\ -B\eta 1 \\ -BB0 \\ -BB1 \end{bmatrix} .$$

The first two rows are calculated at the first collocation point, selected as X = -1.0 + XINT/2.0, and the next two at the second point, X = -1.0 + 1.5*XINT.

The above matrix equation is solved by a complex matrix inversion routine (CMINV) and a multiplication to yield the coefficients NU(I,J), I,J = 1,2. (i.e., ν_{00},ν_{01},ν_{10}, and ν_{11}).

The presence of the step function in the equations greatly simplifies subsequent calculations. A matrix solution is used again but only a single left side matrix need be calculated and inverted. As successive collocation points are reached, all previous coefficients have been calculated and they are used to calculate a new right hand side vector.

```
      SUBROUTINE COEFF(XINT,L)
C
      IMPLICIT COMPLEX*16 (A,B,I,N,R,T,D,C)
      INTEGER*4 I,J,M,IROW,ICOL,IR,IC,IT
      REAL*8 X,XN,XINT
C
      DIMENSION AA2(4,4),BB2(4),CC2(4),AA(2,2),BB(2),CC(2),LL2(4),LL(2),
     1MM2(4),MM(2)
C
      COMMON/COF/NU(2,24),TH00,TH01,TH10,TH11,R
      COMMON/INTG/INT(5,24)
C
      X=-1.0D0 + XINT/2.0D0
      IROW=0
C
CC    BEGIN MATRIX MANIPULATION. ROWS ARE X VARIABLE.
C
      DO 1000 J=1,L
C
      XN=-1.0D0
      DO 900 I=1,J
      IF(I.EQ.2) GO TO 900
      M=J-I+1
C
CC    RECOVER THE INTEGRALS.
      RI0= R*INT(1,M)
      RI1= X*RI0 - R*INT(2,M)
      BB0= TH10*RI0 + TH11*RI1
      BB1= TH00*RI0 + TH01*RI1
C
CC    SWITCH TO FIRST FOUR OR LATER COEFFICIENTS.
      IF(J.GT.2) GO TO 9011
C
CCC
CC    THE REFERENCE BLADE EQUATION.
      IROW= 1 + IROW
      AA2(IROW,1)=(1.0D0,0.0D0)
      AA2(IROW,2)=DCMPLX(X,0.0D0)
      AA2(IROW,3)= RI0
      AA2(IROW,4)= RI1
      BB2(IROW)=-BB0
C
CC    THE ADJACENT BLADE EQUATION.
      IROW=IROW + 1
      AA2(IROW,1)= RI0
      AA2(IROW,2)= RI1
      AA2(IROW,3)=(1.0D0,0.0D0)
      AA2(IROW,4)=DCMPLX(X,0.0D0)
```

```
      BB2(IROW)=-BB1
C
      IF(J.EQ.1) GO TO 900
C
CC    NOW SOLVE FOR THE COEFFICIENTS
C
      CALL CMINV(AA2,4,D,LL2,MM2)
C
CC    MULTIPLY THE RESULT
C
      DO 1 IR=1,4
      CC2(IR)=0.0D0
      DO 1 IC=1,4
    1 CC2(IR)= AA2(IR,IC)*BB2(IC) + CC2(IR)
C
CC    PLACE THE FIRST FOUR IN THE COEFFICIENT VECTOR.
C
      NU(1,1)=CC2(1)
      NU(1,2)=CC2(2)
      NU(2,1)=CC2(3)
      NU(2,2)=CC2(4)
      GO TO 900
C
CC    NOW, WE CALCULATE THE REMAINING COEFFICIENTS.
C
 9011 IF(I.GT.2) GO TO 9012
      REF=NU(1,1) + NU(2,1)*RI0 + NU(1,2)*X + NU(2,2)*RI1
      ADJ=NU(2,1) + NU(1,1)*RI0 + NU(2,2)*X + NU(1,2)*RI1
      RHSR=-REF - B30
      RHSA=-ADJ - BB1
      GO TO 900
C
 9012 CONTINUE
      A=X-XN
C
      IF(I.EQ.J) GO TO 997
      REF=NU(1,I)*A + NU(2,I)*(RI1 - XN*RI0)
      ADJ=NU(2,I)*A + NU(1,I)*(RI1 - XN*RI0)
      RHSR=RHSR - REF
      RHSA=RHSA - ADJ
      IF(I.NE.J) GO TO 900
  997 IF(J.GT.3) GO TO 998
C
CC    FILL THE MATRICES
      AA(1,1)=A
      AA(1,2)=RI1 - XN*RI0
      AA(2,1)=RI1 - XN*RI0
      AA(2,2)=A
```

```
C
CC      SOLVE.
C
        CALL CMINV(AA,2,D,LL,MM)
C
CC      MULTIPLY FOR THE RESULT
C
  998   NU(1,J)=AA(1,1)*RHSR + AA(1,2)*RHSA
        NU(2,J)=AA(2,1)*RHSR + AA(2,2)*RHSA
  900   XN=XN + XINT
 1000   X=X + XINT
C
        RETURN
        END
```

C-III. Subroutine INTEGR

Because of the variety of integrals required, they are calculated as soon as possible and stored for further reference in the matrix INT(5,m) carried by Common INTG.

Since the integrals are of the same form as those encountered in the Laplace solution, the same solution is used, with minor differences for the differing exponent J range. Subroutine ZSUM, borrowed from Elder [Ref. 7] and modified for B = E = 0.0, is utilized for the majority of the integrations. In the event that the Oswatitsch parameter is taken as zero, Subroutine COR is utilized to calculate the 'correction integral'.

INTEGR provides five different integrals, for the following sets of P and J values,

P \ J	1	2	3
0		x	x
ρ	x	x	x

for the ranges 0 to $X_n = -1.0 + XINT/2.0 + \sum_{n=2}^{L-1} XINT$ because

$$\int_0^X H(S-X_n)f(S)dS = \int_{X_n}^X f(S)dS = \int_0^{X-X_n} f(U)dU,$$

where

$$U = X-S.$$

Thence, the integrals are calculated stepwise, i.e. the range of integration starts as 0 to X_0, then X_0 to X_1, etc., until all necessary integrals are obtained.

```
      SUBROUTINE INTEGR(XINT,L)
C
      IMPLICIT REAL*8(A-H,O-Z)
      COMPLEX*16 COR1,COR2,COR3,INT,SUM1,SUM2,SUM3
      INTEGER*4 P
C
      COMMON/HOLD/B,C,D,E,EPS,RHO,P,LIM
      COMMON/INTG/INT(5,24)
C
      P=1
      PI=3.141592653589793
 2500 FORMAT('0','COR1=',2D13.5,/,' COR2=',2D13.5,/,' COR3=',2D13.5)
C
C     CALCULATIONS OF INTEGRALS
      DO 1 I=1,2
      IF(I.EQ.1) GO TO 2
      B=0.0D0
      E=B
      P=0
    2 CONTINUE
      XO=-XINT/2.0D0
      XA=1.0D-08
      IF(P.EQ.0) XA=1.0D-03
C
      COR1=0.0D0
      COR2=0.0D0
      COR3=0.0D0
C
      IF(B.GT.EPS.OR.P.EQ.0) GO TO 3
C
C     CASE FOR K.NE.0   DL=0
C
C     COMPUTE CORRECTION
C
      XA=RHO/100.0D0
      AR=E/XA
    4 SS=DSIN(AR)
      CC=DCOS(AR)
      CALL CS(CCC,SSS,AR)
      ARG=DSQRT(2.0D0*PI/E)
      SSS=ARG*(0.5D0-SSS)
      CCC=ARG*(0.5D0-CCC)
      CALL COR(XA,D,E,1,CC,SS,SSS,CCC,COR1)
      CALL COR(XA,D,E,2,CC,SS,SSS,CCC,COR2)
      CALL COR(XA,D,E,3,CC,SS,SSS,CCC,COR3)
C
      WRITE(6,2500)(COR1,COR2,COR3)
C
```

```
C       COMPUTE REMAINDER OF THE INTEGRAL
C
    3 DO 1 M=1,L
C
        XO=XINT + XO
        IF(I.EQ.2) GO TO 5
        SUM1=DCMPLX(0.0D0,0.0D0)
        CALL ZSUM(XA,XO,1,SUM1)
        K=1
        INT(K,M)= SUM1 + COR1
    5 CALL ZSUM(XA,XO,2,SUM2)
        K=2 + 2*(I-1)
        INT(K,M)= SUM2 + COR2
        CALL ZSUM(XA,XO,3,SUM3)
        K=K + 1
        INT(K,M)= SUM3 + COR3
C
        XA=XO
        COR1=SUM1 + COR1
        COR2=SUM2 + COR2
        COR3=SUM3 + COR3
C
    1 CONTINUE
        RETURN
        END
```

C-IV. Subroutines COR and ZSUM

Subroutine COR is an adaptation of the more general routine for the 'correction integral' used in the Porous Tunnel Wall program described in Appendix D-V.

Subroutine ZSUM is a modification of Elder's [Ref. 7] pyramided Simpson's Rule integration routine to include $p = 0$ corrections (see Section III-D).

C-V. Subroutine CMINV

Subroutine CMINV inverts the complex matrices for Subroutine COEFF. It is an outgrowth of a Library Subroutine.

```
      SUBROUTINE COR(XA,D,E,J,C,S,SS,CC,COR)
C     ..................................................................
CCC
CCC                        SUBROUTINE COR
CCC   COMPUTATION OF THE CORRECTION TO INTEGRAL U**(J-2.5)*COS OR
CCC   SIN(DU+E/U) FOR THE CASE OF DL=0 AND J=1 AND 2.
CCC
C     ..................................................................
      IMPLICIT REAL*8(A-H,O-Z)
      COMPLEX*16 COR
      DIMENSION SI(4),CI(4)
C
C
      IF(J.GE.2) GO TO 12
C
C
      DEN=-1.0D0
      Z=1.0D0/DSQRT(XA)
      DO 10 I=1,4
      IF(I.EQ.1) GO TO 11
      DEN=DEN + 2.0D0
      Z=XA*Z
      SI(I)=2.0D0*(Z*S + E*CC)/DEN
      CI(I)=2.0D0*(Z*C - E*SS)/DEN
      GO TO 15
   11 SI(1)=SS
      CI(1)=CC
   15 CONTINUE
      CC=CI(I)
   10 SS=SI(I)
      GO TO 14
   12 DO 13 I=1,3
      SI(I)=SI(I+1)
   13 CI(I)=CI(I+1)
C
      SI(4)=0.0D0
      CI(4)=0.0D0
   14 CONTINUE
C
CCC   UTILIZE THE SIN AND COS TRUNCATED SERIES TO OBTAIN THE FINAL
CCC   INTEGRAL CORRECTION.
C
      SCOR=SI(1)+D*(CI(2)-D*(SI(3)/2.0D0+D*CI(4)/6.0D0))
      CCOR=CI(1)-D*(SI(2)+D*(CI(3)/2.0D0-D*SI(4)/6.0D0))
      COR= DCMPLX(CCOR,-SCOR)
      RETURN
      END
```

```
      SUBROUTINE ZSUM(XA,XO,J,SUM)
C
CCCC
```

```
C
CC
CC      ESTABLISH THE RIGHT END POINT
C
        U=XO
        AA=C*U-B/U
        BB=D*U+E/U
        CC=D*U-E/U
        YOR=YR(U,J,AA,BB)
        YOI=YI(U,J,AA,BB)
        EE=DEXP(AA)*U**(J-2)/(U*DSQRT(U))
        FF=DFLOAT(J)-2.5D0+C*U+B/U
        YORP=EE*(DCOS(BB)*FF-CC*DSIN(BB))
        YOIP=(-EE)*(DSIN(BB)*FF+CC*DCOS(BB))
C
CC      ESTABLISH INTERVAL
C
        DINT=XO-XA
        SOR=0.0D0
        SOI=0.0D0
        SER=0.0D0
        SEI=0.0D0
        SUMR=0.0D0
        SUMI=0.0D0
C       INITIAL SPACING AND NUMBER OF TERMS IN EVEN SUM
        SP=2.0D0
        K=1
C
CC      LOOP  SPECIFYING INTERVAL
C
        DO 100 M=1,LIM
        H=DINT/SP
C       SET OLD EVEN SUM INTO ODD SUM
        SOR=SOR+SER
        SOI=SOI+SEI
        XE=XA+H
C       ZEROIZE EVEN SUM
        SER=0.0D0
        SEI=0.0D0
C
CC      LOOP TO ESTABLISH EVEN SUM
C
        DO 10 I=1,K
        AA=C*XE-B/XE
        IF(AA.LE.(-172.0D0)) GO TO 4
        BB=D*XE+E/XE
        YER=YR(XE,J,AA,BB)
        YEI=YI(XE,J,AA,BB)
```

```
      GO TO 5
    4 YER=0.0D0
      YEI=0.0D0
    5 CONTINUE
      SER=SER+YER
      SEI=SEI+YEI
   10 XE=XE+2.0D0*H
C
CC    FORM THE INTEGRAL
C
      TEMPR=SUMR
      TEMPI=SUMI
      SUMR=H*(7.0D0*(YAR+YOR)+16.0D0*SER+14.0D0*SOR)/15.0D0
      SUMR=SUMR+H**2*(YARP-YORP)/15.0D0
      SUMI=H*(7.0D0*(YAI+YOI)+16.0D0*SEI+14.0D0*SOI)/15.0D0
      SUMI=SUMI+H**2*(YAIP-YOIP)/15.0D0
      L=M
C
CC    TEST FOR CONVERGENCE
C
      TTTR=DABS(TEMPR-SUMR)
      TTTI=DABS(TEMPI-SUMI)
      IF(TTTR.LE.EPS.AND.TTTI.LE.EPS) GO TO 101
C
CC    PROVIDE FOR ERROR STATEMENT IF NO CONVERGENCE
C
      IF(M.EQ.LIM) GO TO 1
      GO TO 9
    1 WRITE(6,2)
    9 K=K*2
      SP=SP*2.0D0
  100 CONTINUE
  101 CONTINUE
C
CC    IF E=B=0, COMPUTE THE LEFT END POINT TERMS.
C
      IF(P.NE.0) GO TO 102
      IF(J.NE.2) GO TO 102
      IF(XA.GT.1.0D-02) GO TO 102
C
      SUMR=2.0D0*(1.0D0 + C*XA/3.0D0 - (D*XA-C*XA)**2/10.0D0)*DSQRT(XA)
     1 + SUMR
      SUMI=2.0D0*(XA/3.0D0 + C*XA*XA/5.0D0)*D*DSQRT(XA) - SUMI
      SUMI=-SUMI
  102 CONTINUE
      SUM=DCMPLX(SUMR,SUMI)
      RETURN
      END
```

```
      SUBROUTINE CMINV(A,N,D,L,M)                                       MINV  10
      COMPLEX*16 A,D,BIGA,HOLD                                          MINV  20
      DIMENSION A(1),L(1),M(1)                                          MINV  30
C     ...................................................................MINV  60
C                                                                       MINV  80
C        PURPOSE                                                        MINV 120
C           INVERT A COMPLEX MATRIX (A) = (B)+I(C)                      MINV 130
C                                                                       MINV 140
C        DESCRIPTION OF PARAMETERS                                      MINV 150
C           A - INPUT MATRIX, DESTROYED IN COMPUTATION AND REPLACED BY  MINV 160
C               RESULTANT INVERSE.                                      MINV 170
C           N - ORDER OF MATRIX A                                       MINV 180
C           D - RESULTANT DETERMINANT                                   MINV 190
C           L - WORK VECTOR OF LENGTH N                                 MINV 200
C           M - WORK VECTOR OF LENGTH N                                 MINV 210
C                                                                       MINV 220
C        REMARKS                                                        MINV 260
C           MATRIX A MUST BE A GENERAL MATRIX                           MINV 270
C                                                                       MINV 280
C        METHOD                                                         MINV 290
C           THE STANDARD GAUSS-JORDAN METHOD IS USED. THE DETERMINANT   MINV 300
C           IS ALSO CALCULATED. A DETERMINANT OF ZERO INDICATES THAT    MINV 310
C           THE MATRIX IS SINGULAR.                                     MINV 320
C     ...................................................................MINV 540
C                                                                       MINV 550
C        SEARCH FOR LARGEST ELEMENT                                     MINV 570
      D=DCMPLX(1.0D0,0.0D0)                                             MINV 580
      NK=-N                                                             MINV 590
      DO 80 K=1,N                                                       MINV 600
      NK=NK+N                                                           MINV 610
      L(K)=K                                                            MINV 620
      M(K)=K                                                            MINV 630
      KK=NK+K                                                           MINV 640
      BIGA=A(KK)                                                        MINV 650
      DO 20 J=K,N                                                       MINV 660
      IZ=N*(J-1)                                                        MINV 670
      DO 20 I=K,N                                                       MINV 690
      IJ=IZ+I                                                           MINV 700
   10 IF(CDABS(BIGA) - CDABS(A(IJ))) 15,20,20                           MINV 710
   15 BIGA=A(IJ)                                                        MINV 720
      L(K)=I                                                            MINV 730
      M(K)=J                                                            MINV 740
   20 CONTINUE
C
C        INTERCHANGE ROWS
```

```
C                                                                       MINV 750
      J=L(K)                                                            MINV 760
      IF(J-K) 35,35,25                                                  MINV 770
   25 KI=K-N                                                            MINV 780
      DO 30 I=1,N                                                       MINV 790
      KI=KI+N                                                           MINV 800
      HOLD=-A(KI)                                                       MINV 810
      JI=KI-K+J                                                         MINV 820
      A(KI)=A(JI)                                                       MINV 830
   30 A(JI) =HOLD                                                       MINV 840
C                                                                       MINV 850
CC         INTERCHANGE COLUMNS                                          MINV 860
C                                                                       MINV 870
   35 I=M(K)                                                            MINV 880
      IF(I-K) 45,45,38                                                  MINV 890
   38 JP=N*(I-1)                                                        MINV 900
      DO 40 J=1,N                                                       MINV 910
      JK=NK+J                                                           MINV 920
      JI=JP+J                                                           MINV 930
      HOLD=-A(JK)                                                       MINV 940
      A(JK)=A(JI)                                                       MINV 950
   40 A(JI) =HOLD                                                       MINV 960
C                                                                       MINV 970
CCC        DIVIDE COLUMN BY MINUS PIVOT (VALUE OF PIVOT ELEMENT IS      MINV 980
C          CONTAINED IN BIGA)                                           MINV 990
C                                                                       MINV1000
   45 IF(CDABS(BIGA)) 48,46,48
   46 D=DCMPLX(0.0D0,0.0D0)
      RETURN                                                            MINV1030
   48 DO 55 I=1,N                                                       MINV1040
      IF(I-K) 50,55,50                                                  MINV1050
   50 IK=NK+I                                                           MINV1060
      A(IK)=A(IK)/(-BIGA)                                               MINV1070
   55 CONTINUE                                                          MINV1080
C                                                                       MINV1090
CC         REDUCE MATRIX                                                MINV1100
C                                                                       MINV1110
      DO 65 I=1,N                                                       MINV1120
      IK=NK+I                                                           MINV1130
      HOLD=A(IK)                                                        MINV1140
      IJ=I-N                                                            MINV1150
      DO 65 J=1,N                                                       MINV1160
      IJ=IJ+N                                                           MINV1170
      IF(I-K) 60,65,60                                                  MINV1180
   60 IF(J-K) 62,65,62                                                  MINV1190
   62 KJ=IJ-I+K                                                         MINV1200
      A(IJ)=HOLD*A(KJ)+A(IJ)                                            MINV1210
   65 CONTINUE                                                          MINV1220
```

```
C
CC          DIVIDE ROW BY PIVOT                                          MINV1230
C                                                                        MINV1240
                                                                         MINV1250
      KJ=K-N                                                             MINV1260
      DO 75 J=1,N                                                        MINV1270
      KJ=KJ+N                                                            MINV1280
      IF(J-K) 70,75,70                                                   MINV1290
   70 A(KJ)=A(KJ)/BIGA                                                   MINV1300
   75 CONTINUE                                                           MINV1310
C                                                                        MINV1320
CC          PRODUCT OF PIVOTS                                            MINV1330
C                                                                        MINV1340
      D=D*BIGA                                                           MINV1350
C                                                                        MINV1360
CC          REPLACE PIVOT BY RECIPROCAL                                  MINV1370
C                                                                        MINV1380
      A(KK)=1.0/BIGA                                                     MINV1390
   80 CONTINUE                                                           MINV1400
C                                                                        MINV1410
CC          FINAL ROW AND COLUMN INTERCHANGE                             MINV1420
C                                                                        MINV1430
      K=N                                                                MINV1440
  100 K=(K-1)                                                            MINV1450
      IF(K) 150,150,105                                                  MINV1460
  105 I=L(K)                                                             MINV1470
      IF(I-K) 120,120,108                                                MINV1480
  108 JQ=N*(K-1)                                                         MINV1490
      JR=N*(I-1)                                                         MINV1500
      DO 110 J=1,N                                                       MINV1510
      JK=JQ+J                                                            MINV1520
      HOLD=A(JK)                                                         MINV1530
      JI=JR+J                                                            MINV1540
      A(JK)=-A(JI)                                                       MINV1550
  110 A(JI) =HOLD                                                        MINV1560
  120 J=M(K)                                                             MINV1570
      IF(J-K) 100,100,125                                                MINV1580
  125 KI=K-N                                                             MINV1590
      DO 130 I=1,N                                                       MINV1600
      KI=KI+N                                                            MINV1610
      HOLD=A(KI)                                                         MINV1620
      JI=KI-K+J                                                          MINV1630
      A(KI)=-A(JI)                                                       MINV1640
  130 A(JI) =HOLD                                                        MINV1650
      GO TO 100                                                          MINV1660
  150 CONTINUE
C
      RETURN
      END
```

APPENDIX D

FORMULATION OF THE SONIC POROUS WALL WIND TUNNEL ROUTINE

D-I. Main Program

This Main program is very similar to the Main program detailed in Appendix C-I for the Collocation solution of the cascade problem. Provision is made in this routine, however, for the placement of the 'tunnel wall' at Y = ρ/2 (which will be RHO in this program). Furthermore, two different Oswatitsch parameters may be utilized, one for the airfoil, DL, and one for the wall, DLW. Because the wall has no 'isolated blade' source distribution, TH10 and TH11 do not appear. Also, derivatives are made available so as to calculate the pressure coefficient as well as the velocity potential. Finally, the variable, SIGWL is the porosity factor (see Section V), which can be made variable along the wall (see Subroutine COEFF here).

The Main program not only controls the calculation of the integrals required, by calling Subroutine INTEGR, and obtains the appropriate interference source distribution series coefficients from COEFF, it calculates the potential, POT, and the pressure coefficient, CP, at the selected locations (collocation points) along the chord.

From Section V the potential on the airfoil is

$$\psi(X,0) = \phi_0^0(X,0) + \phi_1(X,0) + \phi_1(X,Y_1=-\rho). \qquad \text{(D-I-1)}$$

Also

$$\psi_X(X,0) = \phi^0_{0X}(X,0) + \phi_{0X}(X,0) + \phi_{1X}(X,Y_1=-\rho). \qquad \text{(D-I-2)}$$

The pressure coefficient is

$$C_P(X,0) = -2[\psi_X(X,0) + iK\psi(X,0)]. \qquad \text{(D-I-3)}$$

By introducing the step-wise-linear series used in the Collocation solution for the cascade (equations III-81 and 82) equation V-2 becomes,

$$\psi(X,0) = -R_2\{[\theta_{00}+\nu_{00}]PI00 + [\theta_{01}+\nu_{01}]PI01 + \sum_{n=2}^{L-1}\nu_{0n}PI0N\}$$

$$+R_3[\nu_{10}PI10+\nu_{11}PI11 + \sum_{n=2}^{L-1}\nu_{1n}PI1N], \qquad \text{(D-I-4)}$$

where,

$$PI00 = \int_{-1}^{X}\frac{Exp[C]}{\sqrt{X-S}}dS, \quad PI01 = X\int_{-1}^{X}\frac{Exp[C]}{\sqrt{X-S}} - \int_{-1}^{X}\frac{Exp[C]}{(X-S)^{-1/2}}dS,$$

$$PI0N = PI01 - XN\cdot PI00, \qquad C = \frac{K^2}{Q_0}(X-S),$$

$$R2 = \rho/2\cdot\sqrt{\frac{Q_0}{\pi}}, \qquad \text{(D-I-5)}$$

and, for PI10, PI11, and PI1N,

$$C = \frac{K^2}{Q_1}(X-S) - \frac{Q_1}{4}\frac{\rho^2}{(X-S)} ,$$

$$R_3 = \rho/2\sqrt{\frac{Q_1}{\pi}} .$$

Then, for the X derivative of the potential, all of the PIxx terms of the potential are preceded by a D, denoting the derivative. The appropriate differentiated integrals are obtained from Section V-A-3.

$$DPI00 = \frac{\partial}{\partial X}\int_{-1}^{X} \frac{Exp[\frac{K^2}{Q_0}(X-S)]}{\sqrt{X-S}}\,dS = \frac{Exp[\frac{K^2}{Q_0}(X-S_n)]}{\sqrt{X-X_n}} \qquad (D\text{-}I\text{-}6)$$

etc.

```
C      MASTER ROUTINE FOR TRANSSONIC WIND TUNNELS. UTILIZES AN ADAPTATION
C      OF COLLOCATION ROUTINES.
C
CC
C
       IMPLICIT REAL*8 (A-C,E-H,S,U-Z)
       IMPLICIT COMPLEX*16 (D,N,Q,R,T,P)
       REAL*8 RHO,PI,DK,DL,DLW,D,TAU
       COMPLEX*16 INT,CP
       INTEGER*4 P
C
CC
       COMMON/HOLD/B,C,D,E,EPS,RHO,DK,DLW,Y,LIM
       COMMON/COF/VU(2,24),TH00,TH01,Q0,Q1,R0,R1,R2,R3,SIGWL
       COMMON/INTG/INT(12,24)
C
     1 FORMAT('1',5X,' DK=',D12.4,2X,' DL=',D12.4,2X,' RHO=',D12.4,2X,' L
      1=',I2,2X,' DLW=',D12.4)
C
       PI=3.141592653589793
       LIM=50
       EPS=1.0D-8
       XMAX=1.0D0
       TEMP=0.0D0
C
CCCC   ..........................................................
CCC    INITIALIZATION SECTION
CCC    SET THE CONTROLLING VARIABLES   DK,DL,RHO, AND L.
C
       EHO=35.0D0/12.0D0
       DK=.1D0
       TAU=.06D0
       DL=1.559D0*(2.4D0*TAU)**(2.0D0/3.0D0)
       DLW=DL
       L=10
C
       RHO=EHO/2.0D0
C
CC     ..........................................................
       WRITE(6,1) DK,DL,EHO,L,DLW
C
       IF(DK.GT.0) GO TO 2
       A=0.0D0
       GO TO 3
     2 A= DK*DK/(DL*DL + 4.0D0*DK*DK)
```

```
    3 B= DL*RHO*RHO/4.0D0
      C= DL*A
      D= 2.0D0*DK*A
      E= DK*RHO*RHO/2.0D0
C
      Q0= DCMPLX(DL,2.0D0*DK)
      Q1= DCMPLX(DLW,2.0D0*DK)
      R2=-1.0D0/CDSQRT(PI*Q0)
      R3= 1.0D0/CDSQRT(PI*Q1)
C
      TH00= -1.0D0
      TH01= -DCMPLX(0.0D0,DK)
C
C     SET THE NUMBER OF STATIONS ON THE FOIL, STATION ONE, AND INTERVAL
      XINT=-(-1.0D0 - XMAX)/DFLOAT(L)
C
C
C     ..................................................................
C
C     CALL INTEGRALS FOR CALCULATION.
      CALL INTEGR(XINT,L)
      WRITE(6,11) ((K,M,INT(K,M),M=1,L),K=1,12)
   11 FORMAT(  3(' INT(',I2,',',I2,')=',2D12.4,5X))
C
      R0= (RHO/2.0D0)*CDSQRT(Q0/PI)
      R1= (RHO/2.0D0)*CDSQRT(Q1/PI)
C     ..................................................................
C
C     CALCULATION OF THE COEFFICIENTS.
C
      CALL COEFF(XINT,L,DK,RHO)
      WRITE(6,9004) (NU(1,I),NU(2,I),I=1,L)
 9004 FORMAT(//,' THE COEFFICIENTS   ',5X,'NU(1,I)',22X,'NU(2,I)',/,
     1(25X,2D12.4,5X,2D12.4,/))
C
C     SOLVE FOR THE POTENTIALS.
C
      R0=R2
      R1=R3
      X=-1.0D0 + XINT/2.0D0
      DO 7 J=1,L
C
      XN=-1.0D0
      DO 4 I=1,J
      IF(I.EQ.2) GO TO 4
C
      M=J-I+1
C
```

```
C       REFERENCE BLADE
        PI00= INT(5,M)
        PI01= X*PI00 - INT(6,M)
        DPI00= CDEXP(DK*DK*(X - XN)/Q0)/DSQRT(X - XN)
        DPI01= 0.5D0*PI00 + X*DPI00 - DK*DK*INT(6,M)/Q0
C       ADJACENT BLADE
        PI10= INT(9,M)
        PI11= X*PI10 - INT(10,M)
        DPI10= DK*DK*PI10/Q1 + Q1*RHO*RHO*INT(7,M)/4.0D0 - .5D0*INT(8,M)
        DPI11= 0.5D0*PI10 + X*DPI10 - DK*DK*INT(10,M)/Q1 - Q1*RHO*RHO*INT(
       28,M)/4.0D0
C
C
        IF(I.GT.1) GO TO 8
C       FIRST, THE CONSTANT TERMS.
C
        POT= R0*((TH00  + NU(1,1))*PI00 + (TH01  + NU(1,2))*PI01)  +
       2 R1*(NU(2,1)*PI10 + NU(2,2)*PI11)
        DPOT= R0*((TH00  + NU(1,1))*DPI00+ (TH01  + NU(1,2))*DPI01) +
       2 R1*(NU(2,1)*DPI10 + NU(2,2)*DPI11)
        XN= XN + 2.0D0*XINT
        GO TO 4
C
C       NOW THE REMAINING TERMS.
C
      8 POT= POT + R0*NU(1,I)*(PI01 - XN*PI00) +
       2 R1*NU(2,I)*(PI11 - XN*PI10)
        DPOT= DPOT + R0*NU(1,I)*(DPI01 - XN*DPI00) +
       2 R1*NU(2,I)*(DPI11 - XN*DPI10)
C
        XN=XN + XINT
      4 CONTINUE
C
        CP=-2.0D0*(DPOT + (0.0D0,1.0D0)*DK*POT)
C
      5 WRITE(6,6) X,POT,DPOT,CP
      6 FORMAT(///,4X,' X=',D12.4,' POT=',2D12.4,' DPOT=',2D12.4,' CP=',
       2 2D12.4)
C
        X=X+XINT
      7 CONTINUE
C
        STOP
        END
```

D-II. Subroutine COEFF

As the Main routine, this routine differs only in certain details from the Collocation routine for the cascade. Of greatest importance is the handling of the wall boundary condition equation, equation (V-5)

$$\phi^{0}_{0Y}(X,Y_0=\rho) + \phi_{0Y}(X,Y_0=\rho) + \phi_{1Y}(X,Y_1=0) +$$

$$\sigma_{w\ell}\{[\phi^{0}_{0X}(X,Y_0=\rho) + \phi_{0X}(X,Y_0=\rho) + \phi_{1X}(X,Y_1=0)]$$

$$+ iK[\phi^{0}_{0}(X,Y_0=\rho) + \phi_{0}(X,Y_0=\rho) + \phi_{1}(X,Y_1=0)]\} = 0. \quad (D\text{-}I\text{-}7)$$

The organization of the solution for the coefficients is the same as that in Appendix C-II save for the inclusion of the SIGWL, the deletion of the isolated adjacent blade potential and normal velocity component, and a slight change in notation.

Illustrated is the approach for varying the porosity. SIGWL is calculated by the appropriate function in COEFF and used as necessary.

```
      SUBROUTINE COEFF(XINT,L,DK,RHO)
C
      IMPLICIT COMPLEX*16 (A,B,I,N,R,T,D,C,Q)
      INTEGER*4 I,J,M,IROW,ICOL,IR,IC,IT
      REAL*8 X,XN,XINT,SIGMA,DK,RHO,ZERO
C
      DIMENSION AA2(4,4),BB2(4),CC2(4),AA(2,2),BB(2),CC(2),LL2(4),LL(2),
     1MM2(4),MM(2),CHKM(4,4)
C
      COMMON/COF/NU(2,24),TH00,TH01,Q0,Q1,R0,R1,R2,R3,SIGWL
      COMMON/INTG/INT(12,24)
C
      IROW=0
      X=-1.0D0 + XINT/2.0D0
C
C     BEGIN MATRIX MANIPULATION. ROWS ARE X VARIABLE.
C
      DO 1000 J=1,L
C
      SIGWL=5.0D0*(X+1.0D0)
      XN=-1.0D0
      DO 900 I=1,J
      IF(I.EQ.2) GO TO 900
      M=J-I+1
C
C     RECOVER THE INTEGRALS.
      RI00 = R0*INT(2,M)
      RDI00= R2*(DK*DK*INT(3,M)/Q0 + Q0*RHO*RHO*INT(1,M)/4.0D0 -
     2 .5D0*INT(2,M))
      RKI00= R2*INT(3,M)
C
      RI01= X*RI00 - R0*INT(3,M)
      RDI01= X*RDI00 + R2*(INT(3,M) - (DK*DK*INT(4,M)/Q0 +
     2 Q0*RHO*RHO*INT(2,M)/4.0D0 + .5D0*INT(3,M)))
      RKI01= X*RKI00 - R2*INT(4,M)
C
      RI10= R1*INT(8,M)
      RDI10= R3*(CDEXP(DK*DK*(X - XN)/Q1)/DSQRT(X - XN))
      RKI10= R3*INT(11,M)
C
      RI11= X*RI10 - R1*INT(9,M)
      RDI11= X*RDI10 + R3*(INT(11,M) - (DK*DK*INT(12,M)/Q1 +
     2 .5D0*INT(11,M)))
      RKI11= X*RKI10 - R3*INT(12,M)
C
      RI00= RI00 + SIGWL*(RDI00 + DK*(0.0D0,1.0D0)*RKI00)
      RI01= RI01 + SIGWL*(RDI01 + DK*(0.0D0,1.0D0)*RKI01)
      IR3= SIGWL*(RDI10 + DK*(0.0D0,1.0D0)*RKI10)
```

```
      IR4= SIGWL*(RDI11 + DK*(0.0D0,1.0D0)*R(I11)
      IRBB=-(TH00*RI00 + TH01*RI01)
C
C     SWITCH TO FIRST FOUR OR LATER COEFFICIENTS.
      IF(J.GT.2) GO TO 9011
C
CC    THE CONSTANT TERMS
C
C     THE REFERENCE BLADE.
  901 IROW= 1 + IROW
      AA2(IROW,1)=(1.0D0,0.0D0)
      AA2(IROW,2)=DCMPLX(X,0.0D0)
      AA2(IROW,3)= RI10
      AA2(IROW,4)= RI11
      BB2(IROW)=0.0D0
C
CC    NOW THE ADJACENT BLADE.
C
      IROW=IROW + 1
      AA2(IROW,1)= RI00
      AA2(IROW,2)= RI01
      AA2(IROW,3)=(1.0D0,0.0D0)        + IR3
      AA2(IROW,4)=DCMPLX(X,0.0D0)        + IR4
      BB2(IROW)= IRBB
C
C
      IF(J.EQ.1) GO TO 900
C
CC    NOW SOLVE FOR THE COEFFICIENTS
C
      CALL CMINV(AA2,4,D,LL2,MM2)
C
CC    MULTIPLY THE RESULT
C
      DO 1 IR=1,4
      CC2(IR)=0.0D0
      DO 1 IC=1,4
    1 CC2(IR)= AA2(IR,IC)*BB2(IC) + CC2(IR)
C
CC    PLACE THE FIRST FOUR IN THE COEFFICIENT VECTOR.
C
      NU(1,1)=CC2(1)
      NU(1,2)=CC2(2)
      NU(2,1)=CC2(3)
      NU(2,2)=CC2(4)
      GO TO 900
C
```

```
C      NOW, WE CALCULATE THE REMAINING COEFFICIENTS.
C
 9011 IF(I.GT.2) GO TO 9012
      REF=NU(1,1) + NU(2,1)*RI10 + NU(1,2)*X + NU(2,2)*RI11
      ADJ= NU(2,1)*(1.0D0 + IR3) + NU(1,1)*RI00 + NU(2,2)*(X + IR4) +
     2 NU(1,2)*RI01
      RHSR=-REF
      RHSA=-ADJ + IRBB
      GO TO 900
C
 9012 CONTINUE
      A1= X - XN
      A2= A1        + (IR4 - XN*IR3)
      IF(I.EQ.J) GO TO 997
C
      REF=NU(1,I)*A1+ NU(2,I)*(RI11 - XN*RI10)
      ADJ=NU(2,I)*A2+ NU(1,I)*(RI01 - XN*RI00)
      RHSR=RHSR - REF
      RHSA=RHSA - ADJ
      GO TO 900
C
  997 IF(J.GT.3) GO TO 998
C
C      FILL THE MATRICES
      AA(1,1)=A1
      AA(1,2)=RI11 - XN*RI10
      AA(2,1)=RI01 - XN*RI00
      AA(2,2)=A2
C
C      SOLVE.
C
      CALL CMINV(AA,2,D,LL,MM)
C
C      MULTIPLY FOR THE RESULT
C
  998 NU(1,J)=AA(1,1)*RHSR + AA(1,2)*RHSA
      NU(2,J)=AA(2,1)*RHSR + AA(2,2)*RHSA
  900 XN=XN + XINT
 1000 X=X + XINT
C
      RETURN
END
```

D-III. Subroutine INTEGR

This routine is similar to that described in Appendix C-III except it is more complex to calculate the additional integrals required.

```
      SUBROUTINE INTEGR(XINT,L)
C
      IMPLICIT REAL*8(A-H,O-Z)
      COMPLEX*16 COR0,COR1,COR2,COR3,SUM0,SUM1,SUM2,SUM3,INT
      INTEGER*4 P
      COMMON/HOLD/B,C,D,E,EPS,RHO,DK,DLW,P,LIM
      COMMON/INTG/INT(12,24)
      PI=3.14159265358979 3
 2500 FORMAT('0','COR0=',2D13.5,/,' COR1=',2D13.5,/,' COR2=',2D13.5,
     1/,' COR3=',2D13.5)
C
C
      DO 10 I=1,4
      IF(I.EQ.3) GO TO 23
      P=1
      IF(I-2) 3,1,2
C     FOR REFERENCE BLADE POTENTIAL GENERATION.
    1 B=0.0D0
      E=0.0D0
      P=0
      GO TO 3
C     FOR ADJACENT BLADE USE IN ALL CASES. DL=0.
    2 A= DK*DK/(DLW*DLW + 4.0D0*DK*DK)
      B=DLW*RHO*RHO/4.0D0
      C=DLW*A
      D=2.0D0*DK*A
      E= DK*RHO*RHO/2.0D0
      IF(I.LT.4) GO TO 3
      P=1
      B=0.0D0
      E=0.0D0
      P=0
    3 CONTINUE
C
C     CALCULATIONS OF INTEGRALS
      X0=-XINT/2.0D0
      XA=1.0D-08
      IF(I.EQ.2.OR.I.EQ.4) XA=1.0D-03
C
      COR0=0.0D0
      COR1=0.0D0
      COR2=0.0D0
      COR3=0.0D0
C
      IF(B.GT.EPS.OR.I.EQ.2.OR.I.EQ.4) GO TO 6
C
C     CASE FOR K.NE.0   DL=0
C
```

```
C       COMPUTE CORRECTION
C
        XA=RHO/100.0D0
        AR=E/XA
        SS=DSIN(AR)
        CC=DCOS(AR)
        CALL CS(CCC,SSS,AR)
        ARG=DSQRT(2.0D0*PI/E)
        SSS=ARG*(0.5D0-SSS)
        CCC=ARG*(0.5D0-CCC)
        IF(I.EQ.2.OR.I.EQ.4) GO TO 5
        CALL COR(XA,D,E,0,CC,SS,SSS,CCC,COR0)
        CALL COR(XA,D,E,1,CC,SS,SSS,CCC,COR1)
    5   CALL COR(XA,D,E,2,CC,SS,SSS,CCC,COR2)
        CALL COR(XA,D,E,3,CC,SS,SSS,CCC,COR3)
C
        WRITE(6,2500)(COR0,COR1,COR2,COR3)
C
C       COMPUTE REMAINDER OF THE INTEGRAL
C
        XA=AL
    6   DO 10 M=1,L
C
        K=(I-1)*4 + 1
        IF(I.GT.2) K=K-2
C
        XO=XINT + XO
C
        IF(I.EQ.2.OR.I.EQ.4) GO TO 8
        CALL ZSUM(XA,XO,0,SUM0)
        INT(K,M)=SUM0 + COR0
        K=K+1
        CALL ZSUM(XA,XO,1,SUM1)
        INT(K,M)=SUM1 + COR1
        K=K+1
    8   CALL ZSUM(XA,XO,2,SUM2)
        INT(K,M)=SUM2 + COR2
        K=K+1
        CALL ZSUM(XA,XO,3,SUM3)
        INT(K,M)=SUM3 + COR3
C
        XA=XO
        COR0=SUM0 + COR0
        COR1=SUM1 + COR1
        COR2=SUM2 + COR2
        COR3=SUM3 + COR3
C
   10   CONTINUE
```

```
C       FOR THE CASE DL=DLW.
   23 DO 24 M=1,L
      DO 24 N=1,6
      N1=N+6
   24 INT(N1,M)=INT(N,M)
      RETURN
      END
```

D-IV. Subroutine COR

Subroutine COR calculates the 'correction integral' when commanded by Subroutine INTEGR, using equation (III-99). The 'correction integral' is obtained by summing the terms of a truncated series, here SI(I) and CI(I), I = 0,1,2, and 3. SI(I) and CI(I) are integrals of the form

$$\int_0^{XA} U^{m/2} \begin{matrix}\cos\\ \sin\end{matrix}(E/U)\, dU$$

which can be evaluated by integration by parts and use of the Fresnel Integrals (see Section III-D). Elder [Ref. 7] noted that this is possible and reasonably accurate for powers of U less than about 1.5. In any event, integrals of larger powers are very small.

COR calculates the terms by liberal use of equations (III-101 and 102). It must be noted that for j = 0 the use of equation (III-101) is not direct, i.e., j = 1 is inserted into (III-101) and the resulting integral on the right hand side is the desired j = 0 integral

$$\int_0^{XA} U^{-5/2} \begin{matrix}\sin\\ \cos\end{matrix}(E/U)dU = \pm\frac{1}{2E}\left\{\int_0^{XA} U^{-3/2} \begin{matrix}\cos\\ \sin\end{matrix}(E/U)dU + 2XA^{-3/2}\begin{matrix}\cos\\ \sin\end{matrix}(E/XA)\right\}$$

Thus, it can be seen why the involved logic is contained in COR so as to calculate ocrrections for j = 0 without destroying the basic form of COR.

Of course, once $j = 0$ and 1 corrections have been calculated no further calculations of terms must be performed as they are deemed adequately small to neglect.

```
      SUBROUTINE COR(XA,D,E,J,C,S,SS,CC,COR)
C     ..................................................................
C
C                          SUBROUTINE COR
C     COMPUTATION OF THE CORRECTION TO INTEGRAL U**(J-2.5)*COS OR
C     SIN(DU+E/U) FOR THE CASE OF DL=0 AND J=0 THROUGH 3.
C
C     THE CORRECTION IS FOR THE ILLBEHAVED PORTION OF THE INTEGRAL NEAR
C     ZERO WHICH CANNOT BE COMPUTED BY NUMERICAL METHODS.  LIMITS ON THE
C     CORRECTION ARE ZERO TO XA.  D AND E ARE FIXED FUNCTIONS OF DK AND
C     RHO.  J IS A FUNCTION OF N.  S AND C ARE THE FUNCTIONS SIN(E/AL)
C     AND COS(E/AL).  SS AND CC ARE FUNCTIONS OF THE BASIC FRESNEL
C     INTEGRALS.
C
C     THE METHOD UTILIZES A TRUNCATED SIN AND COS SERIES APPROXIMATION
C     AND A REDUCTION SUBROUTINE WHICH REDUCES THE INTEGRAL TO A BASIC
C     FUNCTION OF THE FRESNEL INTEGRAL.
C
C     THE VALUES OF THE SIN AND COS INTEGRAL CORRECTION ARE RETURNED ON
C     SCOR AND CCOR RESPECTIVELY
C
C     ..................................................................
C
      IMPLICIT REAL*8(A-H,O-Z)
      COMPLEX*16 COR
      DIMENSION SI(4),CI(4)
C
      IF(J.NE.0) GO TO 17
      TEMPSS=SS
      TEMPCC=CC
      GO TO 18
   17 SS=TEMPSS
      CC=TEMPCC
   18 CONTINUE
C
      IF(J.GE.2) GO TO 12
C
C
      DEN=-1.0D0
      Z=1.0D0/DSQRT(XA)
      DO 10 I=1,4
      IF(I.EQ.1) GO TO 11
      DEN=DEN + 2.0D0
      Z=XA*Z
   11 SI(I)=2.0D0*(Z*S + E*CC)/DEN
      CI(I)=2.0D0*(Z*C - E*SS)/DEN
      GO TO 15
```

```
   11 SI(1)=SS
      CI(1)=CC
   15 CONTINUE
      CC=CI(I)
   10 SS=SI(I)
C
      IF(J.NE.0) GO TO 14
      II=4
      DO 16 I=1,3
      II=II-1
      SI(II+1)=SI(II)
      CI(II+1)=CI(II)
      IF(I.LT.3) GO TO 16
      SI(1)= (CI(1) + 2.0D0*C/DSQRT(XA))/(2.0D0*E)
      CI(1)=-(SI(1) + 2.0D0*S/DSQRT(XA))/(2.0D0*E)
   16 CONTINUE
      GO TO 14
C
   12 DO 13 I=1,3
      SI(I)=SI(I+1)
   13 CI(I)=CI(I+1)
C
      SI(4)=0.0D0
      CI(4)=0.0D0
   14 CONTINUE
C
C     UTILIZE THE SIN AND COS TRUNCATED SERIES TO OBTAIN THE FINAL
C     INTEGRAL CORRECTION.
C
      SCOR=SI(1)+D*(CI(2)-D*(SI(3)/2.0D0+D*CI(4)/6.0D0))
      CCOR=CI(1)-D*(SI(2)+D*(CI(3)/2.0D0-D*SI(4)/6.0D0))
      COR= DCMPLX(CCOR,-SCOR)
      RETURN
      END
```

D-V. Subroutines ZSUM, CMINV, and CS

These subroutines are the same as those used in the Collocation routine for the cascade. The ZSUM routine differs, however, in that the terms required for the 'correction' in the case P = 0 are precisely equations (III-106), to provide greater flexibility.

LIST OF REFERENCES

1. Ashley, H. and Landahl, M., Aerodynamics of Wings and Bodies, Addison-Wesley Publishing Company, Inc., 1965.

2. Barton, M. V., 'Stability of an Oscillating Airfoil in Supersonic Airflow,' Journal of the Aeronautical Sciences, p. 371-376, June 1948.

3. AGARD Report R-611, Comments on NASA Langley Research on Transonic Unsteady Aerodynamics, by S. R. Bland, 4 April 1973.

4. Campbell, G. and Foster, R., Fourier Integrals and Practical Applications, D. Van Nostrand Co., Inc., January 1948.

5. Drake, D. G., 'The Oscillating Two-Dimensional Aerofoil Between Porous Walls,' The Aeronautical Quarterly, p. 226-239, August 1957.

6. Aeronautical Research Council Report 21,489, Wind Tunnel Interference for Oscillating Wings at Transonic Speeds, by D. G. Drake, unpublished, 1 December 1959.

7. Elder, P. R., A Theoretical Analysis of Unsteady Transonic Cascade Flow, Thesis, Naval Postgraduate School, Monterey, Calif., 1972.

8. Gorelov, D. N., "Oscillations of a Plate Cascade in a Transonic Gas Flow," Mekhanika Zhidkosti i Gaza, v. 1, no. 1, pp. 69-74, 1966.

9. Guderley, K. G., 'Theorie schallnaher Stromungen,' Berlin/Gottingen/Heidelberg, Springer, 1957.

10. Hamamoto, I., "Minute Harmonic Oscillations of a Flat Plate Cascade in Transonic Flow," Proceedings of the 10th Japan National Congress for Applied Mechanics, pp. 227-231, 1960.

11. Hosokawa, I., "A Simplified Analysis for Transonic Flows Around Thin Bodies," Symposium Transsonicum, pp. 184-199, Springer-Verlag, 1964.

12. Knopp, K., Theory and Application of Infinite Series, Blackie and Son Limited, 1928.

13. Landahl, M., Unsteady Transonic Flow, p. 3, Pergamon Press, 1961.

14. Lane, F., 'Supersonic Flow Past an Oscillating Cascade with Supersonic Leading-Edge Locus,' Journal of the Aeronautical Sciences, p. 65-66, January 1957.

15. Lin, C. C., Reissner, E., and Tsien, H. S., "On Two-Dimensional Non-Steady Motion of a Slender Body in a Compressible Fluid," Journal of Mathematics and Physics, v. 27, no. 3, pp. 220-231, October 1948.

16. McCune, J. E., 'The Transonic Flow Field of an Axial Compressor Blade Row,' Journal of the Aero/Space Sciences, p. 616-626, October 1958.

17. Miles, J. W., "The Compressible Flow Past an Oscillating Airfoil in a Wind Tunnel," Journal of Aeronautical Sciences, v. 23, no. 7, pp. 671-678, 1956.

18. Murasaki, T., "Sonic Wall Interference and Some Other Problems," Transactions of the Japanese Society of Aerospace Sciences, v. 4, no. 5, pp. 29-56, 1961.

19. National Advisory Committee on Aeronautics Report 1128, Calculations on the Forces and Moments for an Oscillating Wing Aileron Combination in Two-Dimensional Potential Flow at Sonic Speed, by H. C. Nelson and J. H. Berman, 4 September 1951.

20. Oswatitsch, K., and Keune, F., "The Flow Around Bodies of Revolution at Mach Number 1,' Proceedings of the Conference on High Speed Aeronautics, Polytechnic Institute of Brooklyn, January 1955.

21. Rott, N., 'Flugelschwingungsformen in ebener kompressibler Potentialstromung,' Z.f.a. Math. u. Phys., v. 1, fasc. 6, p. 380-410, 1950.

22. Samoylovich, G. S., Unsteady Flow Around and Aeroelastic Vibration in Turbomachine Cascades, English translation FTD-HC-23-242-70, Foreign Technology Division, AFSC, 23 February 1971.

23. Sandeman, R. J., "On the Application of Local Linearization Methods to Choked Wind Tunnel Flow Problems," Symposium Transsonicum, pp. 355-361, Springer-Verlag, 1964.

24. Savkar, S. D., Aeromechanical Instability of a Transonic Cascade, unpublished technical brief, 28 January 1974.

25. Sears, W. R., 'Self-Correcting Wind Tunnels,' Sixteenth Lanchester Lecture to the Royal Aeronautical Society, May 1973, also Calspan Report No. RK-5070-a-2, July 1973.

26. NACA Report 1359, by J. R. Spreiter and A. Y. Alksne, 1958.

27. NASA Report R-73, A Study of the Simulation of Flow with Free-Stream Mach Number 1 in a Choked Wind Tunnel, by J. R. Sprieter, D. W. Smith, and B. J. Hyett, 1960.

28. Spreiter, J. R., "The Local Linearization Method in Transonic Flow Theory," Symposium Transsonicum, pp. 152-183, Springer-Verlag, 1964.

29. National Aeronautics and Space Administration CR-2258, Development of a Nonlinear Unsteady Transonic Flow Theory, by S. S. Stahara and J. R. Spreiter, 1973.

30. Teipel, I., "The Unsteady Air Forces at Mach One," Z.F. Flugwiss, v. 12, pp. 6-14, 1964.

INITIAL DISTRIBUTION LIST

		No. Copies
1.	Defense Documentation Center Cameron Station Alexandria, Virginia 22314	2
2.	Library, Code 0212 Naval Postgraduate School Monterey, California 93940	2
3.	Professor R.W. Bell, Code 57Be Department of Aeronautics Naval Postgraduate School Monterey, California 93940	1
4.	Assoc. Professor M.F. Platzer, Code 57Pl Department of Aeronautics Naval Postgraduate School Monterey, California 93940	11
5.	LT. Paul B. Schlein N233 NMC Pt. Mugu, California 93042	5
6.	Dr. H.J. Mueller (AIR-310) Naval Air Systems Command Washington, D.C. 20360	1
7.	Professor M.H. Vavra, Code 57Va Department of Aeronautics Naval Postgraduate School Monterey, California 93940	1
8.	Professor D.J. Collins, Code 57Co Department of Aeronautics Naval Postgraduate School Monterey, California 93940	1
9.	Professor T.H. Gawain, Code 57Ga Department of Aeronautics Naval Postgraduate School Monterey, California 93940	1
10.	Asst. Professor R.A. Hess, Code 57He Department of Aeronautics Naval Postgraduate School Monterey, California 93940	1

		No. Copies
11.	Professor L.V. Schmidt, Code 57Sx Department of Aeronautics Naval Postgraduate School Monterey, California 93940	1
12.	Professor C. Comstock, Code 53Zk Department of Mathematics Naval Postgraduate School Monterey, California 93940	1
13.	Professor K.E. Woehler, Code 61Wh Department of Physics Naval Postgraduate School Monterey, California 93940	1
14.	Professor A.E. Fuhs, Code 57Fu Department of Aeronautics Naval Postgraduate School Monterey, California 93940	1
15.	Asst. Prof. David A. Archer, Code 53Ac Department of Mathematics Naval Postgraduate School Monterey, California 93940	1